CCFSS Library (1939 - present)   Wei-Wen Yu Cold-Formed Steel Library

01 Aug 1989

Design of automotive structural components using high strength sheet steels the effect of strain rate on compressive mechanical properties of sheet steels

Maher Kassar

Wei-Wen Yu
Missouri University of Science and Technology, wwy4@mst.edu

Follow this and additional works at: https://scholarsmine.mst.edu/ccfss-library

Part of the Structural Engineering Commons

Civil Engineering Study 89-4
Structural Series

Twelfth Progress Report

DESIGN OF AUTOMOTIVE STRUCTURAL COMPONENTS
USING HIGH STRENGTH SHEET STEELS

THE EFFECT OF STRAIN RATE ON COMPRESSIVE MECHANICAL PROPERTIES
OF SHEET STEELS

by

Maher Kassar
Research Assistant

Wei-Wen Yu
Project Director

August 1989

Department of Civil Engineering
University of Missouri-Rolla
Rolla, Missouri

TABLE OF CONTENTS

TABLE OF CONTENTS (Cont.)

LIST OF TABLES

LIST OF TABLES (cont.)

LIST OF TABLES (cont.)

LIST OF FIGURES

LIST OF FIGURES (Cont.)

LIST OF FIGURES (Cont.)

LIST OF FIGURES (Cont.)

LIST OF FIGURES (Cont.)

LIST OF FIGURES (Cont.)

I. INTRODUCTION

Since May 1988, the research project on automotive components sponsored by American Iron and Steel Institute (AISI) at University of Missouri-Rolla (UMR) has been concentrated on a study of the effect of strain rate on mechanical properties of sheet steels and the structural behavior and strength of cold-formed steel members subject to impact loads.

The results of the tensile dynamic mechanical properties of three selected sheet steels, in the virgin condition as well as for the steels subjected to different amount of cold stretchings, were established in 1988 and early 1989. Details of the tension coupon tests were presented in the Eleventh Progress Report[1].

During the past few months, the UMR study primarily involved the experimental determination of the dynamic mechanical properties in compression for the same sheet steels used in the Eleventh Progress Report. The strain rates used for these compression coupon tests were similar to those used for the tension tests. They ranged from 10^{-4} to 1.0 in./in./sec. Details of the compression coupon tests are discussed herein.

This phase of study began with a review of the available literature relating to the efffect of the strain rate on the mechanical properties of sheet steels in compression. The literature survey is summarized in Section II. Section III presents the detailed information obtained from 54 compression tests. This section also discusses the strain rate effects on the compressive mechanical properties of the sheet steels tested. In

addition to the compression coupon tests, the test data presented in the Eleventh Progress Report for tension coupons tests have been reevaluated for the purpose of predicting the tensile dynamic mechanical properties under high strain rates. The newly developed equations and the corresponding graphical presentations are given in Section IV. Finally, all the research findings are summarized in Section V.

II. REVIEW OF LITERATURE

A. GENERAL

An extensive review of literature on the effect of strain rate on tensile mechanical properties of steels was presented in the Eleventh Progress Report[1]. This chapter presents a survey of available literature on the effect of strain rate on the compressive mechanical properties of steels and aluminums.

Because mechanical properties such as yield strength and tensile strength can vary with strain rate, it is often necessary to determine these properties under the conditions that closely match the expected deformation rates in service[2].

Strain rate (ϵ) is the rate of change of strain (ϵ) with respect to time (t) :

$$\epsilon' = d\epsilon \, / \, dt \qquad (2.1)$$

where ϵ can be either the engineering or the true strain. For a constant strain rate experiment, the strain rate is simply the total strain divided by the duration of the test[2]:

$$\epsilon' = \epsilon \, / \, t \qquad (2.2)$$

The unit of strain rate is the inverse of time sec^{-1}. When ϵ in Eq 2.1 is the engineering strain, then:

$$d\epsilon/dt = (1/L_o)(dL/dt) = V/L_o \qquad (2.3)$$

where L_o is the original length of the specimen, and V is the velocity at which the specimen is being deformed. A constant crosshead speed in a mechanical testing machine yields a constant engineering strain rate defined by Eq 2.3.

B. DYNAMIC TESTING FOR VARIOUS STRAIN RATES

Standard tests are usually performed at a strain rate of around 10^{-3} in./in./sec.[2] Tests at higher strain rates require special equipment and experimental techniques. These tests fall into four regimes roughly defined by the experimental techniques that are used to achieve the specified strain rate.

Low Strain-Rate Regime. A typical mechanical test is performed at a strain rate of around 10^{-3} in./in./sec., which yields a strain of 0.5 in 500 seconds. The equiment and techniques generally can be extended to strain rates as high as 0.1 in./in./sec. without difficulty.

Medium Strain-Rate Regime. In this regime, the experimental techniques are similar to those used at low strain-rates, but special equipment is required. Servo-hydraulic load frames equipped with high-capacity valves can be used to generate strain rates as high as 200 in./in./sec. Another experimental technique developed for compression testing in this strain-rate regime is the cam plastometer, described in Reference 2. When more qualitative medium strain-rate test results are desired, the drop test, which is also described in Reference 2, may be appropriate.

High Strain-Rate Regime. At strain rates greater than 200 in./in./sec., the required crosshead speed exceeds that easily achieved with screw-driven or servo-hydraulic frames. To generate high strain rates, experimental techniques that make use of projectile impacts and wave propagation phenomena have been employed. Techniques based on the Hopkinson bar have been used successfully to perform dynamic compression tests at strain rates exceeding 10^4 in./in./sec. with a maximum strain up to 0.3 in./in. At these high strain rates, inertia forces begin to

affect the validity of tests. Higher strain rates and larger strains are possible with the rod impact (Taylor) test. In this experiment, the complicated stress wave propagation phenomena strongly influence the measurement and should be accounted for numerically.

Very high Strain-Rate Regime. Very high strain rates are also possible. They are generally found only in shock fronts produced by very high vilocity impacts or in the detonation of explosives[2].

The strain rate regimes are summarized in Table 2.1. For more details concerning the experimental techniques mentioned above see Reference 2.

C. EFFECT OF STRAIN RATE ON COMPRESSIVE MECHANICAL PROPERTIES

It has become known that the mechanical properties of the vast majority of engineering materials are susceptible to the rate of application of the load either in tension or compression since the beginning of this century. For most materials, the proportional limit, yield strength, and tensile strength tend to increase at a higher strain rate. The following sections discuss the effect of strain rate on compressive mechanical properties of steels and aluminums.

a. Steel. In 1955, Alder and Phillips[3] studied the combined effects of stratn rate and temperature on compressive mechanical properties of steel, copper, and aluminum. The stress-strain curves were determined for these three materials at constant true strain rates in the range from 1 to 40 in./in./sec. The maximum compressive strain was 50% for temperatures ranging from 930° to 1200° C. The tests were conducted using the cam plastometer compression machine which was designed by Orwan and Los[8] in 1950. Table 2.2 presents their experimental results for steels at various strain, strain rate, and temperature. It can be observed from this table

that the increase in strain rate or decrease in temperature resulted in the increase of the stress at any given compression strain. The effect of strain rate on the stress for a given strain could be expressed by a reasonable expression as follows:

$$\sigma = \sigma_o \ \dot{\epsilon}^m \tag{2.4}$$

where

σ = true stress

$\dot{\epsilon}$ = true strain rate

m = strain rate sensitivity exponent

σ_o = the stress at unit strain rate

The values of σ_o and m obtained from Alder and Phillips ' work are given in Tables 2.3 and 2.4, respectively. It can be seen that m tends to increase while σ_o decreases and/or the temperature increases.

In 1957, Cook[4] used the cam plastometer machine to determine the compressive yield strengths for twelve different types of steel at 900, 1000, 1100, and 1200 deg. C combined with constant strain rates of 1.5, 8, 40, and 100 in./in./sec. The experimental results obtained from this investigation for low, medium and high carbon steels are given in Figs. 2.1 through 2.3, respectively. These curves illustrate the relationships between yield strengths and natural strains for three steels tested at different temperatures and strain rates. It is observed from the results of Cook, and Alder and Phillips that the yield strengths of steels increase as the strain rate increases and/or the temperature decreased. However, a noticeable feature of many of the curves of this investigation is the drop in yield strength at high strains which is contributed, as Cook concluded, to the predominance of thermal softening of the steels

over strain hardening as the compression proceeds. Comparison of the three curves shown in Figs. 2.1 to 2.3 for the three carbon steels also reveals that the tendency for the stress to drop increases with the steel carbon content.

By using the Split Hopkinson method, Davies and Hunter[5] investigated in 1963 the dynamic compression mechanical behavior of some metals including steel. The compressive loading cycles was of 30 micro-seconds duration which generated strain rates in the range of 10^3 to 10^4 in./in./sec. The results obtained from this investigation indicated that the ratio of the dynamic to static yield strength of the mild steel used is 2.6.

b. Aluminum. Structural aluminums were found to be less strain rate sensitive than steel in both compression and tension.

Alder and Phillips[3] also performed compression tests on aluminum to study the combined effects of strain rate and temperature using the cam plastometer compression testing machine. The compression tests on aluminum were conducted under the strain rate range of 1 to 40 in./in./sec. combined with temperatures ranging from -190° C to 550° C. Figure 2.4 shows typical stress versus logarithmic strain rate curves at various temperatures. It is observed from this figure that the stress at a given strain increases as the strain rate increases and/or the temperature decreases. Table 2.5 presents the experimental results for aluminum. The values of σ_o and m according to Equation 2.4 are given in Tables 2.6 and 2.7, respectively. No drop in stress was observed at high strains as in the case of steel.

Commercially pure aluminum specimens were tested by Hockett[6] in 1959

at room temperature using the cam plstometer compression testing machine

at three strain rates of 0.23, 0.455, and 1.46 in./in./sec. From the

measurements of load and time throughout each test, true stress versus

true strain curves were plotted. These curves fit an equation of the form:

$$\sigma = A (1 - e^{B\epsilon}) + C \epsilon \qquad (2.5)$$

where σ is the true stress, ϵ is the true strain, A, B, and C are param-

eters determined from the tests, and e is the base of natural logarithm.

The parameters A and C were found to be dependent upon temperature and

strain rate, increasing with decreasing temperature and with large in-

creases in strain rate. The parameter B was found to be essentially in-

dependent of temperature, but a large increase of strain rate produces

an increase in B.   Table 2.8 presents the values of the parameters A, B

and C as a result of the compression tests conducted on commercially pure

aluminum at constant true strain rates along with the statistical param-

eters which were obtained from fitting the experimental data to Equation

2.5.

Tests in compression and tension for a large number of metals under

high strain rates were performed by Lindholm and Yeakley[7] in 1968. Figure

2.5 shows stress-strain curves for 1100-0 aluminum in both tension and

compression at various strain rates. The lower strain rate tests were

performed on a standard Instron testing machine and the rest of the tests

were performed using the Split Hopkinson Pressure Bar. For the comparison

between the tension and compression data, all values of stress, strain,

and strain rate are true values. It has been observed from the results

of many tests that for very low strain rates, the stress levels in tension

and compression agree well, although the increase in flow stress with increasing strain rate differs in detail. Figure 2.6 shows a number of compression stress-strain data for 6061-T6 aluminum alloy, for which the wide variation in strain rate appears to have negligible effect on the stress levels. This is found to be true for other high-strength aluminum alloys according to Lindholm and Yeakley. As a result, the equivalence of the data obtained from the Split Hopkinson Pressure Bar with that obtained at low strain rates from an Instron machine indicates that wave propagation and inertia forces are not contributing any significant error to the measurements in the dynamic tests.

III. EXPERIMENTAL PROGRAM

A. MATERIALS

Three Types of sheet steels (35XF, 50XF, and 100XF) were selected to study the effect of strain rate on the compressive mechanical properties. These steels were used previously in the Eleventh Progress Report to study the effect of strain rate on the tensile mechanical properties. The chemical compositions for these three materials are listed in Table 3.1.

B. COMPRESSION TESTS

All these three sheet steels listed in Table 3.1 were uniaxially tested in compression in the longitudinal (parallel to the direction of rolling) and transverse (perpendicular to the direction of rolling) directions under three different strain rates of $10^{-4}, 10^{-2},$ and 1.0 in./in./sec. Three identical tests were conducted for each case.

1. ASTM Specifications. The compression tests followed the procedures outlined in the ASTM Specifications listed below:

E9-70   Standard Methods of Compression Testing of Metallic

           Materials at Room Temperature

E83-67   Standard Method of Verification and Classification

           of Extensometers

E111-82   Standard Test Method for Young's Modulus, Tangent

           Modulus and Chord Modulus

2. Specimens. The compression specimens tested in the longitudinal and transverse directions were prepared by the Machine Shop of the Department of Civil Engineering at the University of Missouri-Rolla. The

test specimens were cut from the quarter points of the steel sheets. The sketch in Figure 3.1 shows the compression specimen dimensions for the three materials (35XF, 50XF, and 100XF). The specimen dimensions were selected to fit a Montgomery-Templin compression test fixture. The notches along one edge were for the installation of the knife edges of the compressometer. Special care was taken to ensure that the ends of the specimens were parallel and thus the same length was used for both longitudinal sides of the specimen. A total of 54 coupons were tested in this phase of study. They are summarized in the following Table :

Direction of Testing	Type of Material	Number of Coupons Used
Longitudinal Compression (LC)	100XF-LC	9
	50XF-LC	9
	35XF-LC	9
Transverse Compression (TC)	100XF-TC	9
	50XF-TC	9
	35XF-TC	9

3. Equipment. All compression tests were performed in the same 110 kips 880 Material Test System (Figure 3.2) as previously used for the tension tests. New MTS Compression Platens were installed for conducting the compression tests. An assembly of the equipment used for the com-

pression tests is shown in Figure 3.3. The load was applied to the compression specimen by means of a specially made subpress (Figure 3.4(A)). The subpress base and ram are constructed of a hardened steel in order to minimize their deformation when applying the load. The compression specimen was held in a Montgomery-Templin compression test fixture (Figure 3.4(B)) which contains a series of rollers that may be tightened against the specimen to prevent buckling.

An MTS compressometer (Figure 3.4(C)) with a 1-in. gage length was used to measure strains from zero to 2 percent in./in. A special fixture was designed to fit the MTS compressometer in the compression jig. The classification of this compressometer according to ASTM Designation E83 was found to be dependent on the compressometer range used in the tests. Table 3.2 contains the classifications of four compressometer ranges according to the MTS transducer calibration data. The assembly of specimen, test fixture and subpress are shown in Figures 3.5a and 3.5b. Other equipment used for the tests includes the MTS controller (Figure 3.6), the data acquisition system (Figure 3.7), Data General graphic display terminal (Figure 3.8), Data General MV-10000 mini computer to store and manipulate the data (Figure 3.9), and IBM PS/2 Model 30 personal computer with IBM color plotter (Figure 3.10).

The load was measured by an MTS System Model 380041-06 load cell and associated conditioning, which was calibrated prior to testing according to the procedure of the National Bureau of Standard. The function of this equipment is identical to that for tension tests. For details concerning the function of the MTS machine and the data acquisition system, See Section III.B of the Eleventh Progress Report.

4. <u>Procedure.</u> Prior to testing, the dimensions of the compressive specimens were measured to the nearest 0.001 in. The specimen was then placed in the Montgomery-Templin compression test fixture and the lateral roller supports of the fixture were thightened firmly against the both sides of the specimen. Special care was taken to ensure that the specimen was aligned vertically in the test fixture. Next, the MTS compressometer was attached to one side of the test fixture such that the knife edges of the compressometer smoothly inserted into the notches of the compression specimen. Then, with the specimen, test fixture, and compressometer attached together as a unit, the entire unit was placed in the compression subpress. A small stub is provided on each side of the bottom surface of the test fixture. These stubs fit into indentions on the base of the subpress in order to ensure proper alignment of the subpress ram with the specimen's longitudinal axis. Next step was to place the subpress, with the test fixture, compressometer, and specimen attached, between the compression platens of the MTS loading frame such that the longitudinal axis of the subpress lined up with the centers of the platens. The function generator was then programmed to produce the desired ramp. Figure 3.11 shows a typical function generator ramp waveform. Table 3.3 shows the function generator ramp time and the corresponding strain-rate value. For all the tests, the strain mode was selected to maintain a constant strain rate and Range 4 was chosen for the three MTS modes (i.e., Load, Strain, and Stroke). During the tests, the stress-strain curves were plotted simultaneously on the Data General graphic terminal. The stress-strain data were recorded and stored by a computer for plotting and determination of the mechanical properties at a later

time. Buckling of the unsupported lengths at each end of the specimen limited the obtainable range of the stress-strain curves to approximately 1.8 percent.

C. RESULTS

1. Stess-Strain Curves. The stress-strain curves were plotted by using the Data General graphics software nemed Trendview with the stress-strain data recalled from the computer storage. Figures 3.12 through 3.17 present the compressive stress-strain curves for the following 6 different cases, which were studied under three different strain rates (0.0001, 0.01, and 1.0 in./in./sec.).

Direction of Testing	Type of Material	Figure Number
Longitudinal Compression (LC)	100XF-LC	3.12
	50XF-LC	3.14
	35XF-LC	3.16
Transverse Compression (TC)	100XF-TC	3.13
	50XF-TC	3.15
	35XF-TC	3.17

For the purpose of comparison, each figure includes three stress-strain curves representing the test data obtained from the same material for three different strain rates.

2. Mechanical Properties. The procedures used for determining the mechanical properties of sheet steels are discussed in the subsequent sections (Sections III.C.2.a and III.C.2.b). The mechanical properties so determined are the proportional limit F_{pr}, and the yield point F_y. These tested mechanical properties are presented in Tables 3.4 through 3.9 for each individual test. Tables 3.10 through 3.15 present the av-

erage values of the mechanical properties for each material tested in either longitudinal compression (LC) or transverse compression (TC) under different strain rates (0.0001, 0.01, or 1.0 in./in./sec.).

a. <u>Proportional Limit</u>, F_{pr}. The proportional limit is usually defined as the point above which the stress-strain curve becomes nonlinear. Since it is often difficult to pinpoint the exact location of the true proportional limit, standard methods are normally used so that comparable values of proportional limit may be determined by different researchers. One such method that is commonly used for aircraft structures and also for cold-formed stainless steel members is the 0.01 percent offset method. For this method a straight line with a slope equal to the modulus of elasticity is drawn parallel to the stress-strain curve and offset such that it intersects the strain axis at 0.01 percent strain. The intersection of this line with the stress-strain curve is defined as the proportional limit.

In this study, the 0.01 percent offset method was chosen to obtain the values of the proportional limit for the steels tested in compression under the strain rates of 0.0001 and 0.01 in./in./sec. as demonstrated graphically in Figure 3.18 for the 35XF-TC-4 curve and listed in tables 3.4 through 3.9. Because of the waving effect of the impact load on the stress-strain curves of the tests conducted at the high strain rate of 1.0 in./in./sec., reliable values for the proportional limit were difficult to obtain.

b. <u>Yield Strength or Yield Point</u>, F_y. The method commonly used to determine the yield point of sheet steels depends on whether the stress-strain curve is of the gradual or sharp-yielding type. For the types of

sheet steels tested in this study in compression, the stress-strain curves of the 50XF sheet steel are the sharp-yielding type, while the stress-strain curves of the 35XF and 100XF steels are the gradual-yielding type.

The yield point of the sharp-yielding steel was determined as the stress where the stress-strain curve becomes horizontal. Typical sharp-yielding stress-strain curves are shown in Figure 3.14 for the 50XF steel in the longitudinal direction. For this case, the lower yield point is given in Tables 3.6 and 3.7 for longitudinal and transverse directions, respectively.

For the gradual-yielding type stress-strain curves as shown in Figure 3.18 for 35XF-TC-4 curve, the yield point of 35XF steel was determined by the intersection of the stress-strain curve and the straight line drawn parallel to the elastic portion of the stress-strain curve at an offset of 0.002 in./in. A Fortran 77 code was written to determine the yield points presented in Tables 3.4, 3.5, 3.8 and 3.9 for the gradual-yielding type curves using the Least Square Method.

D. DISCUSSION

The test results presented in Section III.C are discussed in this section with an emphasis on the effects of strain rate on the mechanical properties of the sheet steels tested in both longitudinal compression and transverse compression.

1. Mechanical Properties. The test results indicate that all mechanical properties are affected by the strain rate. Table 3.16 compares the dynamic yield stress determined at the strain rate of 1.0 in./in./sec. and the static yield stress determined at the strain rate

of 0.0001 in./in./sec. The effects of strain rate on proportional limit and yield strength are discussed in the following sections.

a. <u>Yield Strength or Yield Point,</u> F_y. In Table 3.16, the dynamic yield strength, $(F_y)_d$, and the static yield strength, $(F_y)_s$, are compared by using a ratio of $(F_y)_d/(F_y)_s$. In the above expressions, $(F_y)_d$ is the yield strength determined for the strain rate of 1.0 in./in./sec. while $(F_y)_s$ is the yield strength determined for the strain rate of 0.0001 in./in./sec. It can be seen that for all cases, the yield strength of sheet steel increases with the strain rate. The percentage increases in yield strength for the three steels studied in this investigation are: 7% for 100XF steel, 9% to 10% for 50XF steel, and 24% to 33% for 35XF steel when the strain rate increased from 0.0001 to 1.0 in./in./sec. It is observed from this table that the increases in yield strength for the virgin materials are independent of the test direction (LC or TC) for 100XF and 50XF sheet steels. However, for 35XF steel the increase in yield stress in the transverse direction is larger than that in the longitudinal direction.

b. <u>Proportional Limit</u> F_{pr}. Similar to the effect of strain rate on yield strength, the proportional limits of sheet steels increased with the strain rate. The percentage increases in proportional limits for the three materials studied in this investigation are: 9% to 24% for 100XF steel, 4% to 22% for 50XF steel, and 14% to 24% for 35XF steel when the strain rate increased from 0.0001 to 0.01 in./in./sec. It is noted from these values that the amounts of percentage increase in proportional limit are larger than the amounts of percentage increase in yield stress when the strain rate increased from 0.0001 in./in./sec. to 1.0 in./in./sec.

2. <u>Strain Rate Sensitivity.</u> In the literature review, Equation 2.4 gives the relation between the stress and the strain rate at a given strain as follows:

$$\sigma = \sigma_o \, \dot\epsilon^{\,m} \qquad\qquad (3.1)$$

By applying Equation 3.1 to two different strain rates and eliminating σ_o we have

$$m = \ln(\, \sigma_2 / \sigma_1 \,) / \ln(\, \dot\epsilon_2 / \dot\epsilon_1 \,) \qquad\qquad (3.2)$$

for two given values of the flow stress of a material at two different strain rates, the strain rate sensitivty exponent m may be calculated by using Equation 3.2.

Table 3.17 list the values of the strain-rate sensitivities, which were calculated on the basis of Equation 3.2. The value of m_1 was calculated for the yield strengths corresponding to the strain rates of 0.0001 in./in./sec. and 0.01 in./in./sec., while the value of m_2 was calculated for the yield strengths corresponding to the strain rates of 0.01 in./in./sec. and 1.0 in./in./sec. From Table 3.17, it can be seen that, in general, the value of m in compression increases as the strain rate increases. The strain rate sensitivity decreases progressively as the static yield strength level increases.

3. <u>Prediction of Yield Strength in Compression for High Strain Rates.</u> Figures 3.19 through 3.24 copmare the average values of the compressive yield strengths at different strain rates for different cases. The data plotted in these figures are in terms of yield stress vs. logarithmic strain rate. For each case, the following second degree polynomial was developed using the Least Square Method in the strain-rate range of 0.0001 to 1.0 in./in./sec.

$$Y = A + B X + C X^2 \qquad\qquad (3.3)$$

where

      Y = yield stress

      $X = \log(\epsilon^{\cdot})$

      A, B, and C = constants

The polynomial parameters A, B, and C are given at the top of the curve for each case in Figures 3.19 through 3.24. The values of the compressive yield strengths of the steels used in this investigation at higher strain rate (larger than 1.0 and up to 1000 in./in./sec.) could be extrapolated by using the equation or the curve for each individual case.

This report included compression tests for steels in the virgin condition only. The discussion on the combined effects of cold-stretching and strain rate on steel mechanical properties are discussed in details in the Eleventh Progress Report.

IV. ADDITIONAL EVALUATION FOR THE TENSILE TEST DATA PRESENTED

IN THE ELEVENTH PROGRESS REPORT

In the Eleventh Progress Report, the tensile mechanical properties (i.e., yield strength, ultimate strength, and elongation) of the three steels (35XF, 50XF, and 100XF) tested under the strain-rate rage of 0.0001 to 1.0 in./in./sec. were established. These three sheet steels were tested under the virgin condition and different amounts of cold stretching. Half of coupons were tested to study the combined effects of strain rate, cold stretching, and aging on the steel sheet mechanical properties. Figures 3.28 through 3.58 of the Eleventh Progress Report compare the average values of the yield and ultimate tensile strengths at different strain rates for different cases. The test data were plotted in these Figures using semi-log scale and were connected by straight lines. The horizontal scales were limited to the strain rate range from 0.0001 to 1.0 in./in./sec. which was used for all tensile tests.

For the purpose of predicting the values of the yield and ultimate strengths of the steels for higher strain rates above 1.0 in./in./sec., a second degree polynomial equation similar to Equation 3.3 was developed by using the Least Square Method. In these equations, the ultimate and yield strengths are a function of logarithmic strain rate for steels in the virgin condition as well as for steels subjected to different amounts of cold stretching including aged and non-aged conditions. Graphical presentations and the corresponding equations are shown in Figures 4.1 through 4.26. The horizontal axis in these Figures represents the logarithmic strain rate range from 0.0001 to 1000 in./in./sec. The values

of the yield and ultimate strengths at a strain rate higher than 1.0 and

up to 1000 in./in./sec. can be predicted by extrapolation from the curve

or calculated from the equation by using the desired strain-rate value.

V. CONCLUSIONS

This study dealt with the effect of strain rate on mechanical properties of sheet steels.

During the period from May 1988 through December 1988, progress was made on a study of the effect of strain rate on tensile mechanical properties of sheet steels. The results of this investigation were presented in the Eleventh Progress Report.

Since the beginning of 1989 through July of the same year, the work continued to include the study of mechanical properties of sheet steels in compression. This work included a review of literature and testing of 54 compression specimens. The literature survey is presented in Section II. Section III contains the detailed information on the experimental investigation, which includes materials, test specimens, equipment, test procedure, test results, and the discussion of the test data. Additional evaluation of the test data included in the Eleventh Progress Report is presented in Section IV of this report for the purpose of predicting the mechanical properties of sheet steels at strain rates higher than that used in the tension tests.

The following conclusions may be drawn from the study of the effect of strain rate on tensile and compressive mechanical properties of steels:

1. Proportional limit, yield strength, and ultimate strength increase with increasing strain rate.

2. Yield strength is more sensitive to strain rate than ultimate strength.

3. The strain rate sensitivity value is not a constant. In most cases it increases with increasing strain rate.

4. The mechanical properties of sheet steels having low yield strengths are more sensitive for strain rate effect.

5. A second degree polynomial is well fitted to the experimental data for each case in both tension and compression and can provide a better prediction for yield and ultimate strengths at high strain rates above the strain rate-range used in the tests.

The results of this study will be used in the future research work which will include the study of the structural strengths of cold-formed steel stub columns and beams subjected to dynamic loads.

ACKNOWLEDGMENTS

REFERENCES

1. Kassar, M. and Yu, W.W., "Design of Automotive Structural Components Using High Strength Sheet Steels: The Effect of Strain Rate on Mechanical Properties of Sheet Steels", Eleventh Progress Report, Civil Engineering Study 89-2, University of Missouri- Rolla, January 1989.

2. Follansbee, P.S., "High Strain Rate Compression Testing", Metals Handbook , American Society for Metals, Ninth Edition, Volume 8, 1985, pp. 190-207.

3. Alder, J.F., and Phillips, V.A., "The Effect of Strain Rate and Temperature on the Resistance of Aluminum, Copper, and Steel to Compression," Journal of the Institute of Metals , Vol 83, 1954-1955, pp. 80-86.

4. Cook, P.M., "True Stress-Strain Curves for Steel in Compression at High Temperature and Strain Rates, for Application to the Calculation of Load and Torque in Hot Rolling," Conference on The Properties of Materials at High Rates of Strain , Institute of Mechanical Engineers, 1957, pp. 86-97.

5. Davies, E.D.H., and Hunter, S.C., "The Dynamic Compression Testing of Solids by the Method of the Split Hopkinson Pressure Bar," J. Mech. Phys. Solids , Vol 11, 1963, pp. 155-172.

6. Hockett, J.E., "Compression Testing at Constant True Strain Rates," Proc. ASTM , Vol 59, 1959, pp. 1309-1319.

7. Lindholm, U.S., and Yeakley, L.M., "High Strain-Rate Testing: Tension and Compression," Experimental Mechanics , Vol 8, 1968, pp. 1-9.

8. Orwan, E., British Iron and Steel Research Association Report No. MW/F/22/50.

9. Soroushian, P., and Choi, K.B., "Steel Mechanical Properties at Different Strain Rates," Journal of Structural Engineering , Proceedings of the American Society of Civil Engineers, Vol. 113, No. 4, 1987, pp. 663-672.

10. Norris, C.H., Hansen, R.J., Holley, M.J. Jr., Biggs, J.M., Namyet, S., and Minami, J.K., Structural Design for Dynamic Loads , McGraw-Hill Book Company, 1959.

Table 2.1

Experimental Techniques for Various Strain

Rate Regimes for Compression Testing[2]

Strain Rate Regime	Experimental Techniques	Wave Propagation
Low strain rate : $\dot{\epsilon} \leq 0.1 \text{ s}^{-1}$	Standard mechanical testing procedures	Not significant
Medium strain rate : $0.1 \text{ s}^{-1} \leq \dot{\epsilon} \leq 200 \text{ s}^{-1}$	Servo-hydraulic frames, cam plasometer, drop test	Influences load measurement
High strain rate : $200 \text{ s}^{-1} \leq \dot{\epsilon} \leq 10^5 \text{ s}^{-1}$	Hopkinson pressure bar	Affects uniform stress approximation
	Rod Impact (Taylor) test	Analysis required for interpretation of results
Very high strain rate : $\dot{\epsilon} \geq 10^5 \text{ s}^{-1}$	Flyer plate impact	Critical

Table 2.2

Effect of Strain Rate and Temperature on the Stress

Required to Compress Steel[3]

Speci-men Dia., mm.	Temp., °C.	Strain Rate, sec.$^{-1}$	Average Stress (10^3 lb./in.^{2}) to Compress :				
			10%	20%	30%	40%	50%
18	18	slow *	77·5	92·0	98·0	102	105
12	930	4·35	18·6	22·3	23·5	23·9	24·1
		7·4	19·0	22·9	25·1	26·4	26·2
		12·9	20·9	24·0	25·8	27·0	27·1
		23·1	21·6	25·3	27·4	28·6	29·4
12	1000	4·35	14·8	18·3	20·0	20·7	20·1
18		4·35	14·8	17·9	19·6	20·8	20·3
12		7·4	16·4	19·2	21·0	22·1	22·0
18		7·4	15·5	18·6	20·8	22·3	22·2
12		12·9	16·9	19·7	21·4	22·6	22·8
12		23·1	18·6	21·6	22·9	23·9	24·4
18	1060	4·35	12·8	15·2	16·6	17·1	16·3
		7·4	13·6	16·0	17·9	18·7	18·5
		12·9	14·5	16·9	18·6	19·9	20·2
		23·1	15·4	18·4	20·3	21·7	22·1
18	1135	4·35	11·0	12·9	13·8	13·8	13·1
		7·4	11·6	13·6	14·8	15·3	14·7
		12·9	12·4	14·5	15·8	16·7	16·9
		23·1	13·6	15·9	17·4	18·3	18·5
18	1200	4·35	9·0	10·6	11·0	10·9	10·1
		7·4	9·5	10·9	11·7	11·8	11·2
		12·9	10·2	11·6	12·5	12·7	12·5
		23·1	10·9	12·6	13·7	14·3	14·0

Table 2.3

Values of σ_0 for Steels using the Equation[3]

$$\sigma = \sigma_0 * \epsilon^{\cdot m}$$

Temp., °C.	Value of σ_0 for a Compression of:				
	10%	20%	30%	40%	50%
930	16·3	19·4	20·4	20·9	20·9
1000	13·0	15·6	17·3	18·0	16·9
1060	10·9	12·9	14·0	14·4	13·6
1135	9·1	10·5	11·2	11·0	9·9
1200	7·6	8·6	8·8	8·3	7·6

Table 2.4

Values of m for Steels using the Equation[3]

$$\sigma = \sigma_0 * \epsilon^{\cdot m}$$

Temp., °C.	Value of m for a Compression of:				
	10%	20%	30%	40%	50%
930	0·088	0·084	0·094	0·099	0·105
1000	0·108	0·100	0·090	0·093	0·122
1060	0·112	0·107	0·117	0·127	0·150
1135	0·123	0·129	0·138	0·159	0·198
1200	0·116	0·122	0·141	0·173	0·196

Table 2.5

Effect of Strain Rate and Temperature on the Stress

Required to Compress Aluminum[3]

Batch	Speci-men Dia., mm.	Temp., °C.	Strain Rate, sec.⁻¹	Average Stress (10^3 lb./in.²) to Compress :				
				10%	20%	30%	40%	50%
b	12	−190	4·38	28·1	34·1	33·9	32·2	31·6
b	12	−120	4·38	18·6	22·4	24·7	26·3	27·8
b	12	− 75	4·38	17·4	20·9	23·0	24·5	25·8
a	18	− 75	4·38	16·0	19·5	21·5	23·0	24·1
a	18	18	slow*	12·9	15·4	17·0	18·8	20·5
a	18		1·34	14·7	17·2	19·0	20·7	22·1
a	18		2·31	14·9	17·6	19·5	21·1	22·6
a	18		4·38	14·1	17·0	19·2	21·0	22·4
b	12		4·38	14·5	17·2	19·2	20·6	21·9
a	18		7·15	14·6	17·5	19·5	21·3	22·9
a	18		12·9	15·1	17·9	19·8	21·5	23·0
b	12		12·9	15·0	17·9	19·7	21·1	22·3
a	18		23·1	15·3	18·2	20·1	21·8	23·1
a	18		39·3	15·1	18·1	20·1	22·0	23·3
a	18	150	1·34	11·4	13·5	14·9	16·0	16·9
			2·31	11·5	13·8	15·3	16·3	17·2
			4·38	11·9	14·1	15·6	16·7	17·8
			7·15	12·0	14·2	15·7	17·1	17·9
			12·9	12·0	14·2	15·9	17·3	18·2
			23·1	12·1	14·2	15·8	17·2	18·4
			39·3	12·1	14·3	16·0	17·4	18·5
a	18	250	1·34	9·2	10·6	11·5	12·1	12·5
			2·31	9·4	10·7	11·6	12·2	12·6
			4·38	9·5	11·0	12·1	12·7	13·1
			7·15	9·6	11·1	12·1	12·9	13·1
			12·9	9·8	11·6	12·6	13·3	13·6
			23·1	9·8	11·5	12·6	13·4	13·8
a	18	350	1·34	6·3	7·0	7·3	7·5	7·5
			2·31	6·3	7·1	7·6	7·8	7·9
			4·38	6·8	7·7	8·2	8·5	8·6
			7·15†	6·7	7·6	8·2	8·6	8·7
			12·9	7·0	8·1	8·6	9·0	9·1
			23·1	7·3	8·3	9·0	9·4	9·7
			39·3	7·7	8·8	9·5	10·0	10·2
a	18	450	1·34	4·0	4·5	4·6	4·6	4·5
			2·31	4·2	4·6	4·8	4·7	4·7
			4·38	4·4	4·9	5·0	5·0	5·1
			7·15	4·8	5·3	5·5	5·6	5·6
			12·9	5·4	5·8	5·9	6·0	6·1
			23·1	5·2	5·9	6·2	6·3	6·4
			39·3	5·8	6·2	6·5	6·7	6·9

Table 2.6

Values of σ_0 for Aluminums using the Equation[3]

$$\sigma = \sigma_0 * \epsilon^{.m}$$

Metal	Temp., °C.	Value of σ_0 for a Compression of:				
		10%	20%	30%	40%	50%
Al	18	14·6	17·1	18·9	20·6	22·0
	150	11·4	13·5	15·0	16·1	17·0
	250	9·1	10·5	11·4	11·9	12·3
	350	6·3	6·9	7·2	7·3	7·4
	450	3·9	4·3	4·5	4·4	4·3
	550	2·2	2·4	2·5	2·4	2·4

Table 2.7

Values of m for Aluminums using the Equation[3]

$$\sigma = \sigma_0 * \epsilon^{.m}$$

Metal	Temp., °C.	Value of m for a Compression of:				
		10%	20%	30%	40%	50%
Al	18	0·013	0·018	0·018	0·018	0·020
	150	0·022	0·022	0·021	0·024	0·026
	250	0·026	0·031	0·035	0·041	0·041
	350	0·055	0·061	0·073	0·084	0·088
	450	0·100	0·098	0·100	0·116	0·130
	550	0·130	0·130	0·141	0·156	0·155

Table 2.8

Results of Compression Tests on Commercially Pure Aluminum

at Constant True Strain Rates[6]

Based on Equation : $\sigma = A * (1 - e^{B\epsilon}) + C * \epsilon$

Strain Rate, $\dot{\epsilon}$, per sec	Variance of Fit. s_f^2	Standard Deviation of Fit, s_f	First Param-eter, A	Stand-ard De-viation of A, s_A	Second Param-eter, B	Stand-ard De-viation of B, s_B	Third Param-eter, C	Stand-ard De-viation of C, s_C	Num-ber of Points n
2.30×10^{-1}....	347 103	589.2	11 303	237	−25.92	1.46	13 496	473	70
4.55×10^{-1}....	2 496 161	1 579.2	11 662	637	−19.12	2.54	13 220	1 221	89
1.46..........	2 749 815	1 685.3	10 972	515	−22.49	2.80	15 750	1 037	124

Table 3.1

Chemical Compositions of the Sheet Steels Used

AISI Designa.	Thick in.	C	Mn	P	S	Si	V	Cu	Al	Cb	Zr
035XF	0.085	.070	.40	.007	.017	--	.08	--	--	--	---
050XF	0.077	.081	.96	.017	.003	.27	--	--	.04	--	---
100XF	0.062	.070	.43	.006	.023	--	--	.11	.056	.064	.08

Table 3.2

Classification of the MTS Compressometer

Range	Maximum Strain in./in.	Maximum Error in./in.	ASTM Classification
100%	0.20	0.000100	Class B-1
50 %	0.10	0.000050	Between Classes A and B-1
20 %	0.04	0.000012	Between Classes A and B-1
10 %	0.02	0.000008	Class A

Table 3.3

Function Generator Ramp Time and the Corresponding

Strain Rate

Ramp Time sec.	Strain Rate in./in./sec.
200	0.0001
20	0.001
2	0.01
0.2	0.1
0.02	1.0

Table 3.4

Tested Mechanical Properties of 100XF Sheet Steel

Longitudinal Compression

Test No.	Strain Rate in./in./sec.	F_{pr} (ksi)	F_y (ksi)	F_{pr}/F_y
LC-1	0.0001	72.87	107.28	0.68
LC-2	0.0001	71.17	108.23	0.66
LC-3	0.0001	69.71	106.37	0.65
LC-4	0.01	87.90	110.51	0.79
LC-5	0.01	88.98	112.18	0.79
LC-6	0.01	*****	111.08	****
LC-7	1.0	*****	115.16	****
LC-8	1.0	*****	116.61	****
LC-9	1.0	*****	112.97	****

Table 3.5

Tested Mechanical Properties of 100XF Sheet Steel

Transverse Compression

Test No.	Strain Rate in./in./sec.	F_{pr} (ksi)	F_y (ksi)	F_{pr}/F_y
TC-1	0.0001	103.82	123.66	0.84
TC-2	0.0001	102.53	120.41	0.85
TC-3	0.0001	104.63	126.91	0.82
TC-4	0.01	113.27	126.42	0.90
TC-5	0.01	113.18	125.14	0.90
TC-6	0.01	113.91	126.91	0.90
TC-7	1.0	******	129.98	****
TC-8	1.0	******	132.62	****
TC-9	1.0	******	132.59	****

Table 3.6

Tested Mechanical Properties of 50XF Sheet Steel

Longitudinal Compression

Test No.	Strain Rate in./in./sec.	F_{pr} (ksi)	F_y (ksi)	F_{pr}/F_y
LC-1	0.0001	37.63	49.95	0.75
LC-2	0.0001	39.05	49.70	0.79
LC-3	0.0001	39.24	49.40	0.79
LC-4	0.01	42.92	52.82	0.81
LC-5	0.01	41.25	52.82	0.78
LC-6	0.01	35.99	51.90	0.69
LC-7	1.0	*****	54.88	****
LC-8	1.0	*****	54.50	****
LC-9	1.0	*****	54.99	****

Table 3.7

Tested Mechanical Properties of 50XF Sheet Steel

Transverse Compression

Test No.	Strain Rate in./in./sec.	F_{pr} (ksi)	F_y (ksi)	F_{pr}/F_y
TC-1	0.0001	38.69	51.07	0.76
TC-2	0.0001	42.65	51.04	0.84
TC-3	0.0001	43.19	51.13	0.84
TC-4	0.01	50.00	53.46	0.93
TC-5	0.01	50.47	53.38	0.94
TC-6	0.01	51.47	53.36	0.96
TC-7	1.0	*****	55.52	****
TC-8	1.0	*****	55.88	****
TC-9	1.0	*****	55.22	****

Table 3.8

Tested Mechanical Properties of 35XF Sheet Steel

Longitudinal Compression

Test No.	Strain Rate in./in./sec.	F_{pr} (ksi)	F_y (ksi)	F_{pr}/F_y
LC-1	0.0001	17.76	29.95	0.59
LC-2	0.0001	17.98	29.79	0.60
LC-3	0.0001	17.63	29.74	0.59
LC-4	0.01	23.15	32.50	0.71
LC-5	0.01	17.94	31.52	0.57
LC-6	0.01	19.00	31.73	0.60
LC-7	1.0	*****	36.69	****
LC-8	1.0	*****	36.27	****
LC-9	1.0	*****	37.76	****

Table 3.9

Tested Mechanical Properties of 35XF Sheet Steel

Transverse Compression

Test No.	Strain Rate in./in./sec.	F_{pr} (ksi)	F_y (ksi)	F_{pr}/F_y
TC-1	0.0001	23.48	32.76	0.72
TC-2	0.0001	22.45	32.44	0.69
TC-3	0.0001	23.42	32.67	0.72
TC-4	0.01	28.60	37.95	0.75
TC-5	0.01	30.34	36.71	0.83
TC-6	0.01	27.26	35.40	0.77
TC-7	1.0	*****	43.17	****
TC-8	1.0	*****	41.00	****
TC-9	1.0	*****	46.17	****

Table 3.10

Average Tested Mechanical Properties of 100XF Sheet Steel

Longitudinal Compression

Strain Rate in./in./sec.	F_{pr} (ksi)	F_y (ksi)	F_{pr}/F_y
0.0001	71.25	107.29	0.66
0.01	88.44	111.26	0.79
1.0	*****	114.91	****

Table 3.11

Average Tested Mechanical Properties of 100XF Sheet Steel

Transverse Compression

Strain Rate in./in./sec.	F_{pr} (ksi)	F_y (ksi)	F_{pr}/F_y
0.0001	103.66	123.66	0.84
0.01	113.45	126.16	0.90
1.0	******	131.73	****

Table 3.12

Average Tested Mechanical Properties of 50XF Sheet Steel

Longitudinal Compression

Strain Rate in./in./sec.	F_{pr} (ksi)	F_y (ksi)	F_{pr}/F_y
0.0001	38.64	49.68	0.78
0.01	40.05	52.51	0.76
1.0	*****	54.79	****

Table 3.13

Average Tested Mechanical Properties of 50XF Sheet Steel

Transverse Compression

Strain Rate in./in./sec.	F_{pr} (ksi)	F_y (ksi)	F_{pr}/F_y
0.0001	41.51	51.08	0.81
0.01	50.65	53.40	0.95
1.0	*****	55.54	****

Table 3.14

Average Tested Mechanical Properties of 35XF Sheet Steel

Longitudinal Compression

Strain Rate in./in./sec.	F_{pr} (ksi)	F_y (ksi)	F_{pr}/F_y
0.0001	17.79	29.83	0.60
0.01	20.03	31.92	0.63
1.0	*****	36.91	****

Table 3.15

Average Tested Mechanical Properties of 35XF Sheet Steel

Transverse Compression

Strain Rate in./in./sec.	F_{pr} (ksi)	F_y (ksi)	F_{pr}/F_y
0.0001	23.12	32.62	0.71
0.01	28.73	36.69	0.78
1.0	*****	43.45	****

Table 3.16

Ratios of Dynamic to Static Compressive Yield Stresses

for Three Sheet Steels Based on Tables 3.10 to 3.15

Type of Sheet Steel	$(F_y)_d/(F_y)_s$
100XF-LC	1.07
100XF-TC	1.07
50XF-LC	1.10
50XF-TC	1.09
35XF-LC	1.24
35XF-TC	1.33

Notes :

$(F_y)_d$ = dynamic yield stress for the strain
rate of 1.0 in./in./sec.

$(F_y)_s$ = static yield stress for the strain
rate of 0.0001 in./in./sec.

Table 3.17

Values of Strain Rate Sensitivities m for Three Sheet

Steels Based on the Changes of the Yield Stresses at

Different Strain Rates

Type of Sheet Steel	m_1	m_2
100XF-LC	0.008	0.007
100XF-TC	0.004	0.009
50XF-LC	0.012	0.009
50XF-TC	0.010	0.008
35XF-LC	0.015	0.031
35XF-TC	0.025	0.037

Notes:

m_1= strain rate sensitivity based on the changes of yield stress between strain rates of 0.0001 in./in./sec. and 0.01 in./in./sec.

m_2= strain rate sensitivity based on the changes of yield stress between strain rates of 0.01 in./in./sec. and 1.0 in./in./sec.
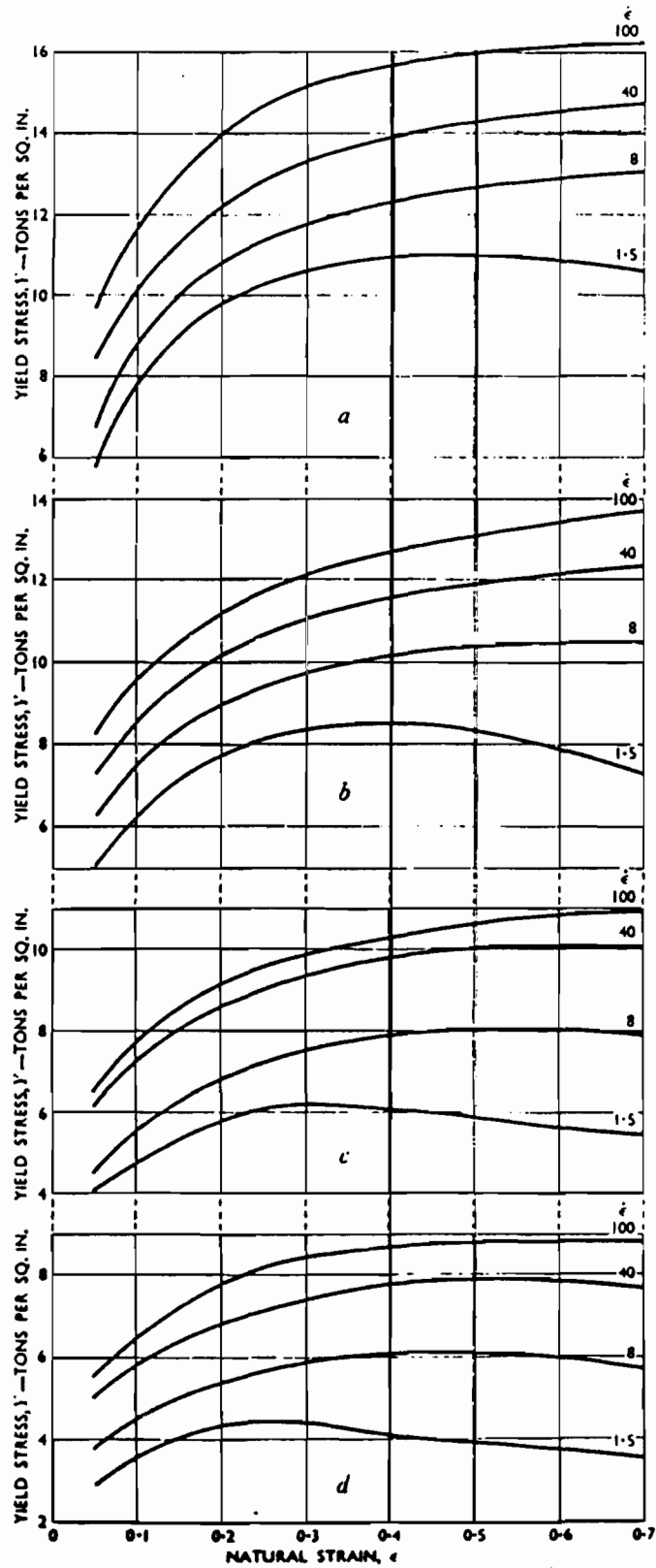
Fig. 2.1 Relationship Between Flow Stress and Natural Strain for
Low-Carbon Steels[4] a) 900 deg. C., b) 1000 deg. C.,
c) 1100 deg. C., and d) 1200 deg. C.
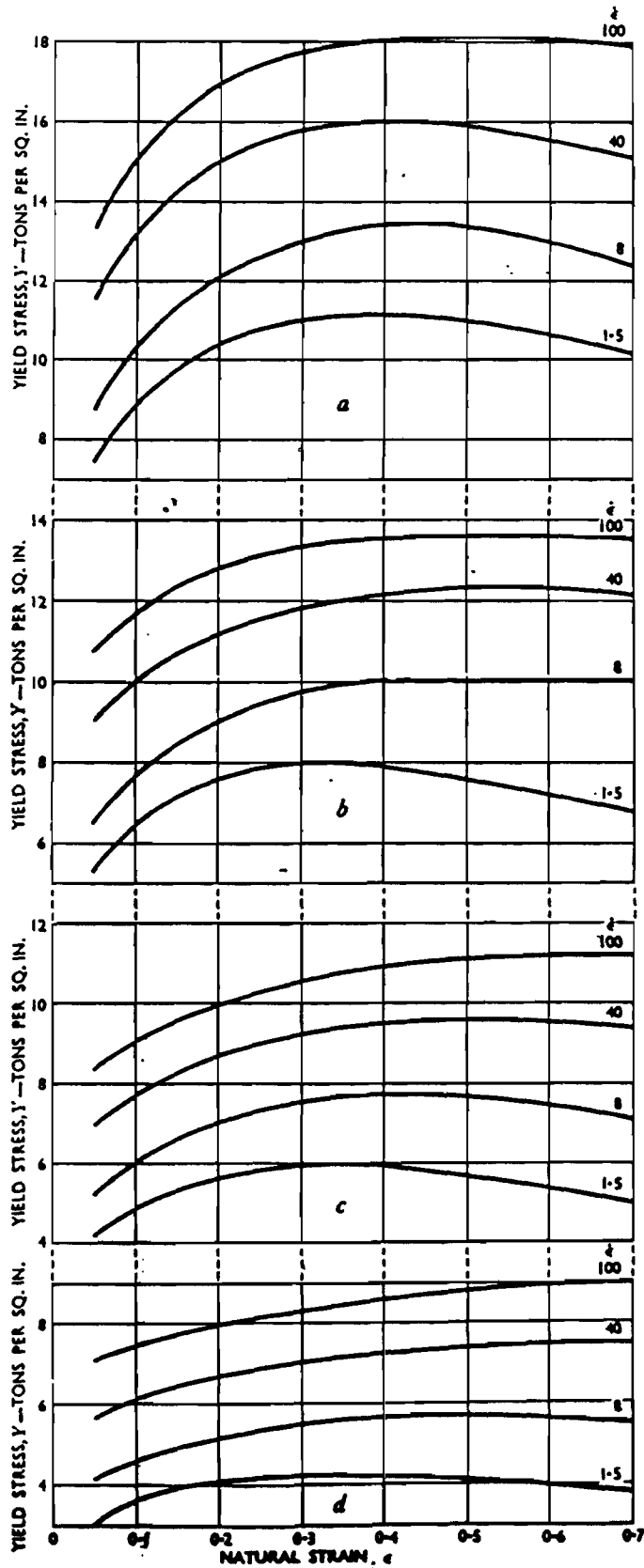
Fig. 2.2 Relationship Between Flow Stress and Natural Strain for
Medium-Carbon Steels[4] a) 900 deg. C., b) 1000 deg. C.,
c) 1100 deg. C., and d) 1200 deg. C.
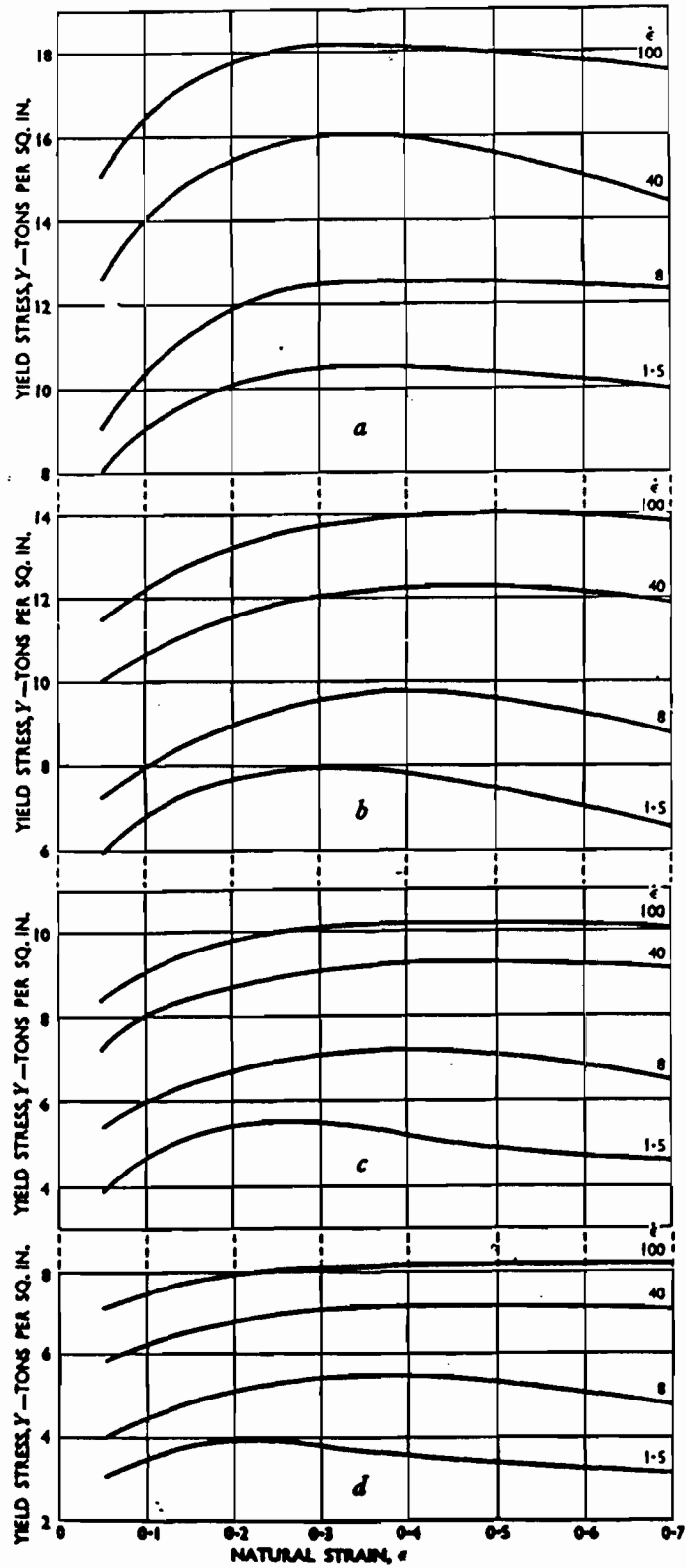
Fig. 2.3 Relationship Between Flow Stress and Natural Strain for
High-Carbon Steels[4] a) 900 deg. C., b) 1000 deg. C.,
c) 1100 deg. C., and d) 1200 deg. C.
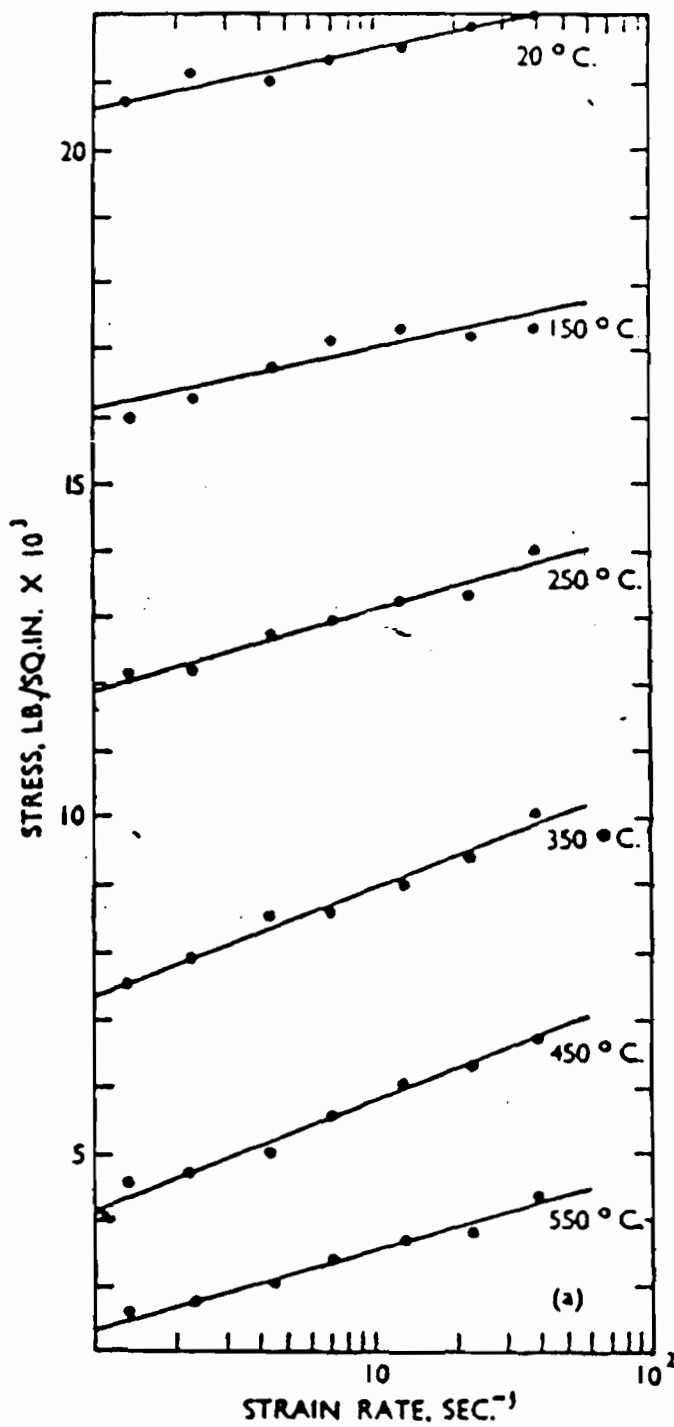
Fig. 2.4 Effect of strain rate on the Stress Required to Compress
Aluminum to 40% Reduction at Various Temperatures[3]
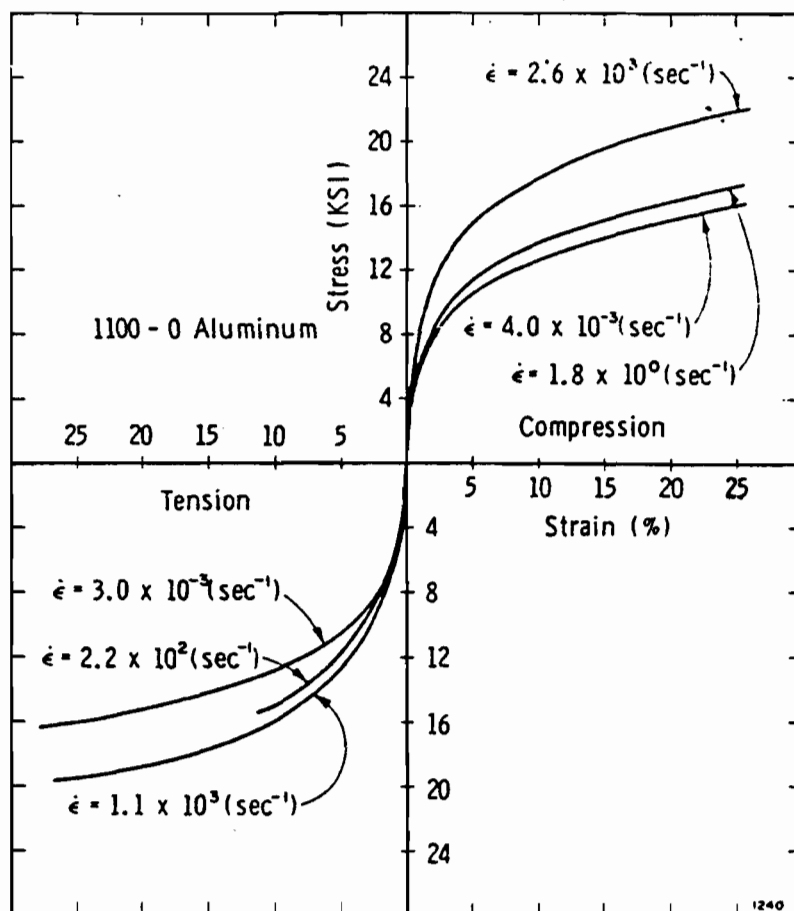
Fig. 2.5 Stress-Strain Curves for 1100-0 Aluminum in Tension and Compression[7]
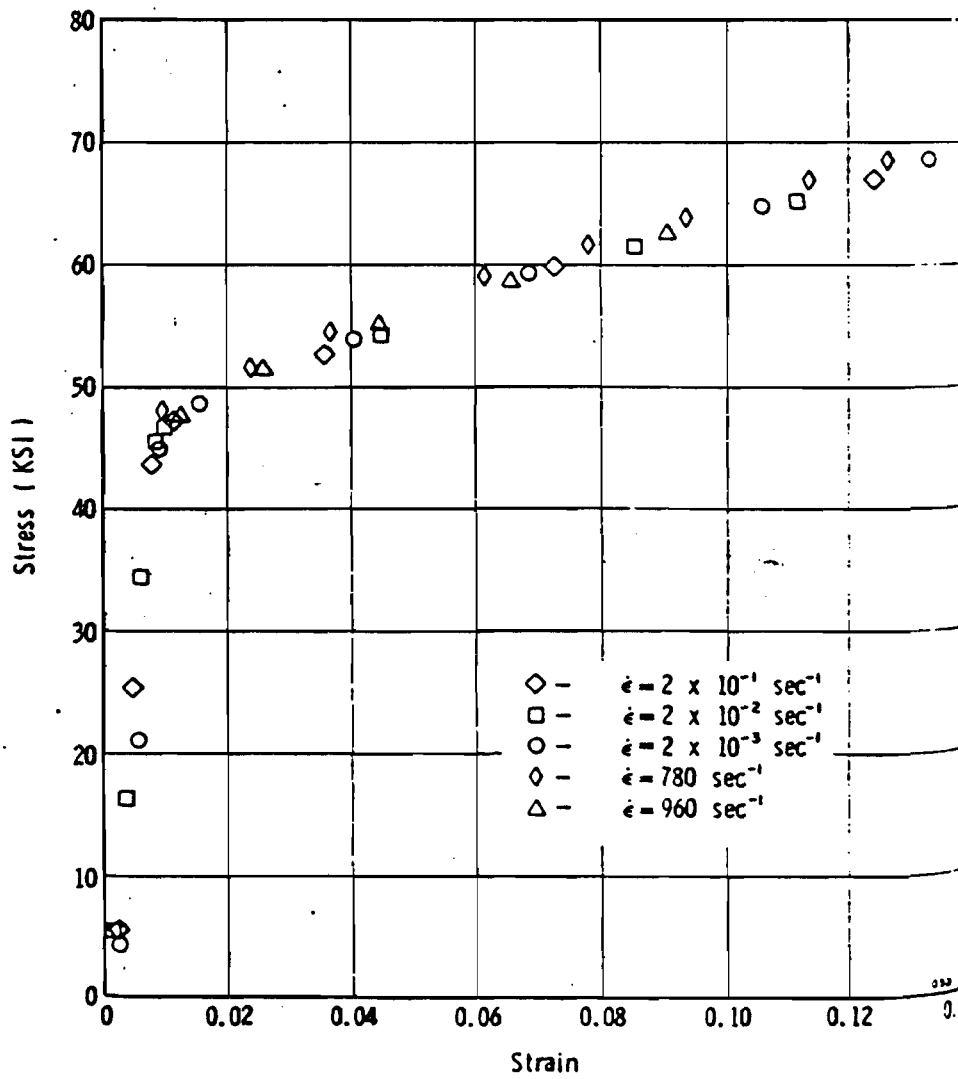
Fig. 2.6 Stress-Strain Curves for 6061-T6 Aluminum in Compression
at Several Strain Rates[7]
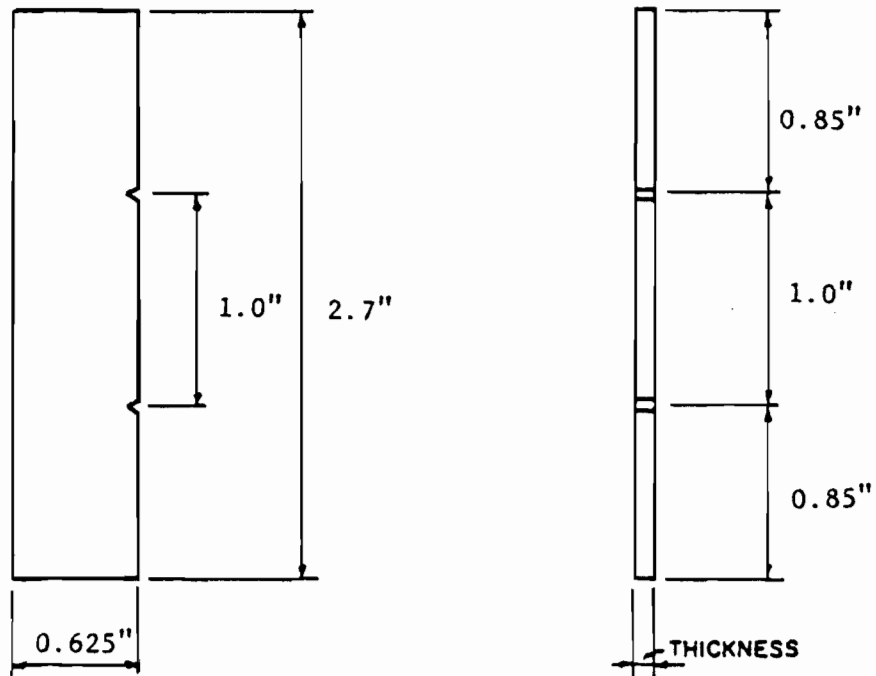
Fig. 3.1 Nominal Dimensions of Compression Coupons Used for All
Sheet Steels
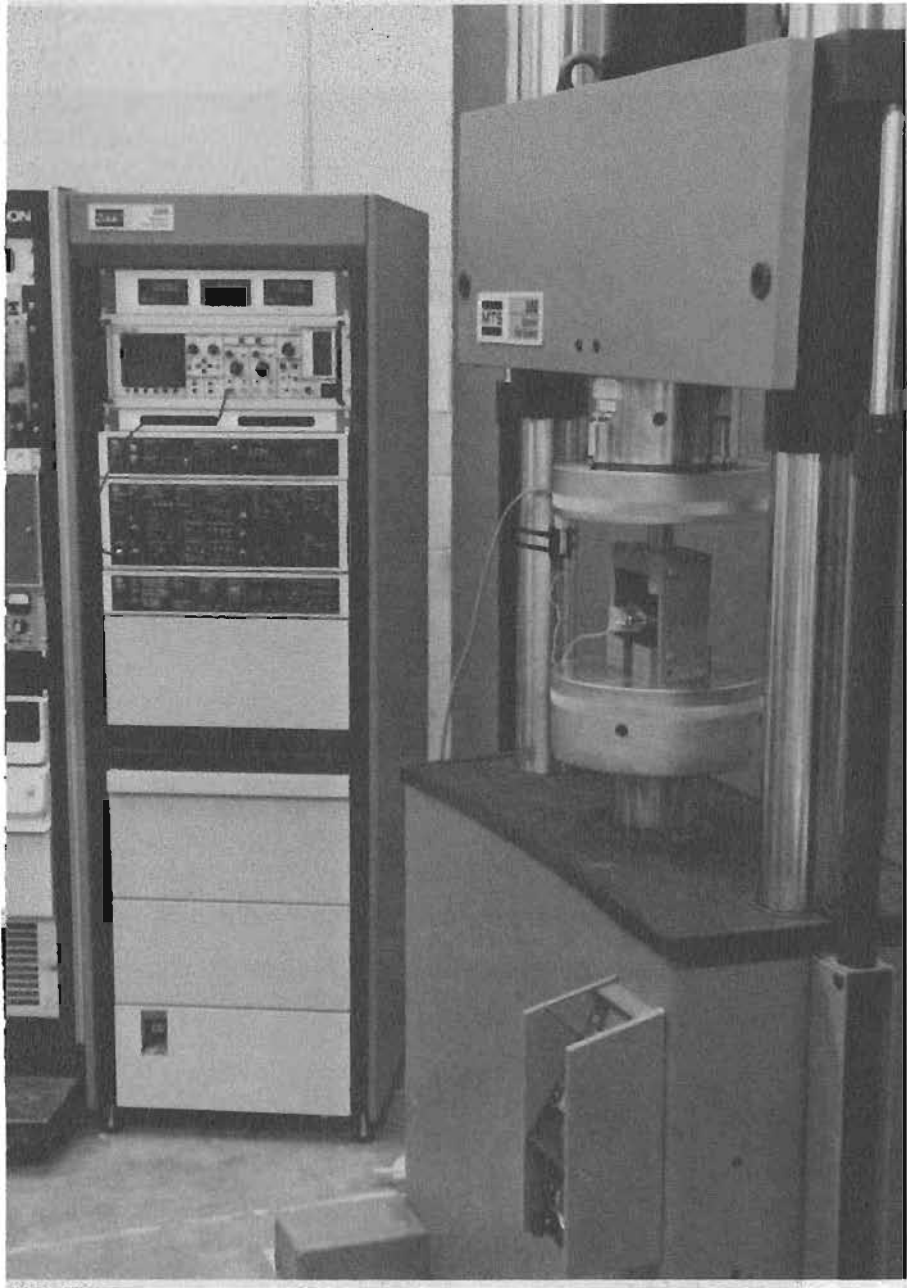
Fig. 3.2 MTS 880 Material Test System Used for Compression Tests

Fig. 3.3 MTS Load Frame, MTS Controller, CAMAC Data Acquisition
System, and Data General Graphic Display Terminal Used
for Compression Tests
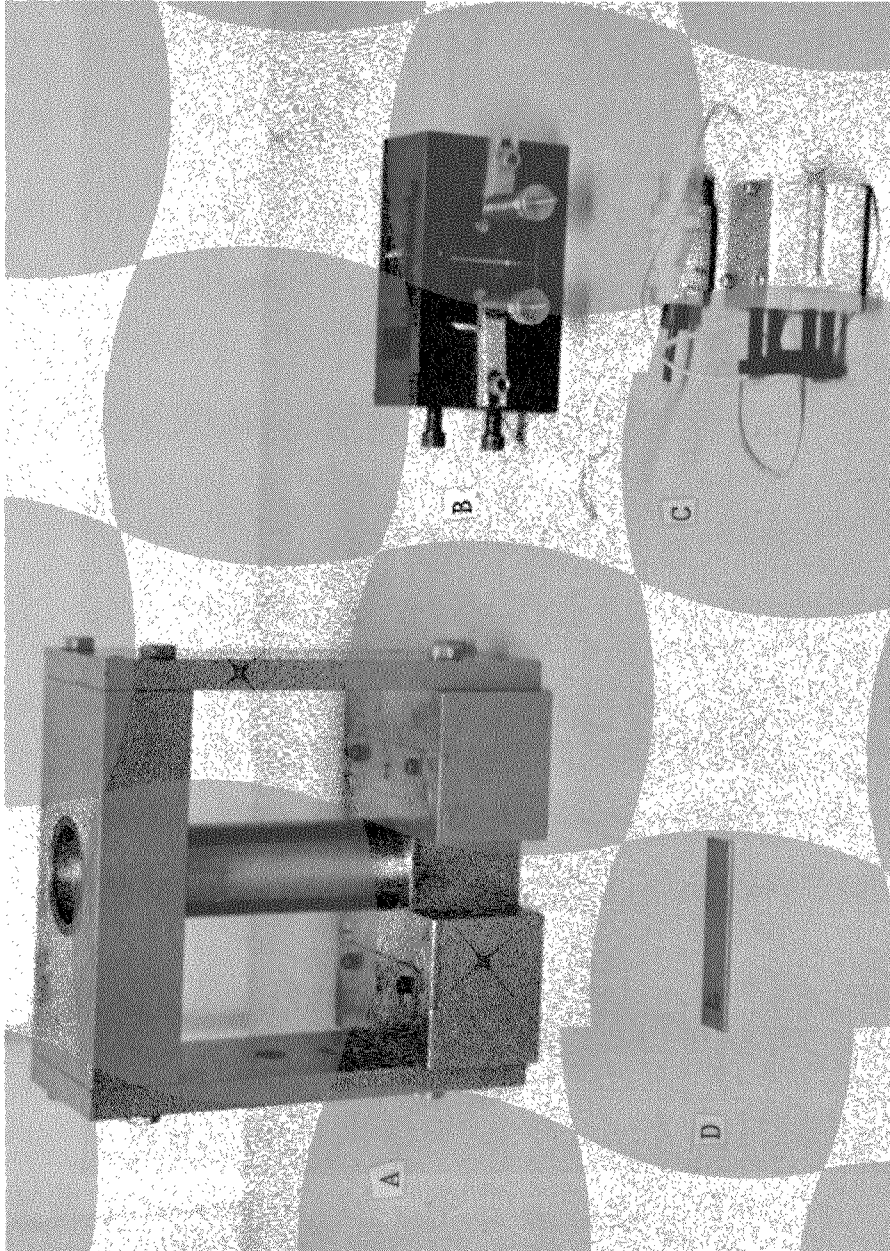
Fig. 3.4 Compression Subpress, Jig, Compressometer, and Test Specimen
Used for Compression Tests

A- Compression Subpress   C- MTS Compressometer
B- Compression Jig   D- Test Specimen
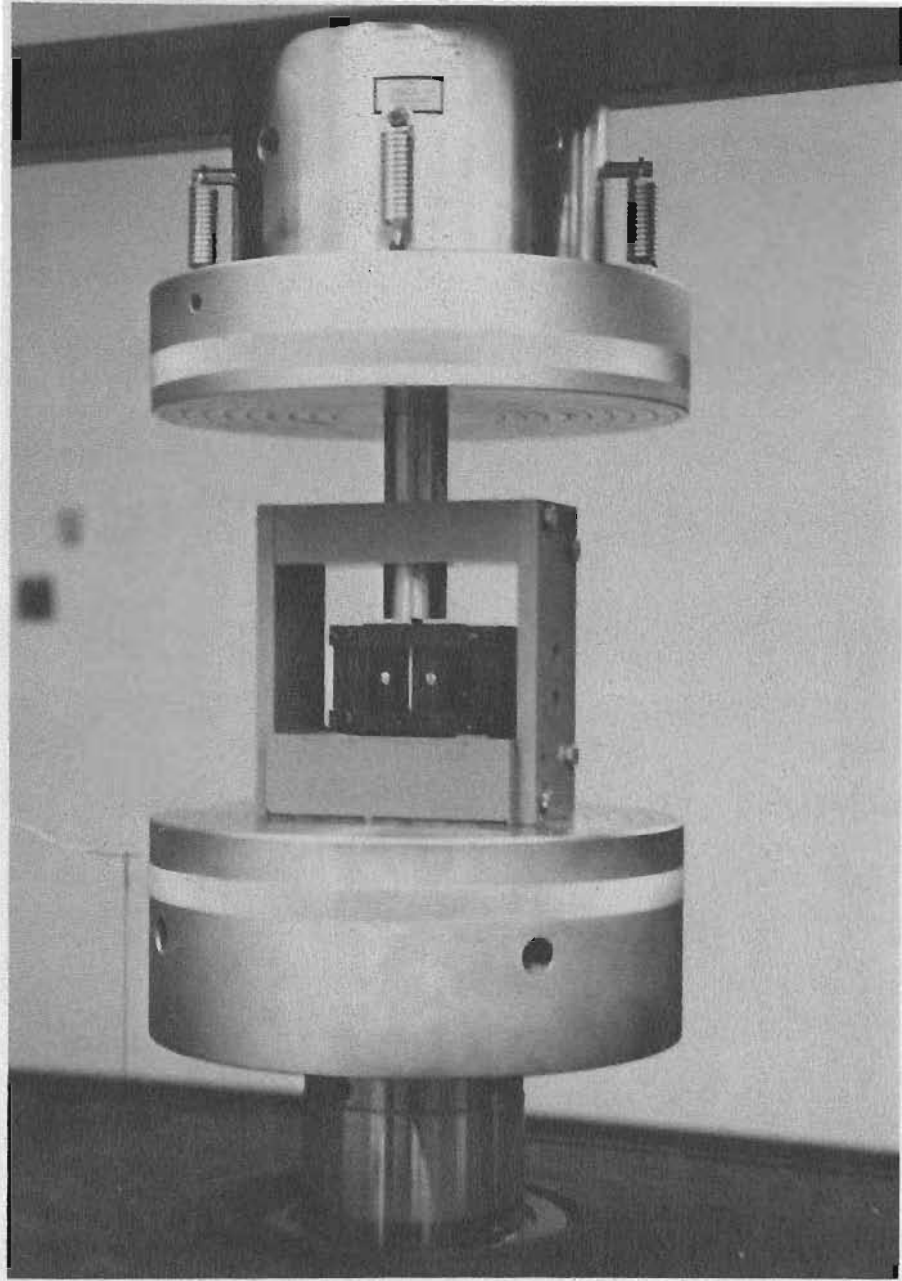
Fig. 3.5a Assembly of Compression Subpress, Jig, and Compressometer
(Front View)
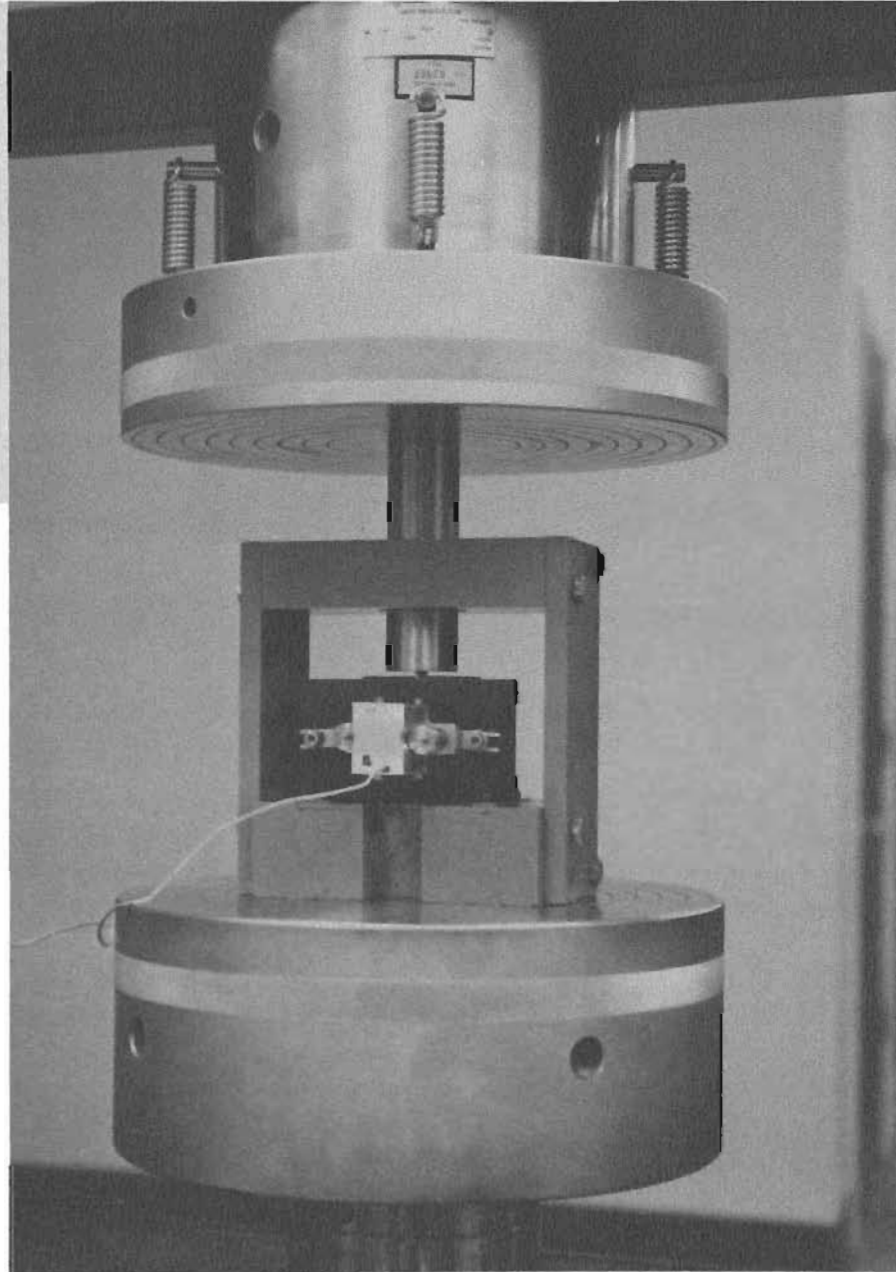
Fig. 3.5b Assembly of Compression Subpress, Jig, and Compressometer
(Back View)
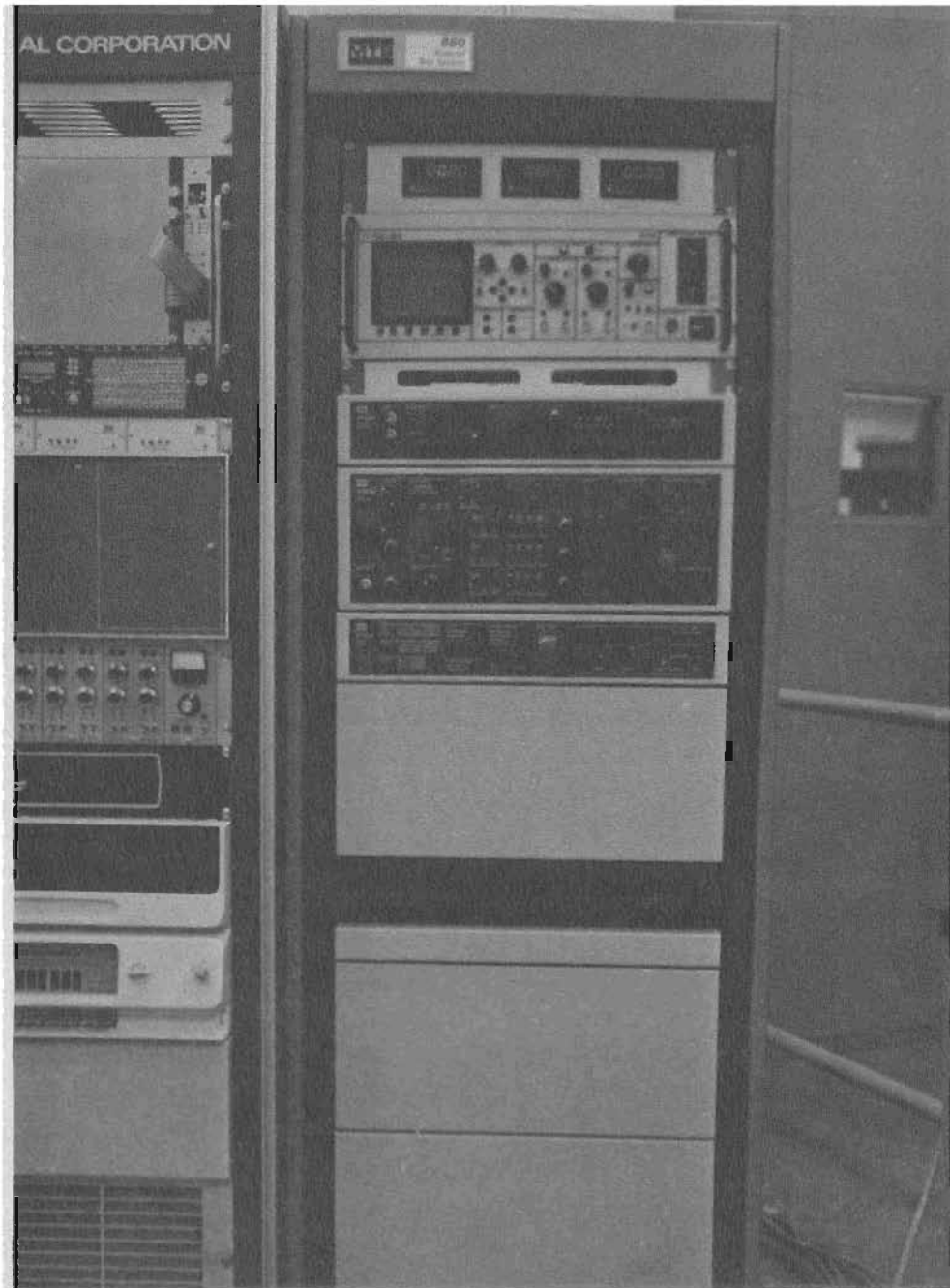
Fig. 3.6 MTS 880 Test Controller and Function Generator
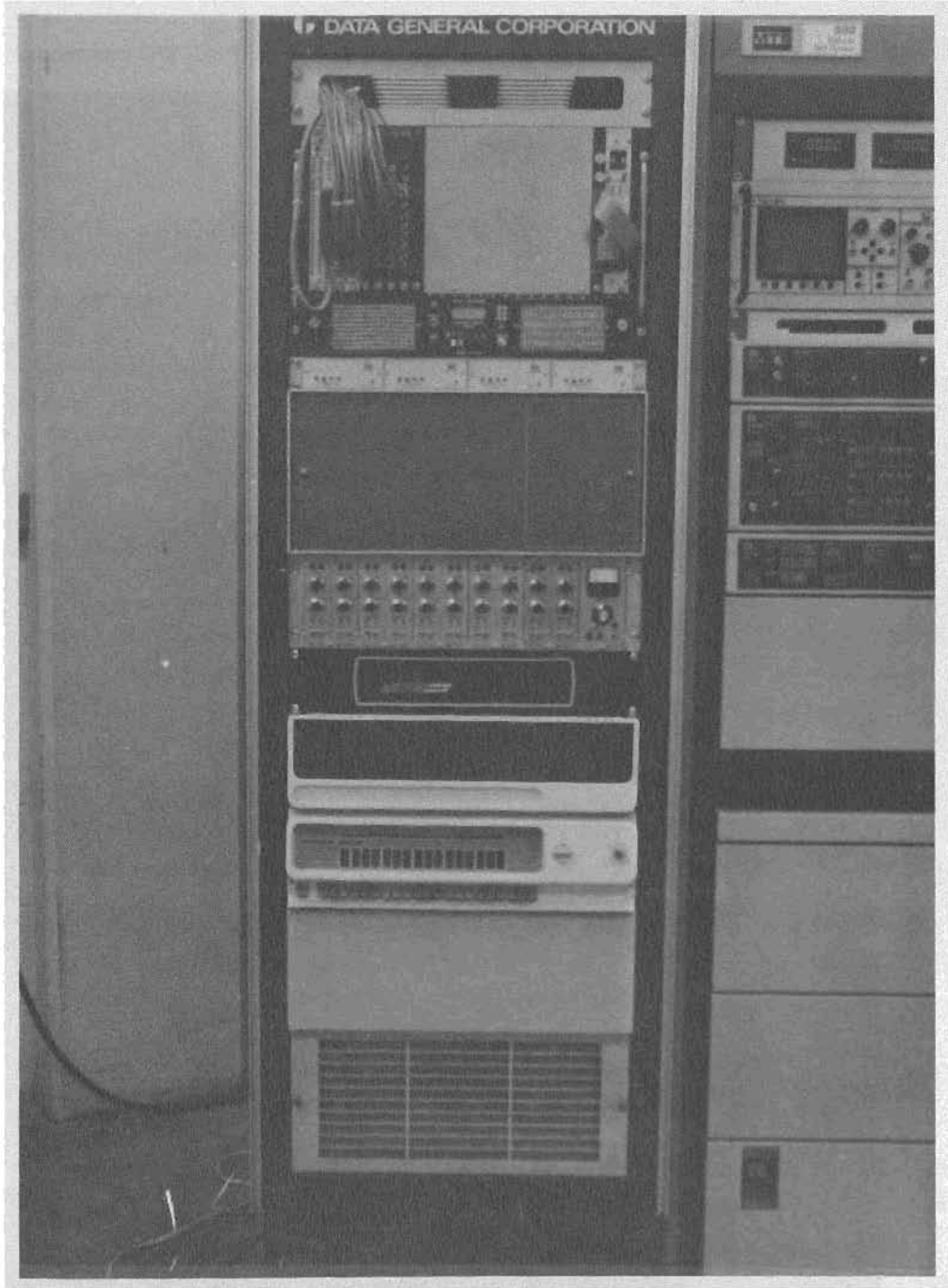
Fig. 3.7 Data Acquisition System
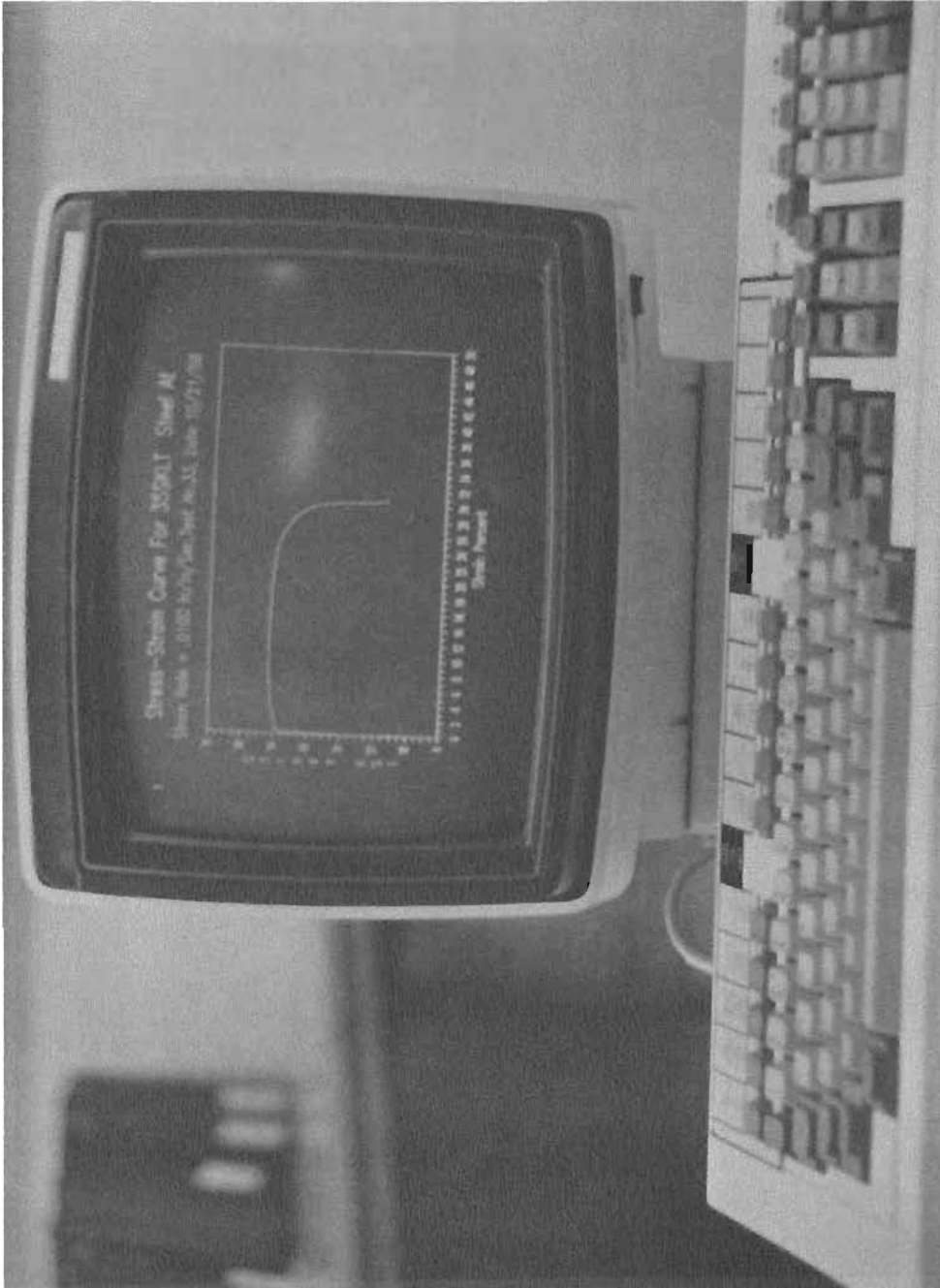
Fig. 3.8 Data General Graphic Display Terminal
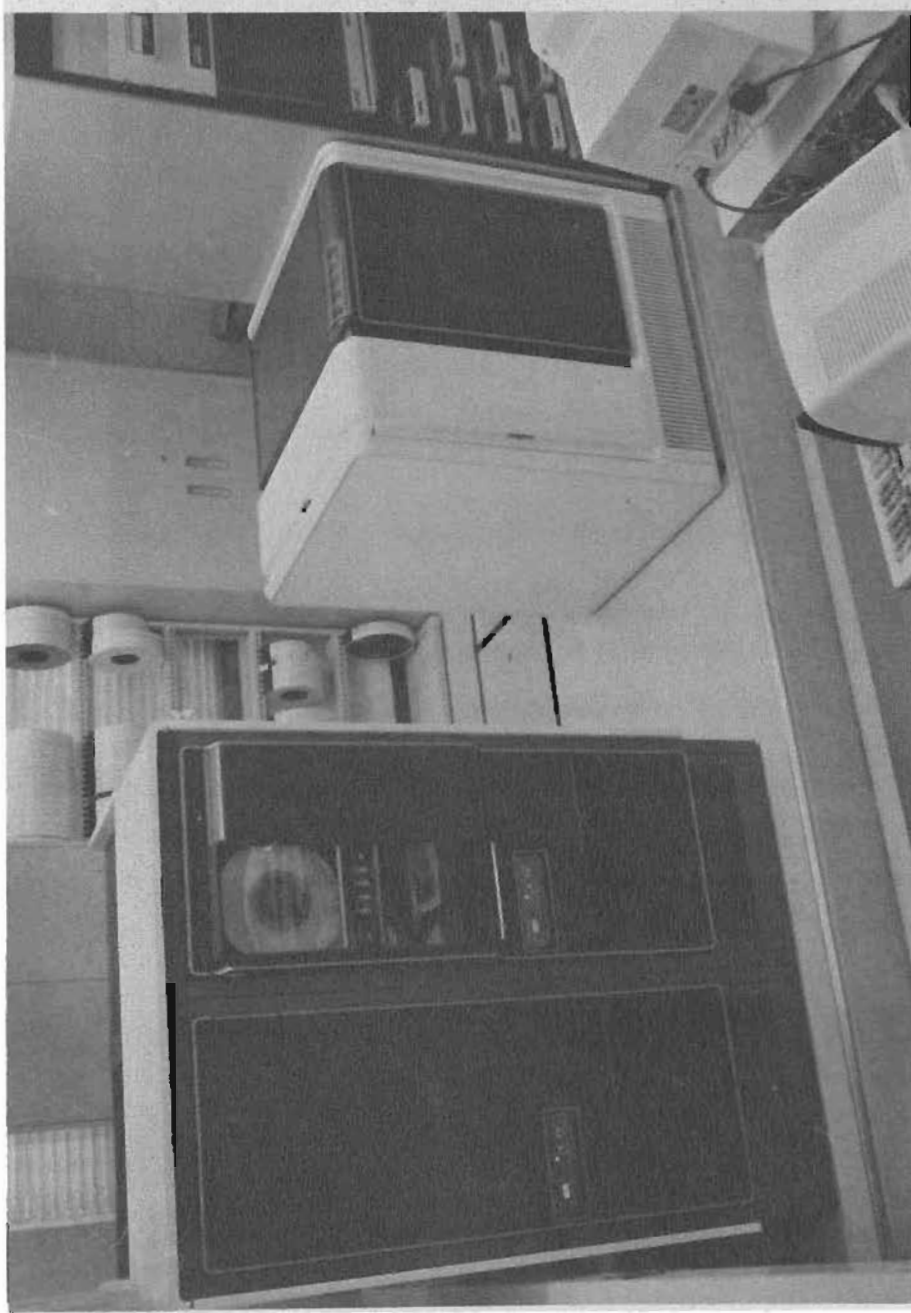
Fig. 3.9 Data General MV-10000 Mini Computer

Fig. 3.10 IBM PS/2 Model 30 Personal Computer with IBM Color Plotter

Strain , in./in.
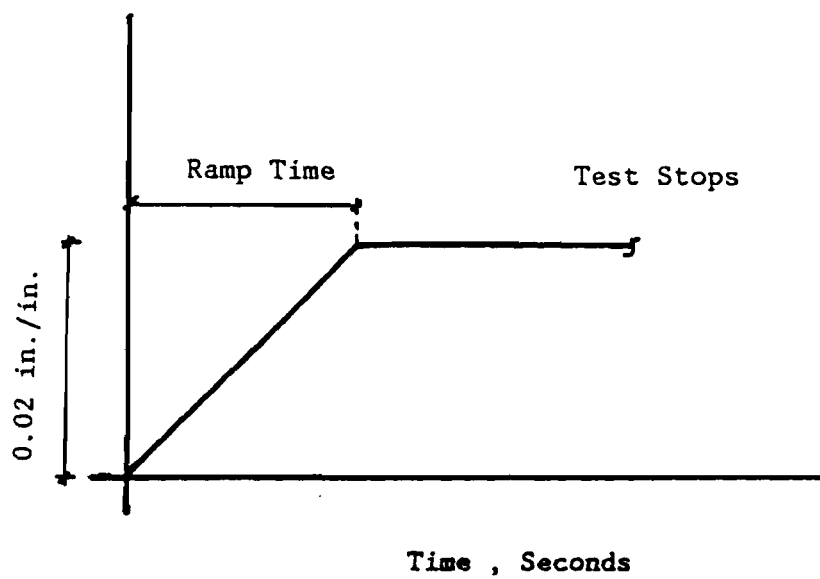
Fig. 3.11 Typical Function Generator Ramp Waveform
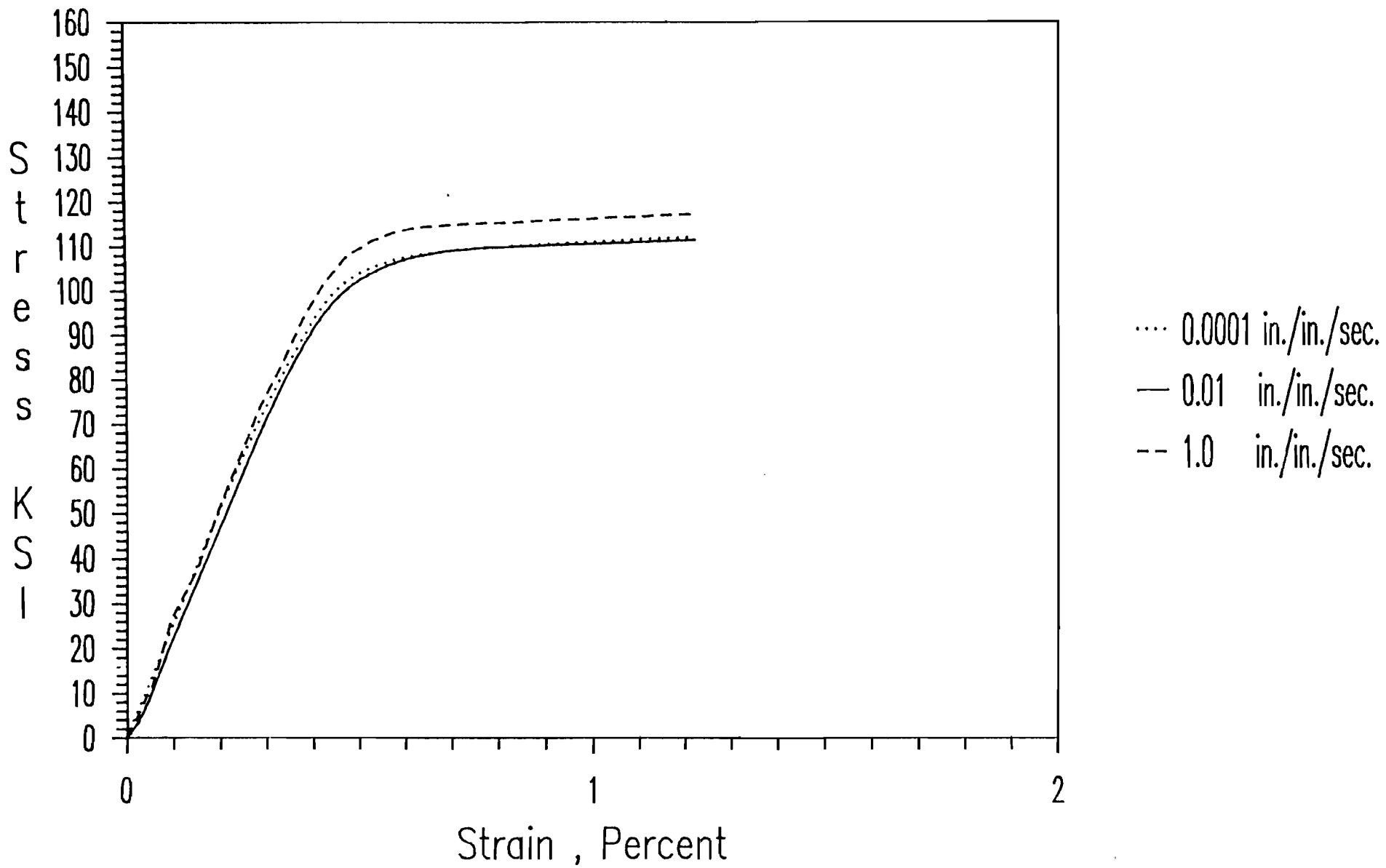
Fig. 3.12 Stress-Strain Curves for 100XF-LC Steel Under Different
Strain Rates
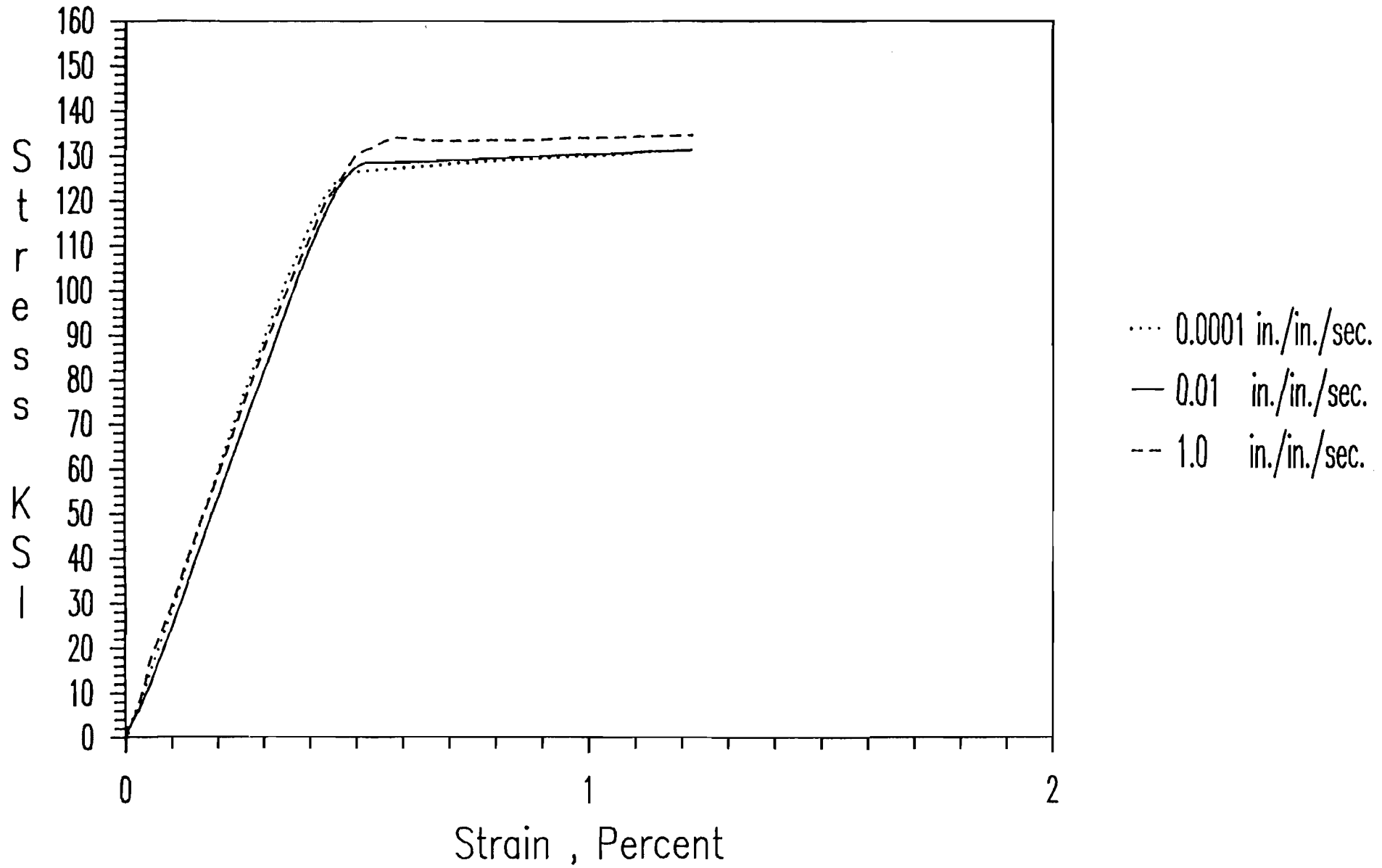
Fig. 3.13 Stress-Strain Curves for 100XF-TC Steel Under Different
Strain Rates
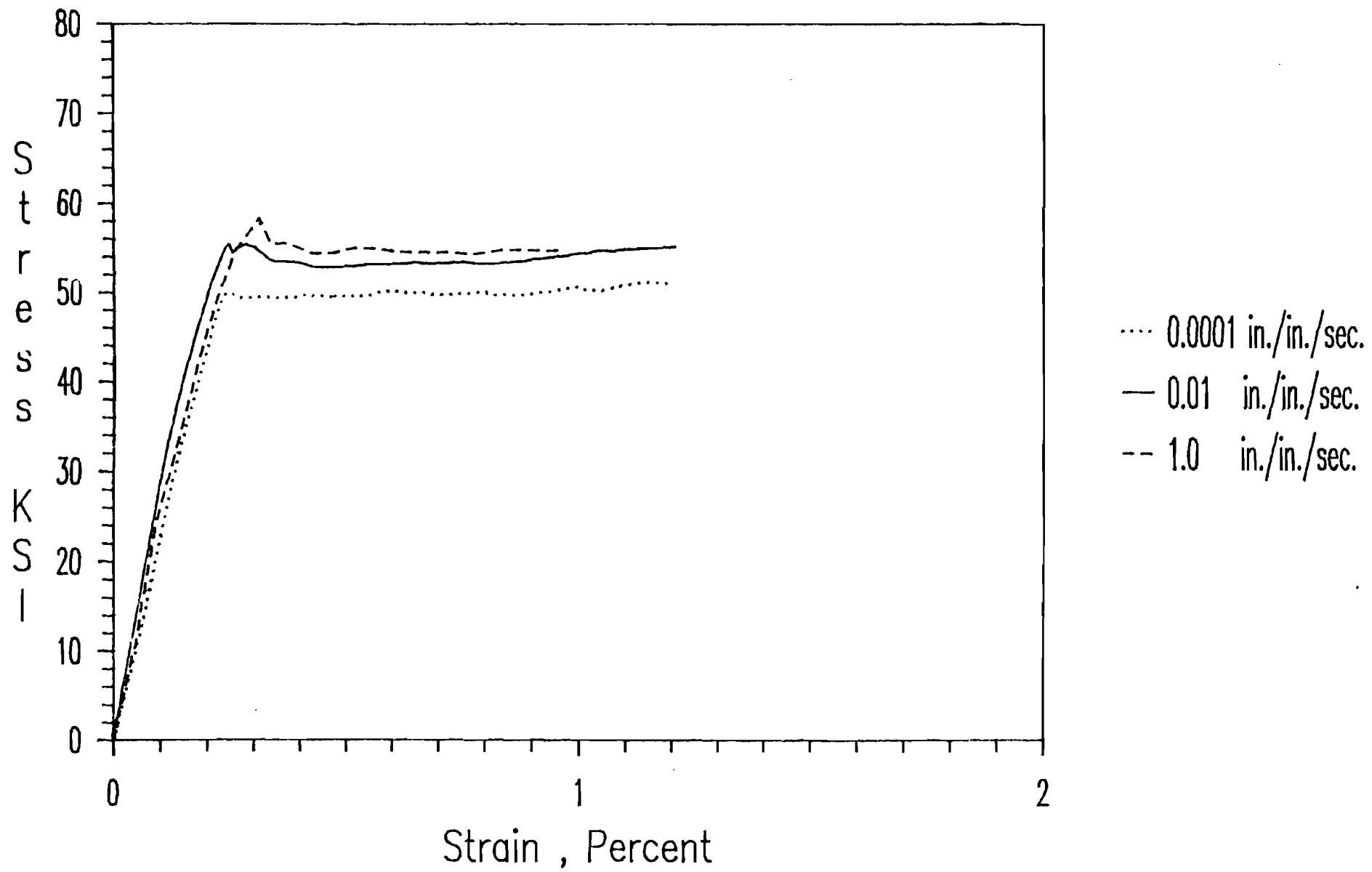
Fig. 3.14 Stress-Strain Curves for 50XF-LC Steel Under Different
Strain Rates
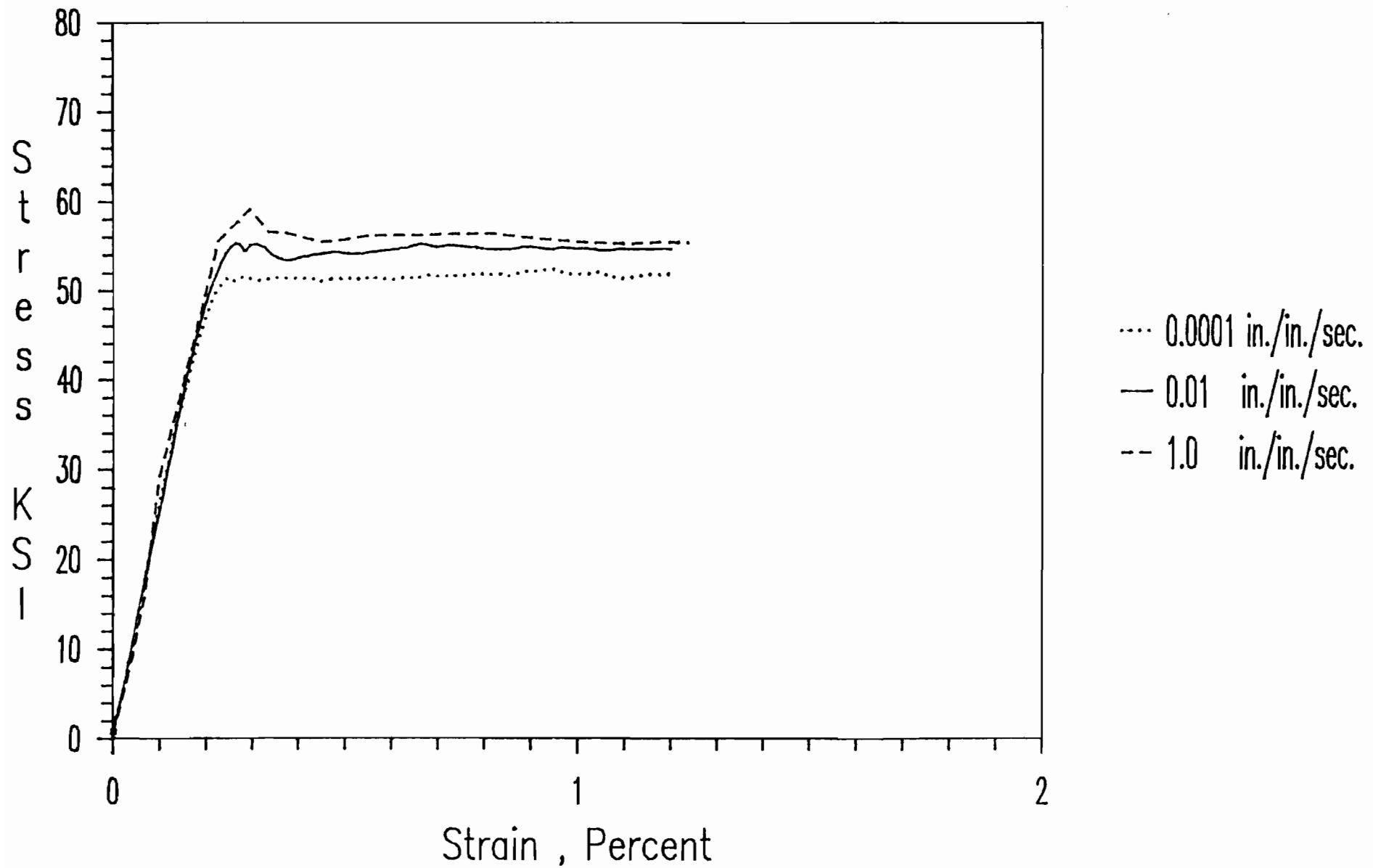
Fig. 3.15 Stress-Strain Curves for 50XF-TC Steel Under Different
Strain Rates
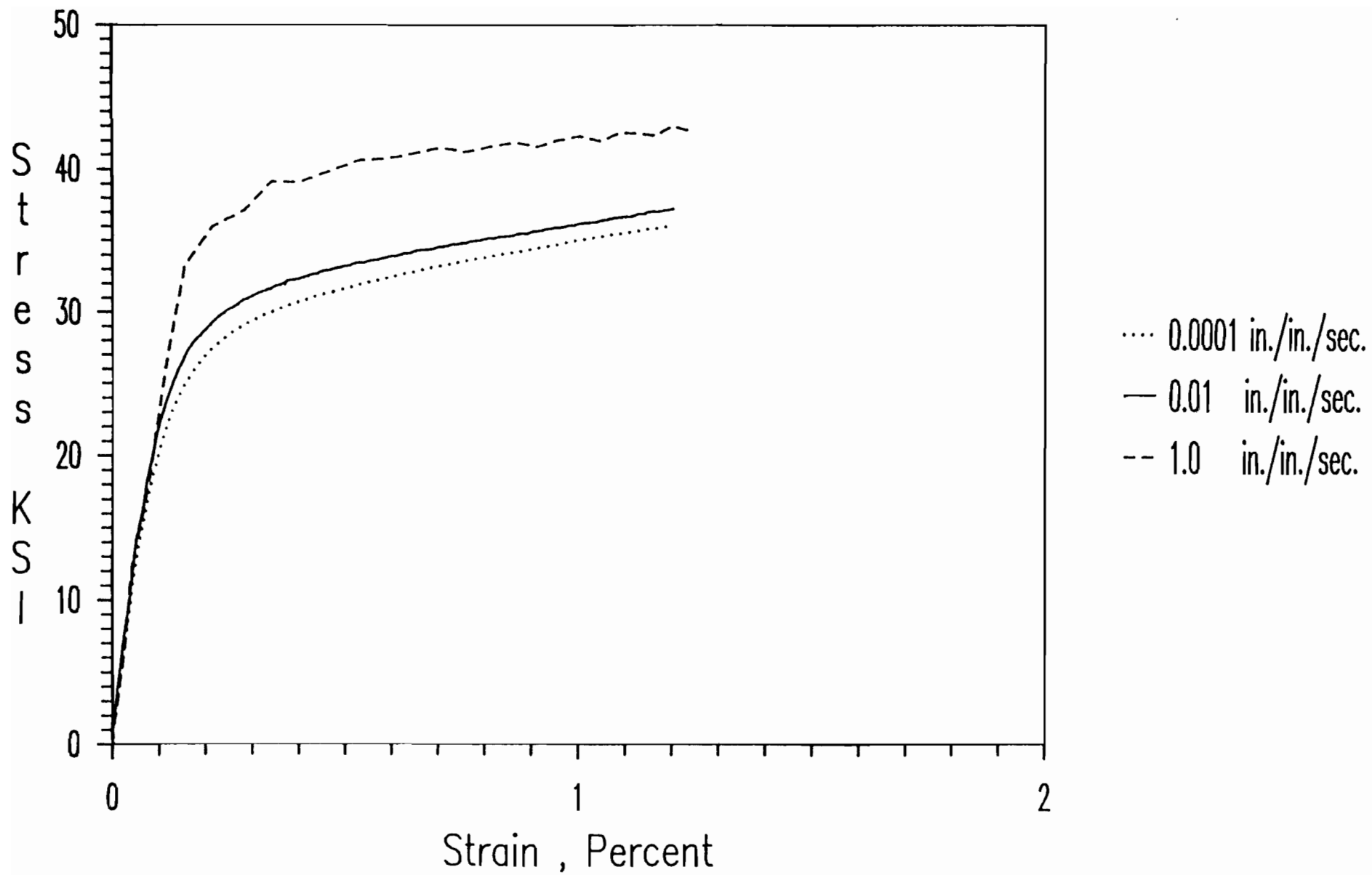
Fig. 3.16 Stress-Strain Curves for 35XF-LC Steel Under Different
Strain Rates
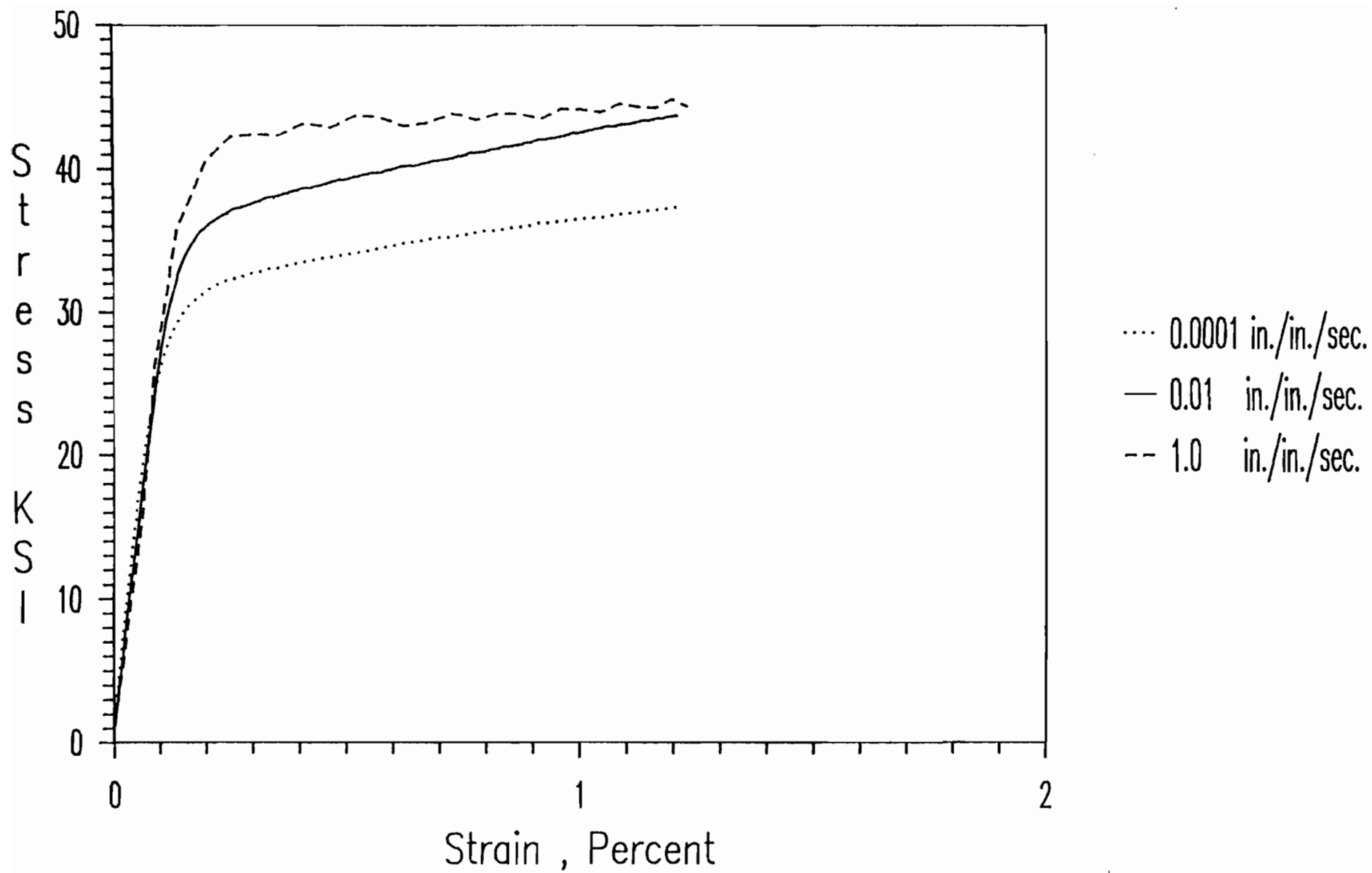
Fig. 3.17 Stress-Strain Curves for 35XF-TC Steel Under Different
Strain Rates
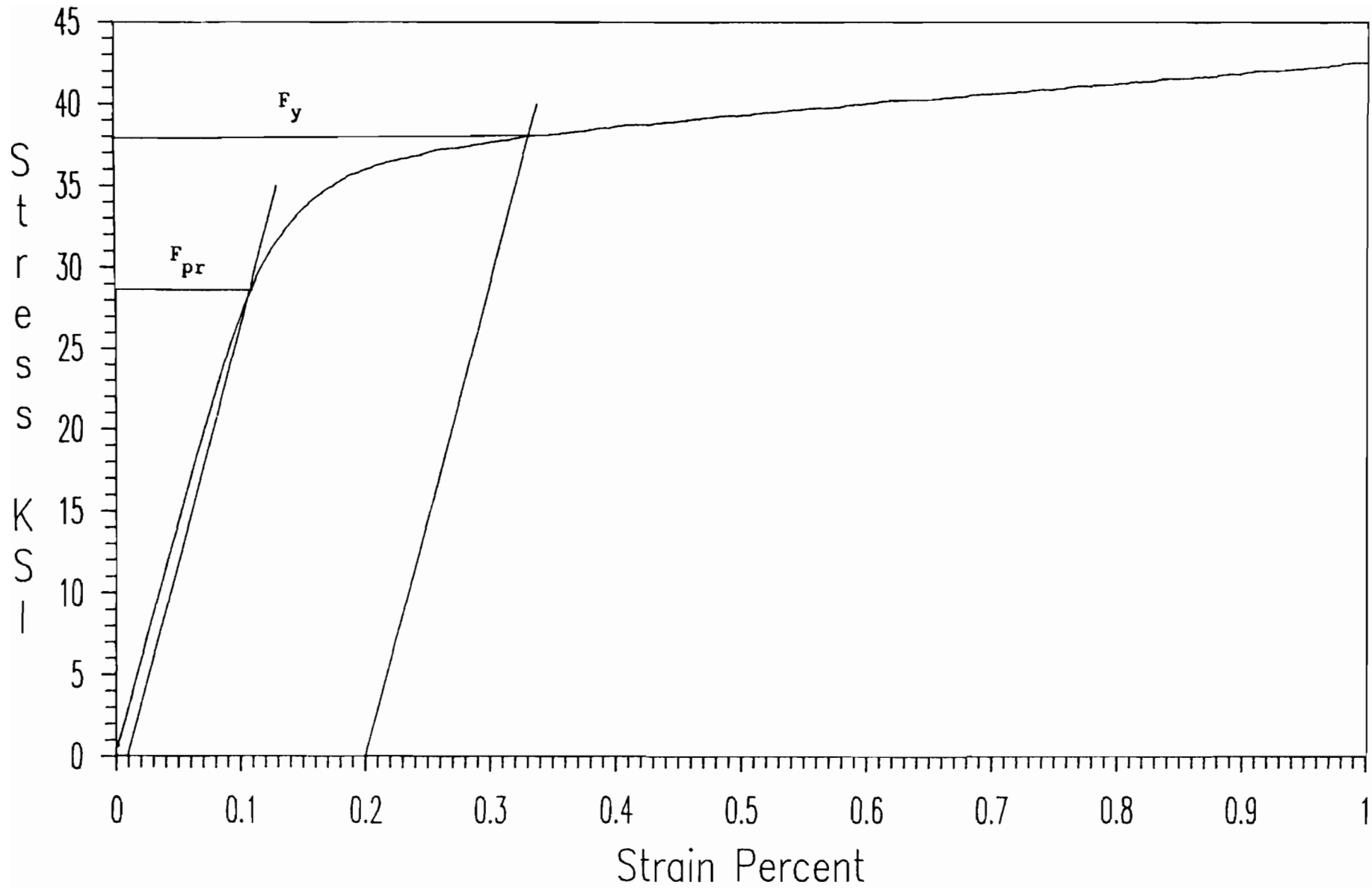
Fig. 3.18 Stress-Strain Curve for Determination of Mechanical
Properties of 35XF-TC-4
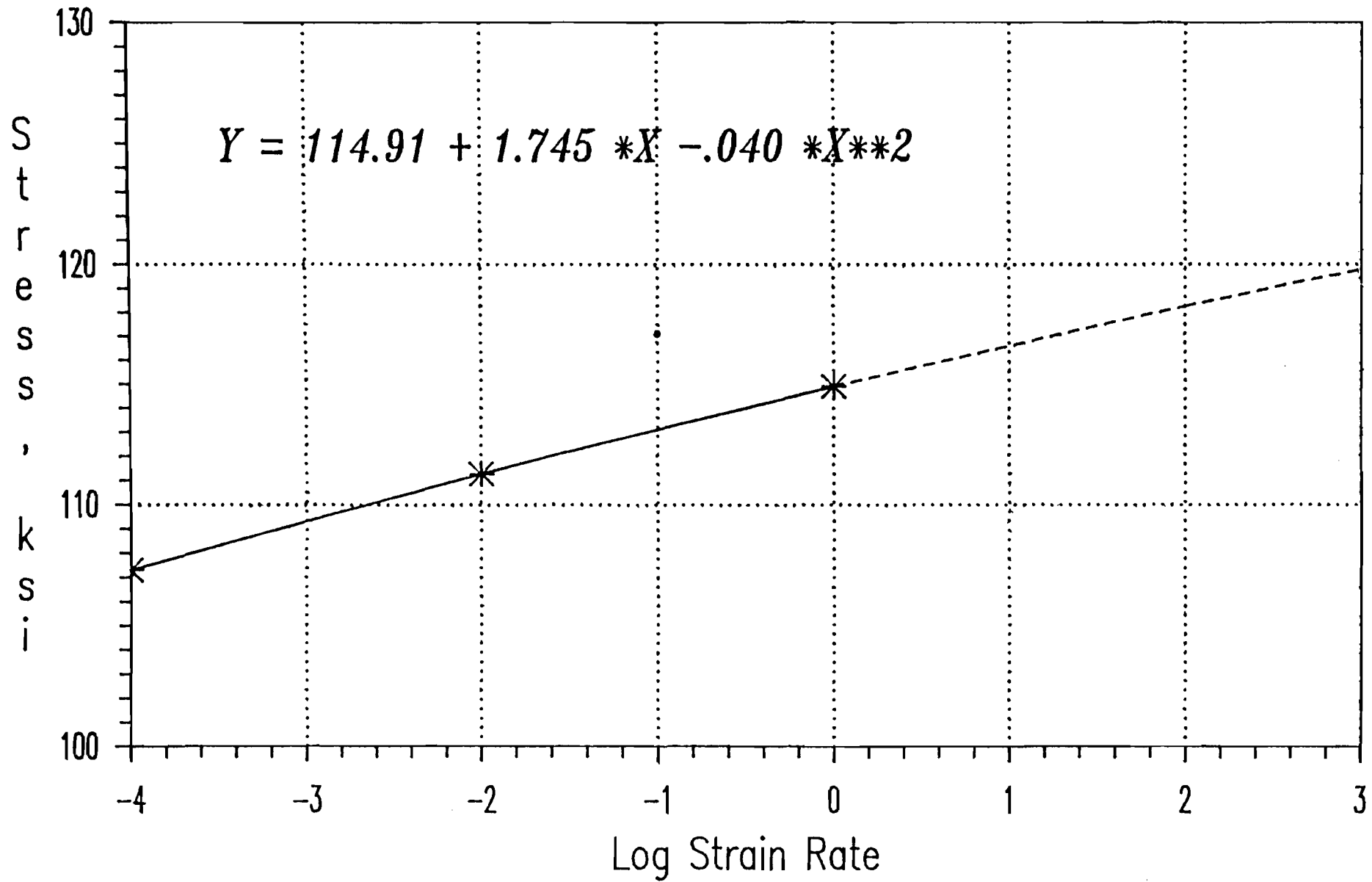
Fig. 3.19 Compressive Yield Stress vs Logarithmic Strain Rate Curve
for 100XF-LC Steel

$$Y = 131.73 + 3.552 * X + .384 * X**2$$
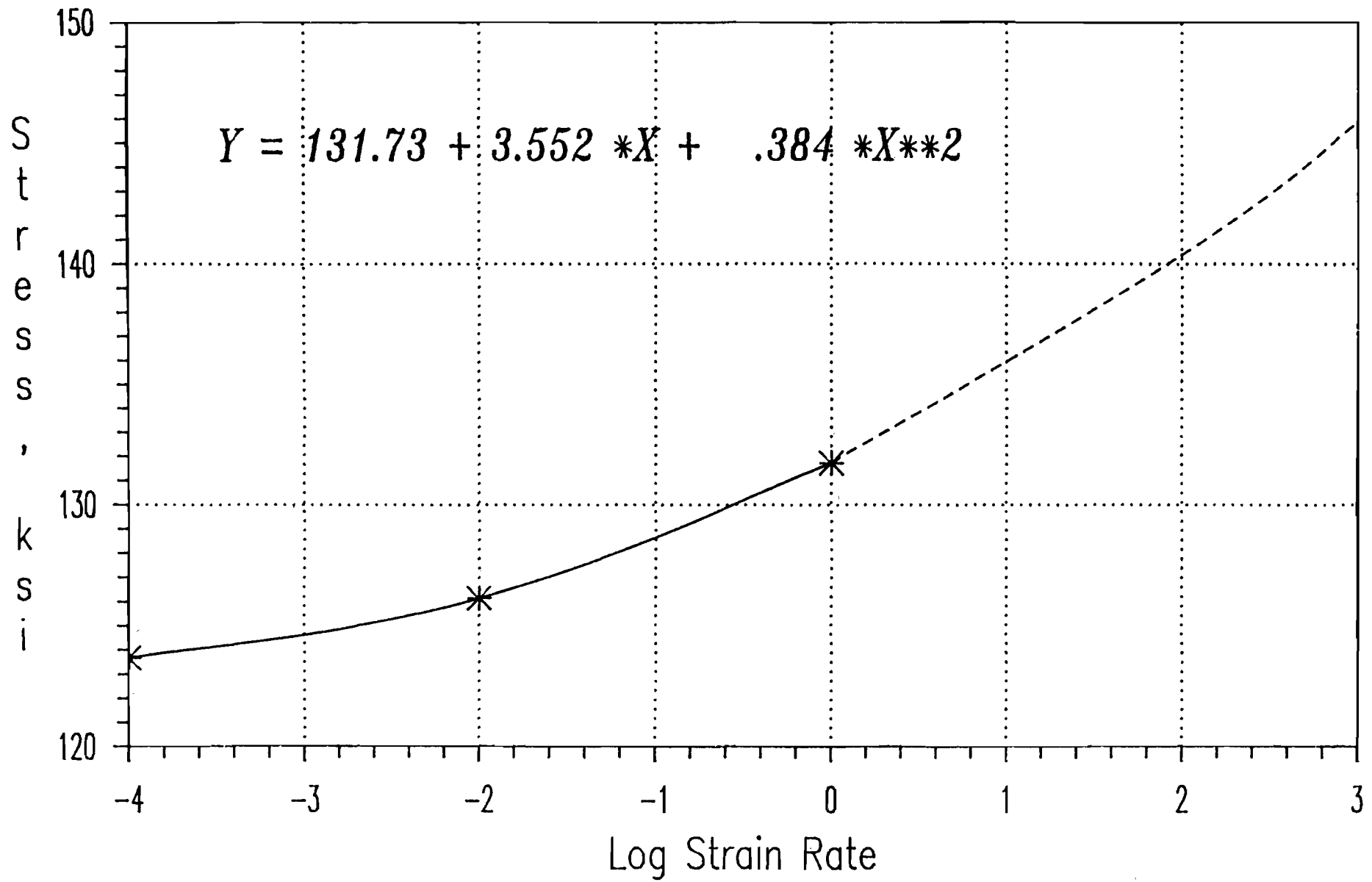
Fig. 3.20 Compressive Yield Stress vs Logarithmic Strain Rate Curve
for 100XF-TC Steel

$$Y = 54.79 + 1.002 *X + -.069 *X**2$$

Stress, ksi
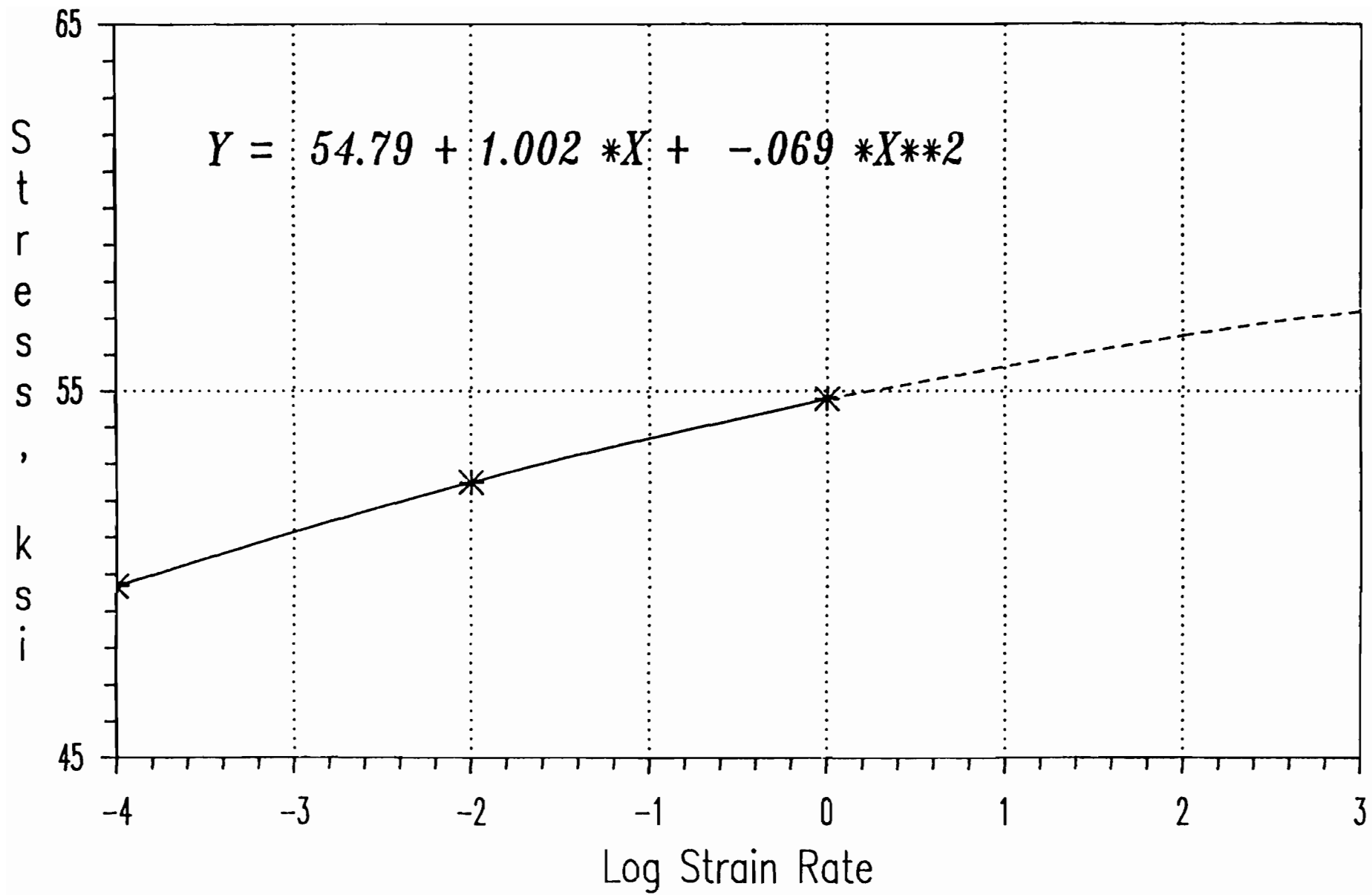
Log Strain Rate

Fig. 3.21 Compressive Yield Stress vs Logarithmic Strain Rate Curve
for 50XF-LC Steel

$$Y = 55.54 + 1.025 * X + -.023 * X**2$$
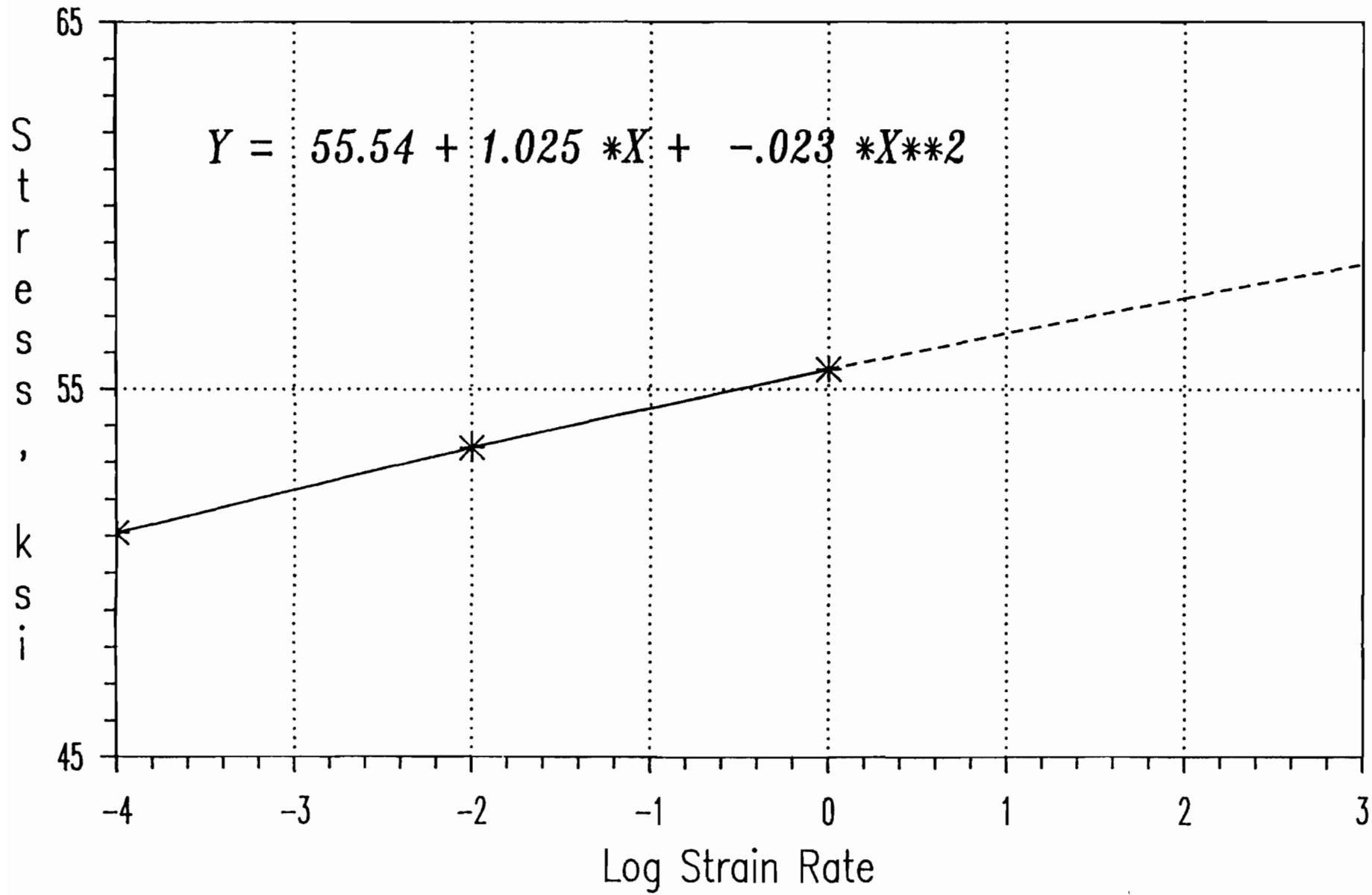
Fig. 3.22 Compressive Yield Stress vs Logarithmic Strain Rate Curve
for 50XF-TC Steel

$$Y = 36.91 + 3.208 * X + .356 * X**2$$
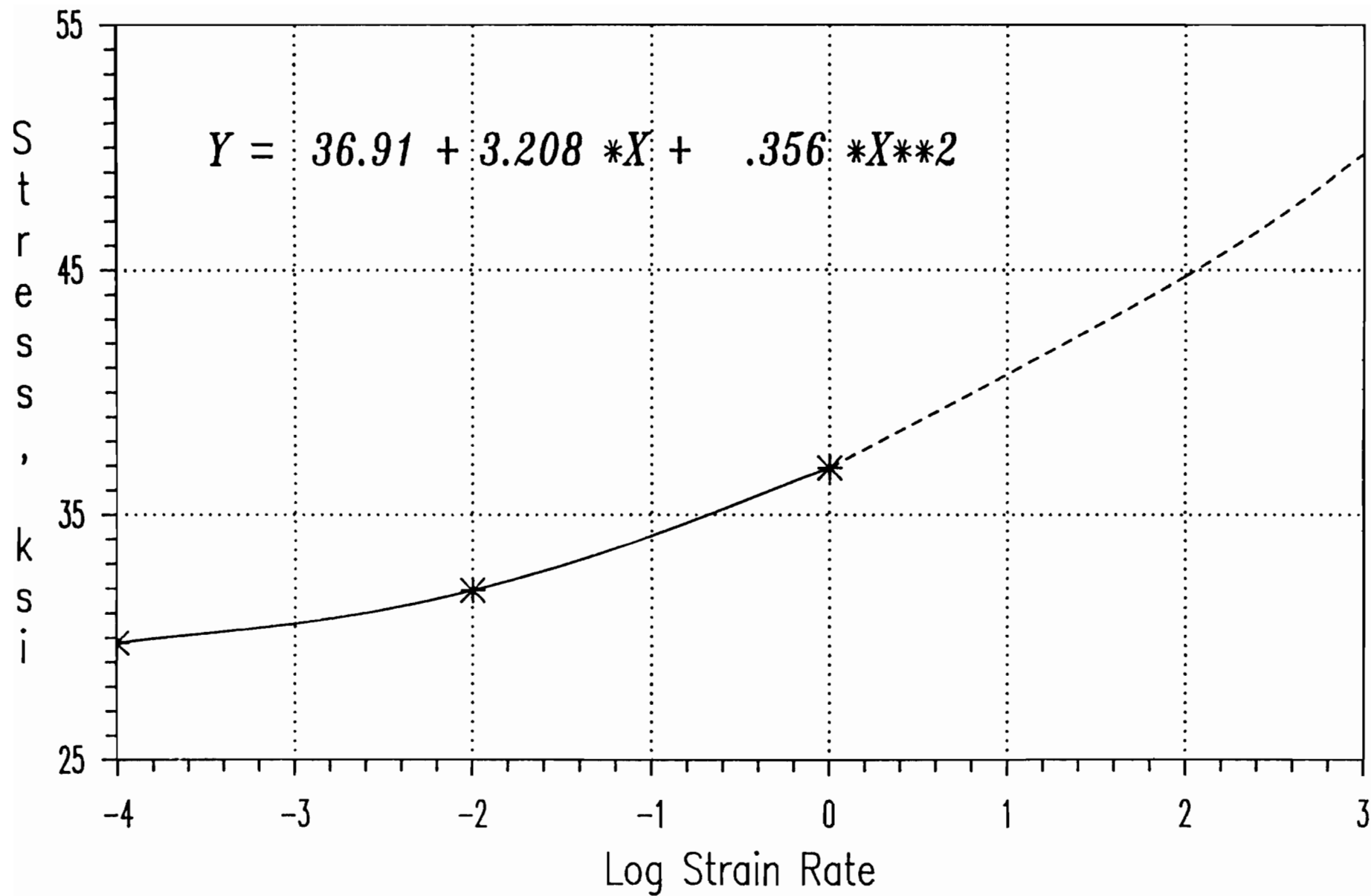
Fig. 3.23 Compressive Yield Stress vs Logarithmic Strain Rate Curve
for 35XF-LC Steel

$$Y = 43.45 + 4.052 *X + .336 *X**2$$
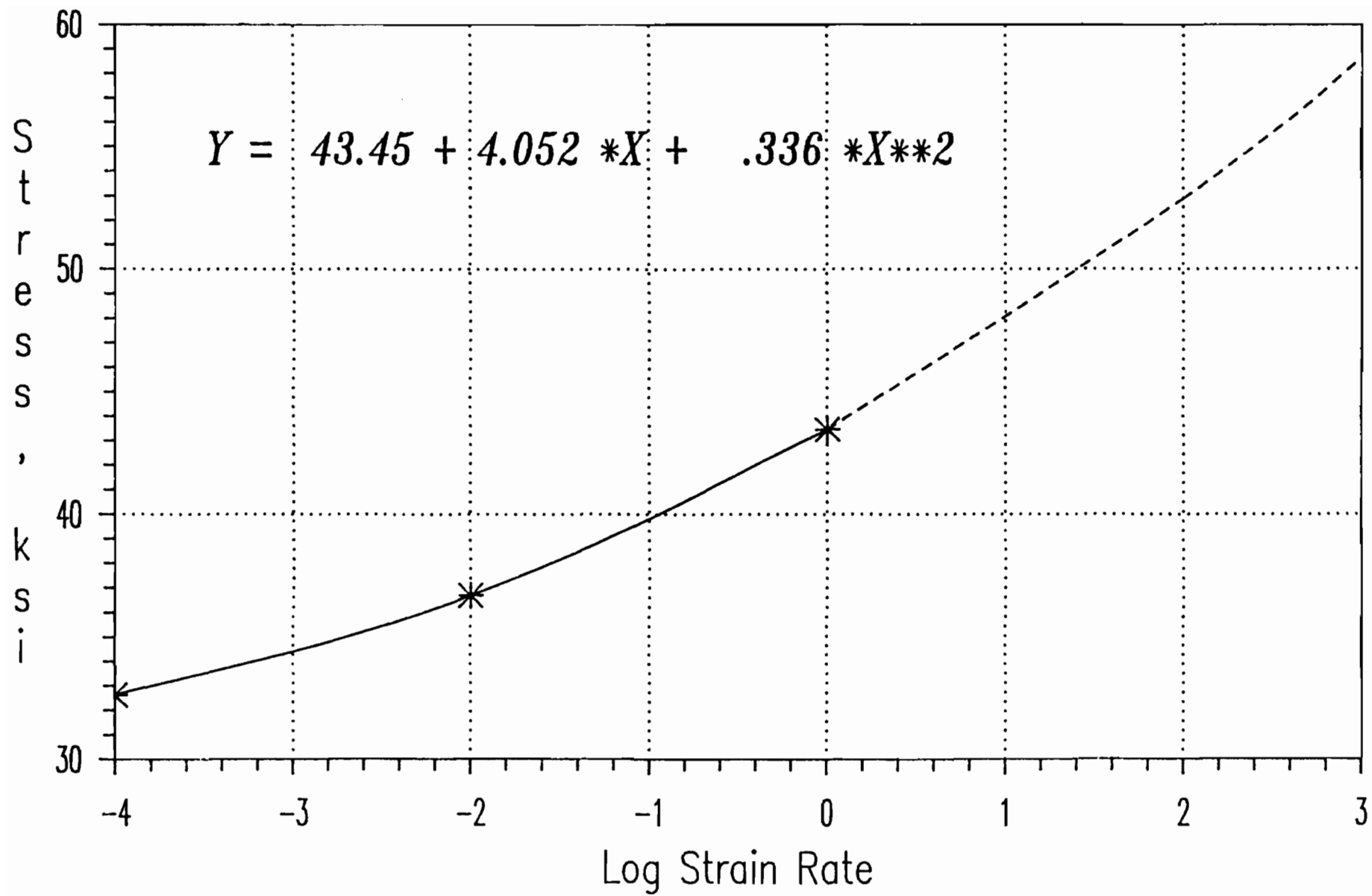
Fig. 3.24 Compressive Yield Stress vs Logarithmic Strain Rate Curve
for 35XF-TC Steel

$$Y = 128.91 + 1.945 * X + .195 * X**2$$
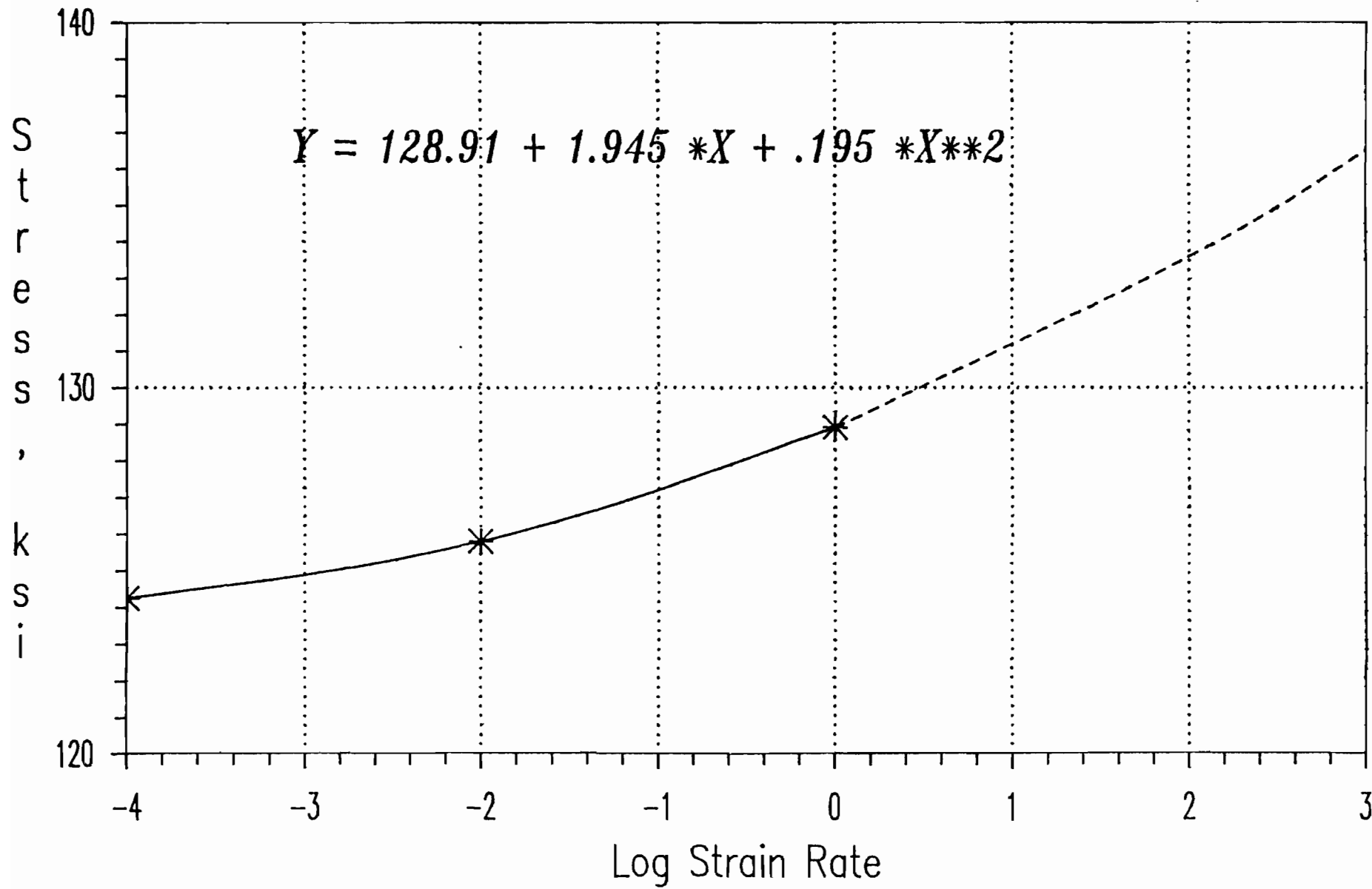
Fig. 4.1 Tensile Yield Stress vs Logarithmic Strain Rate Curve
for 100XF-LT, (Virgin Material)
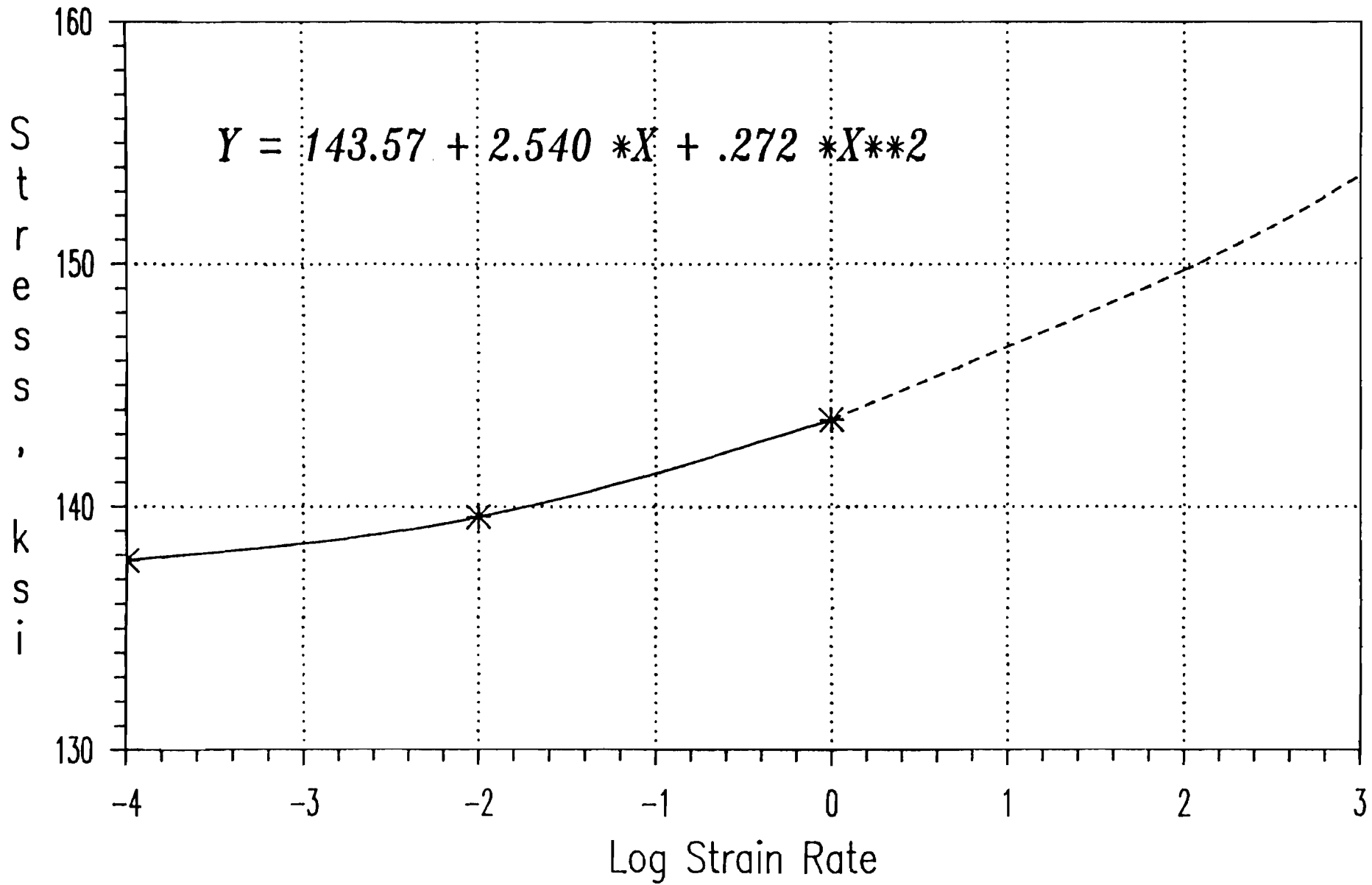
Fig. 4.2 Tensile Yield Stress vs Logarithmic Strain Rate Curve
for 100XF-TT, (Virgin Material)

$$Y = 54.66 + 1.770 *X + .120 *X**2$$
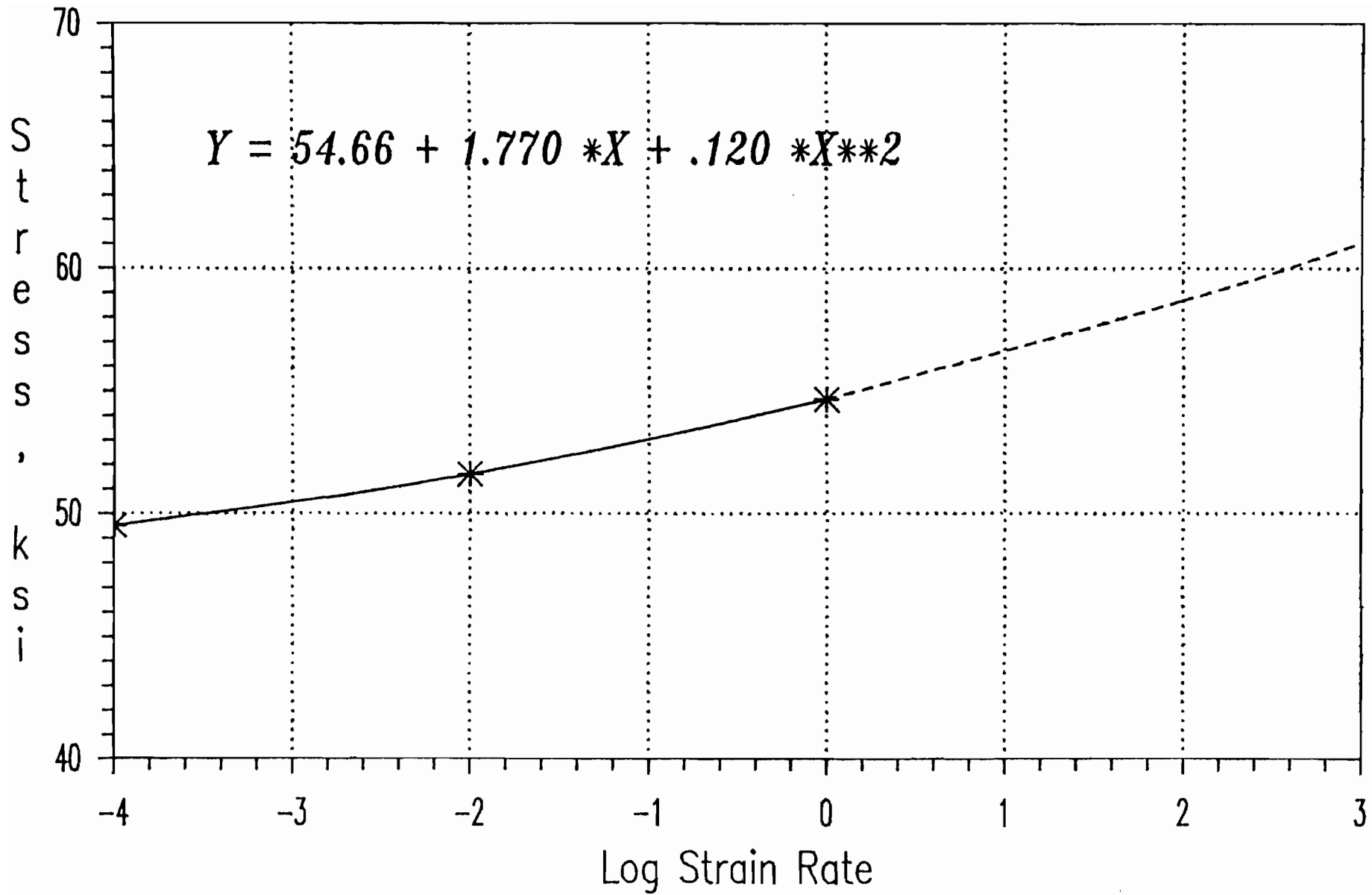
Fig. 4.3   Tensile Yield Stress vs Logarithmic Strain Rate Curve
for 50XF-LT, (Virgin Material)

$$Y = 62.67 + 2.433 *X + .216 *X**2$$
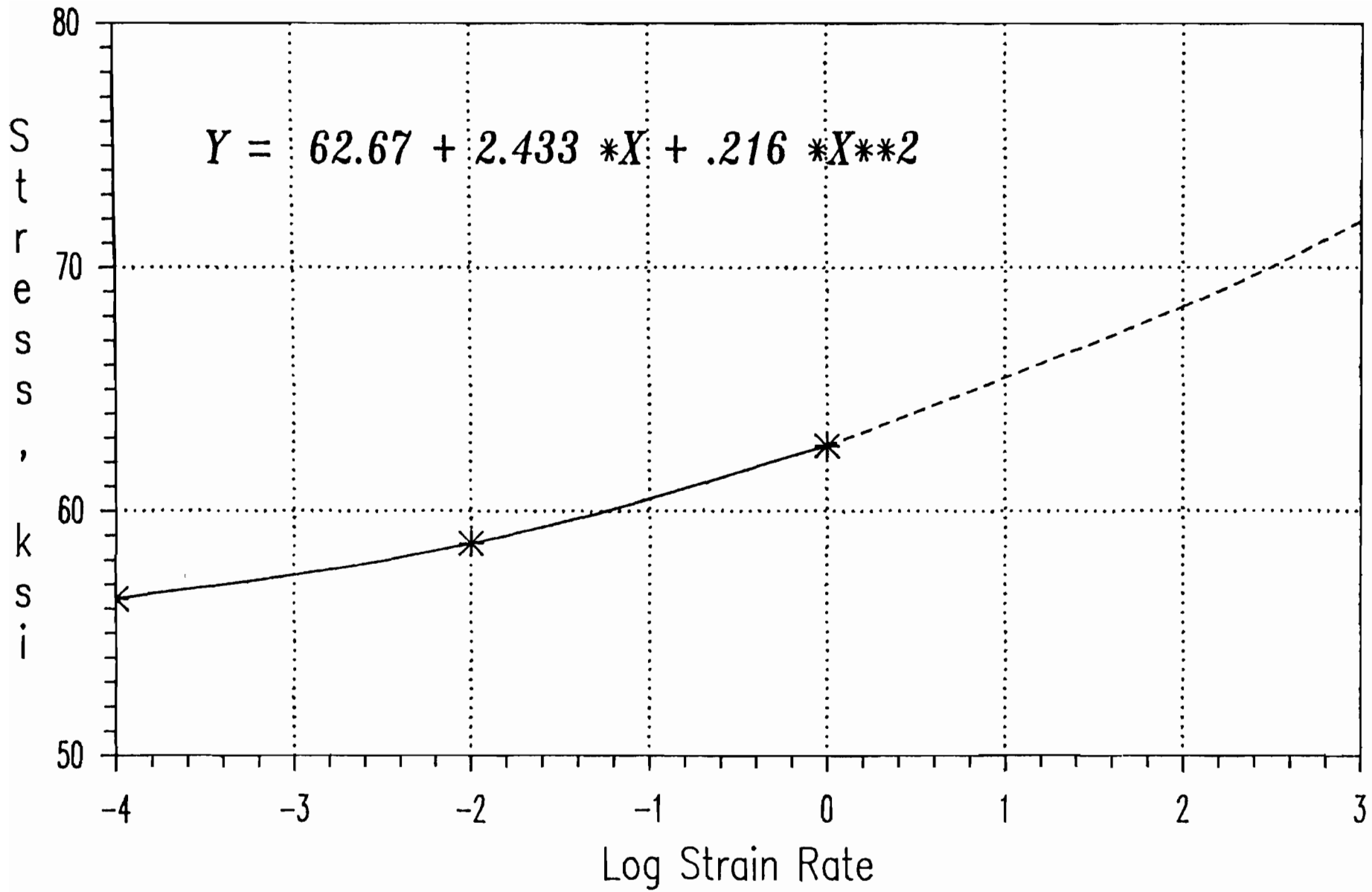
Fig. 4.4 Tensile Yield Stress vs Logarithmic Strain Rate Curve
for 50XF-LT, (2% Cold-Stretched, Non-Aged Material)
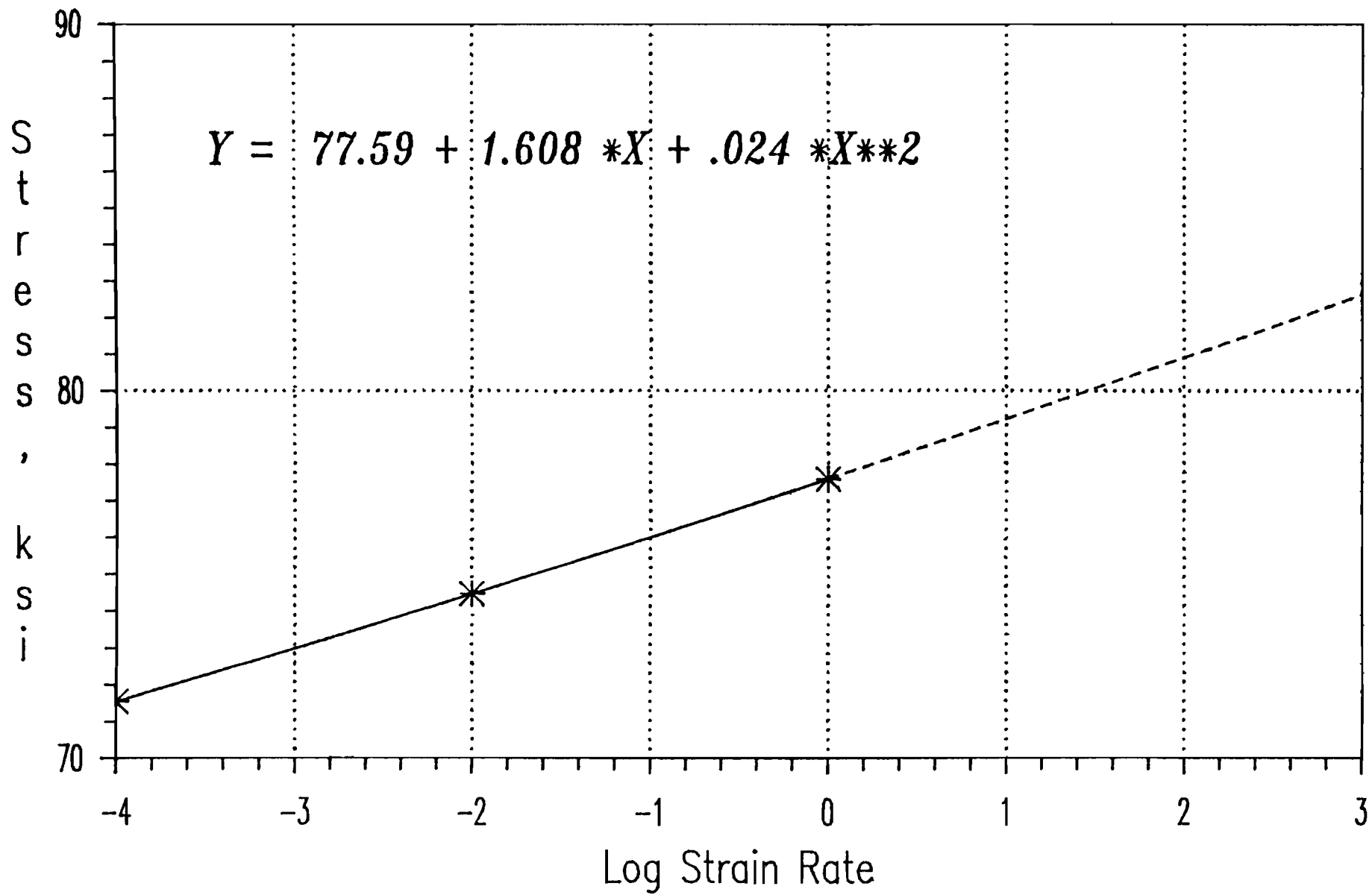
Fig. 4.5 Tensile Yield Stress vs Logarithmic Strain Rate Curve
for 50XF-LT, (8% Cold-Stretched, Non-Aged Material)
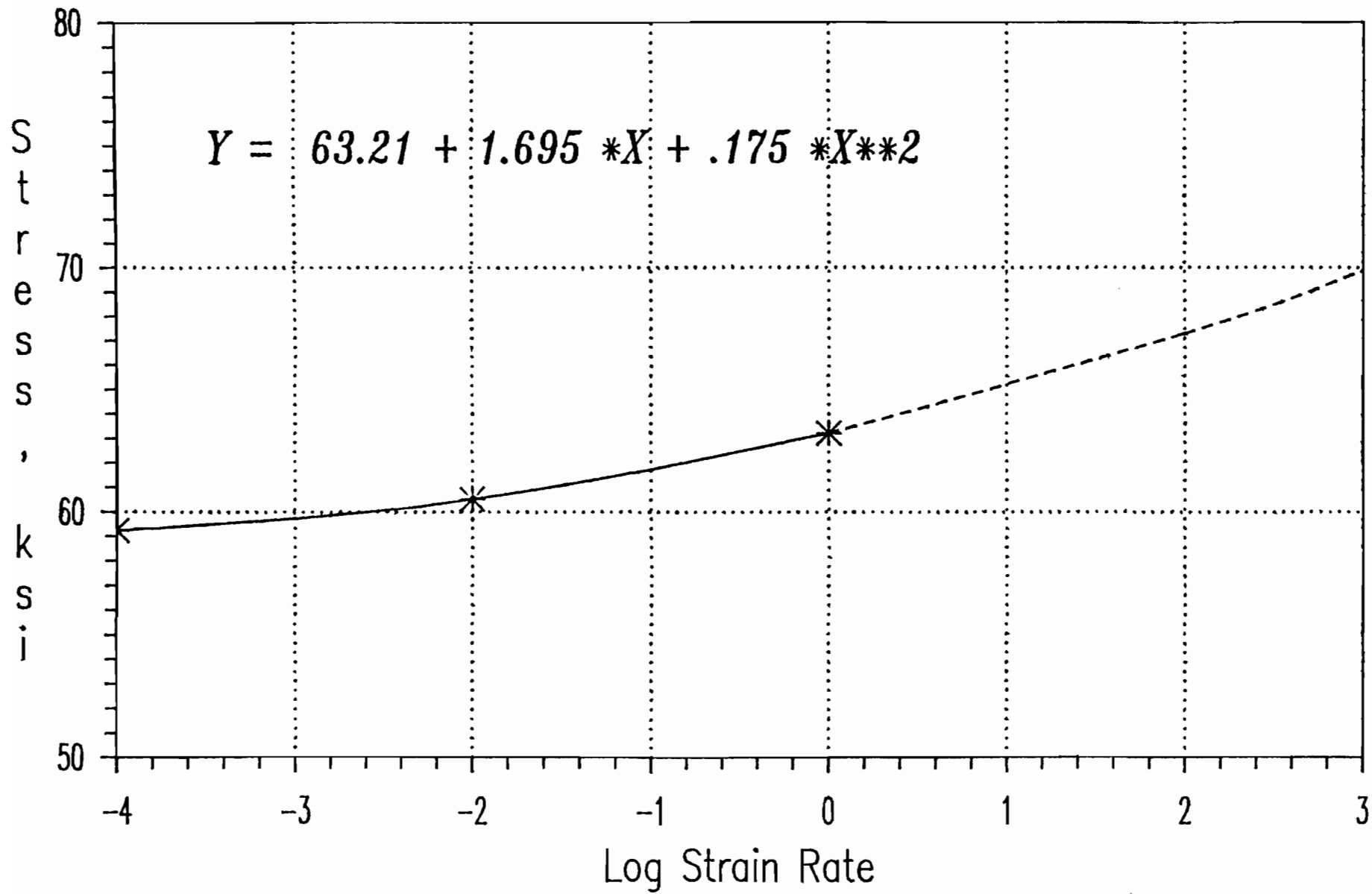
Fig. 4.6 Tensile Yield Stress vs Logarithmic Strain Rate Curve
for 50XF-LT, (2% Cold-Stretched, Aged Material)

$$Y = 75.77 + 1.960 *X + .325 *X**2$$
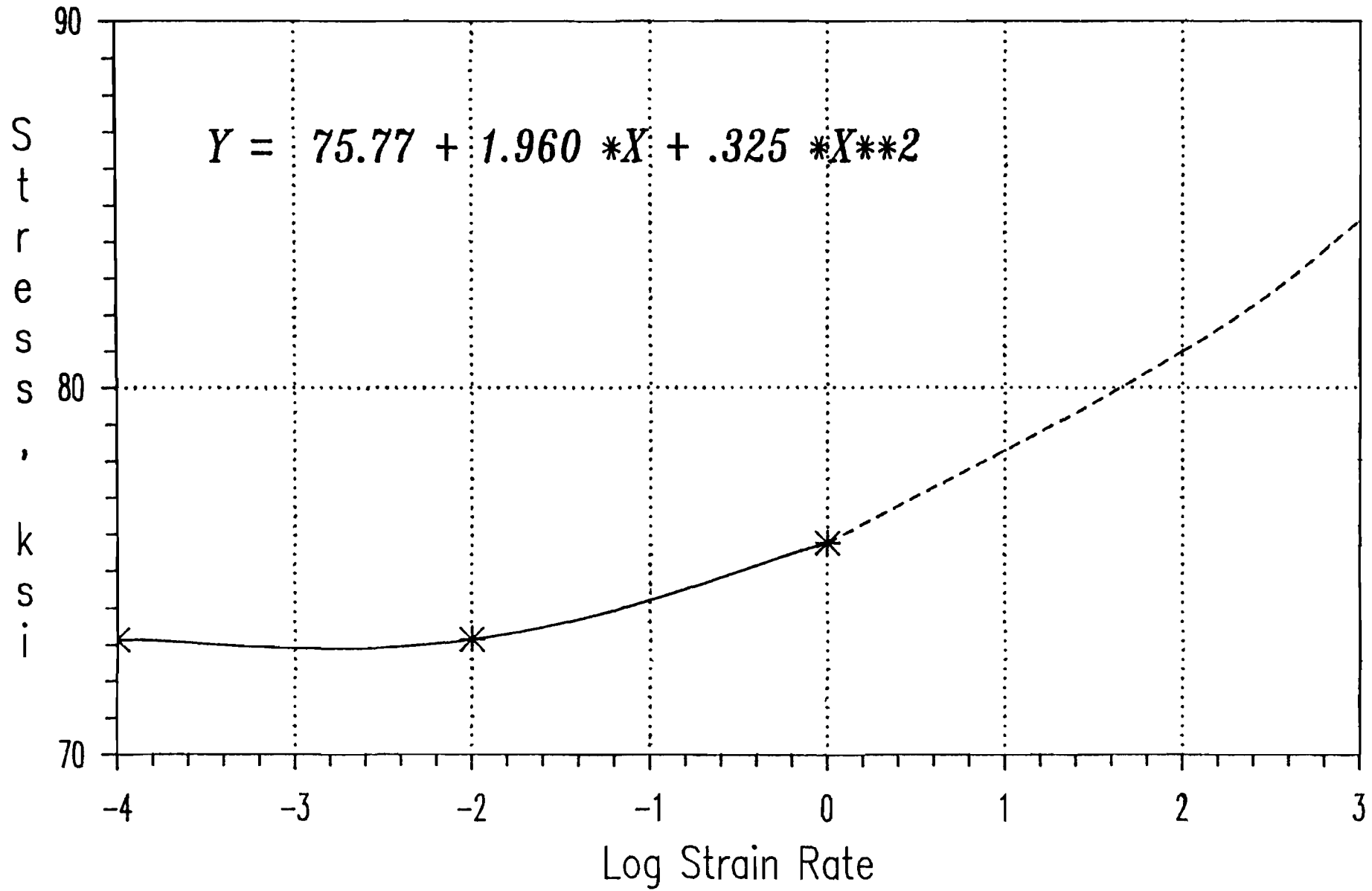
Fig. 4.7 Tensile Yield Stress vs Logarithmic Strain Rate Curve
for 50XF-LT, (8% Cold-Stretched, Aged Material)

$$Y = 78.73 + 2.420 *X + .245 *X**2$$
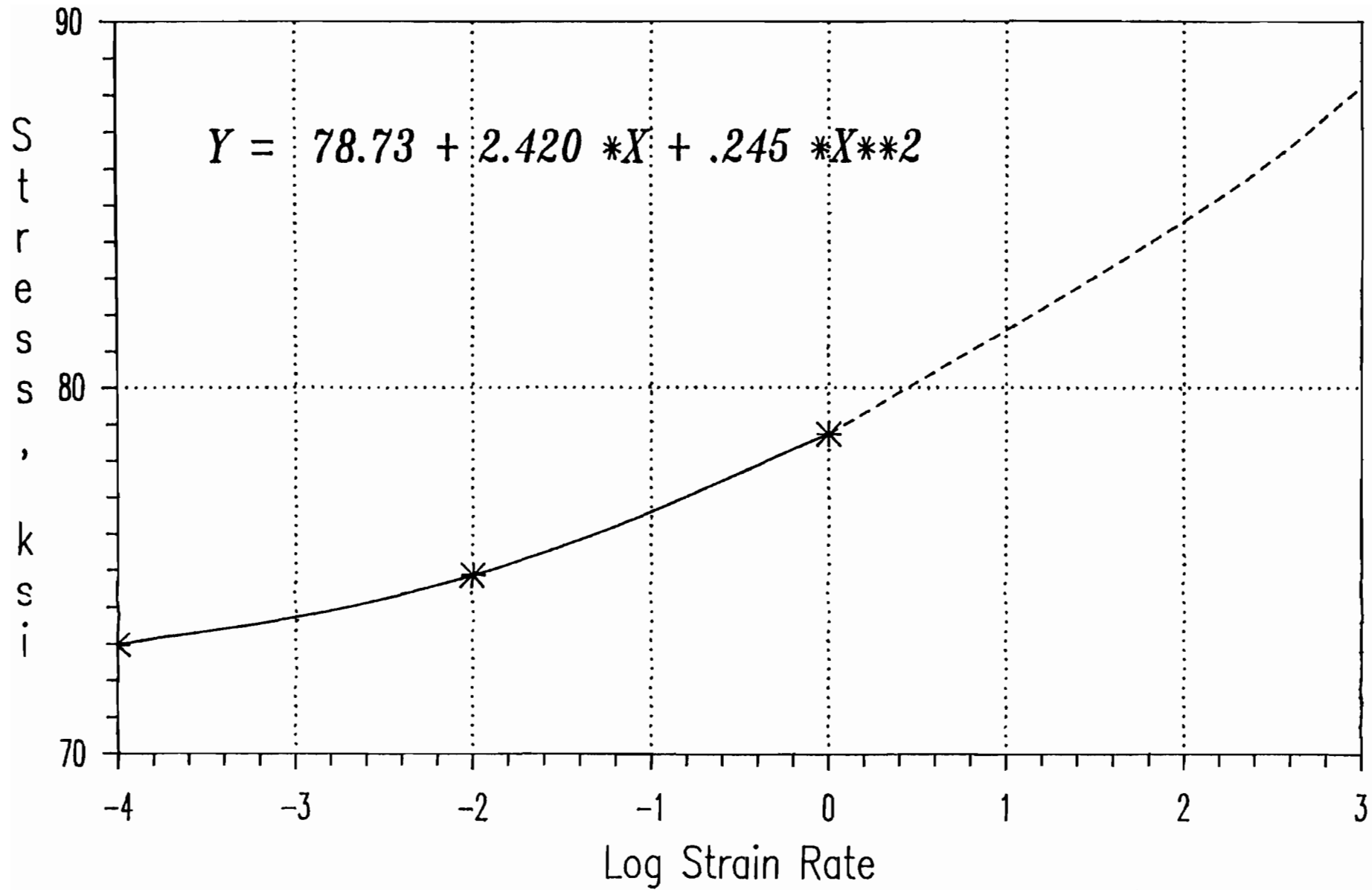
Fig. 4.8   Tensile Ultimate Stress vs Logarithmic Strain Rate Curve
for 50XF-LT, (Virgin Material)

$$Y = 80.32 + 3.992 * X + .541 * X**2$$
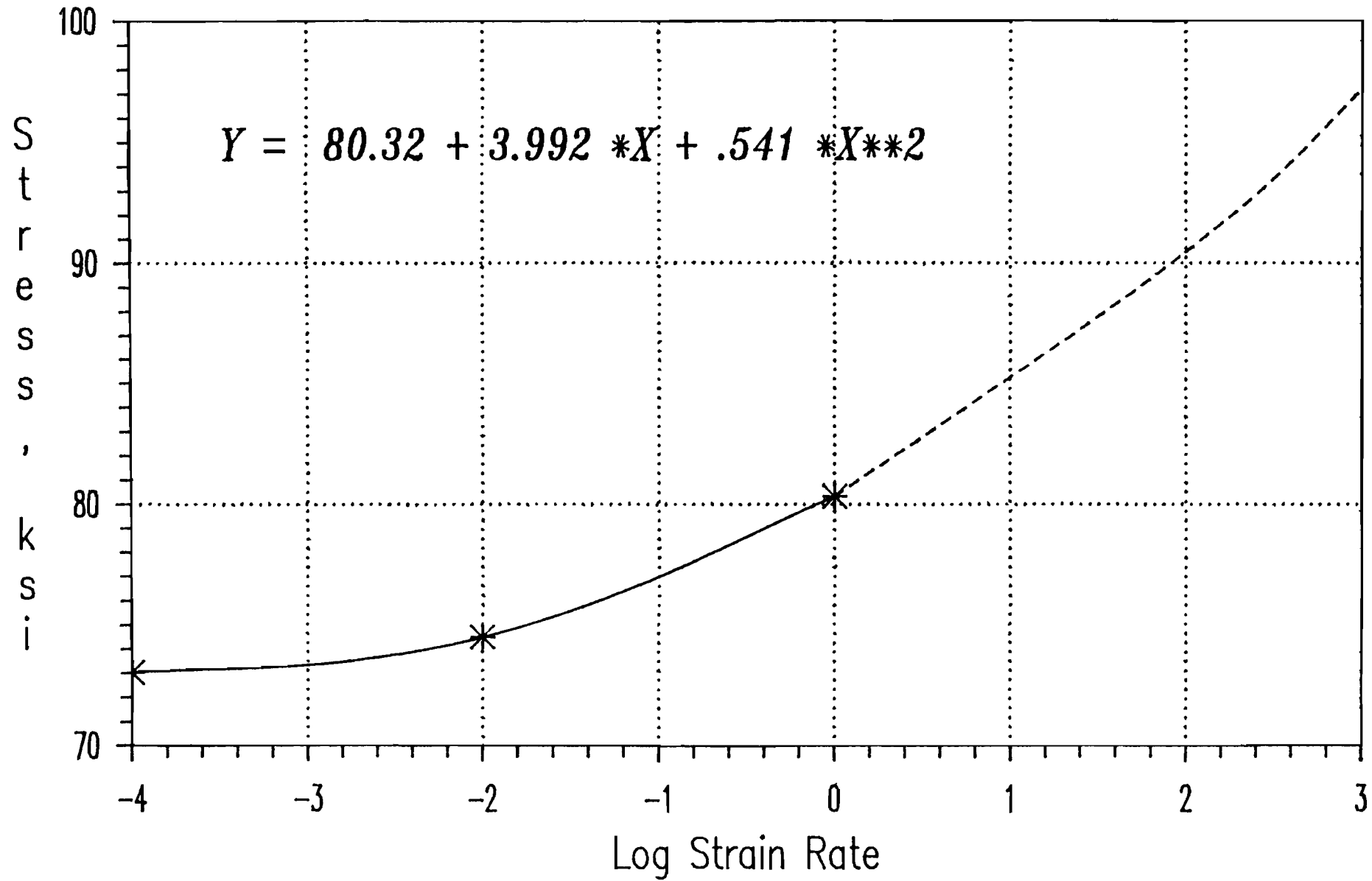
Fig. 4.9   Tensile Ultimate Stress vs Logarithmic Strain Rate Curve
for 50XF-LT, (2% Cold-Stretched, Non-Aged Material)

$$Y = 81.16 + 2.825 *X + .250 *X**2$$
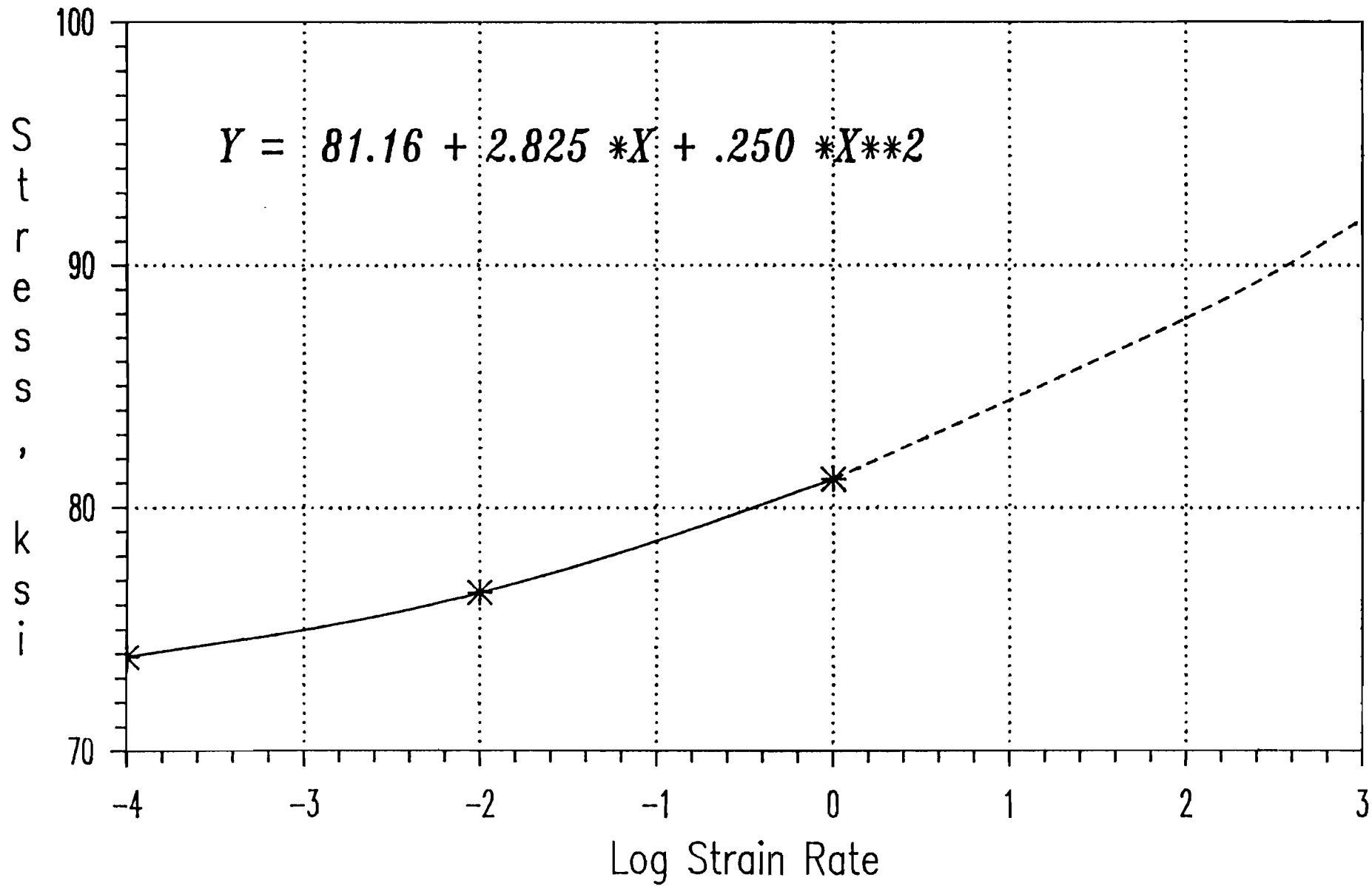
Fig. 4.10 Tensile Ultimate Stress vs Logarithmic Strain Rate Curve
for 50XF-LT, (8% Cold-Stretched, Non-Aged Material)
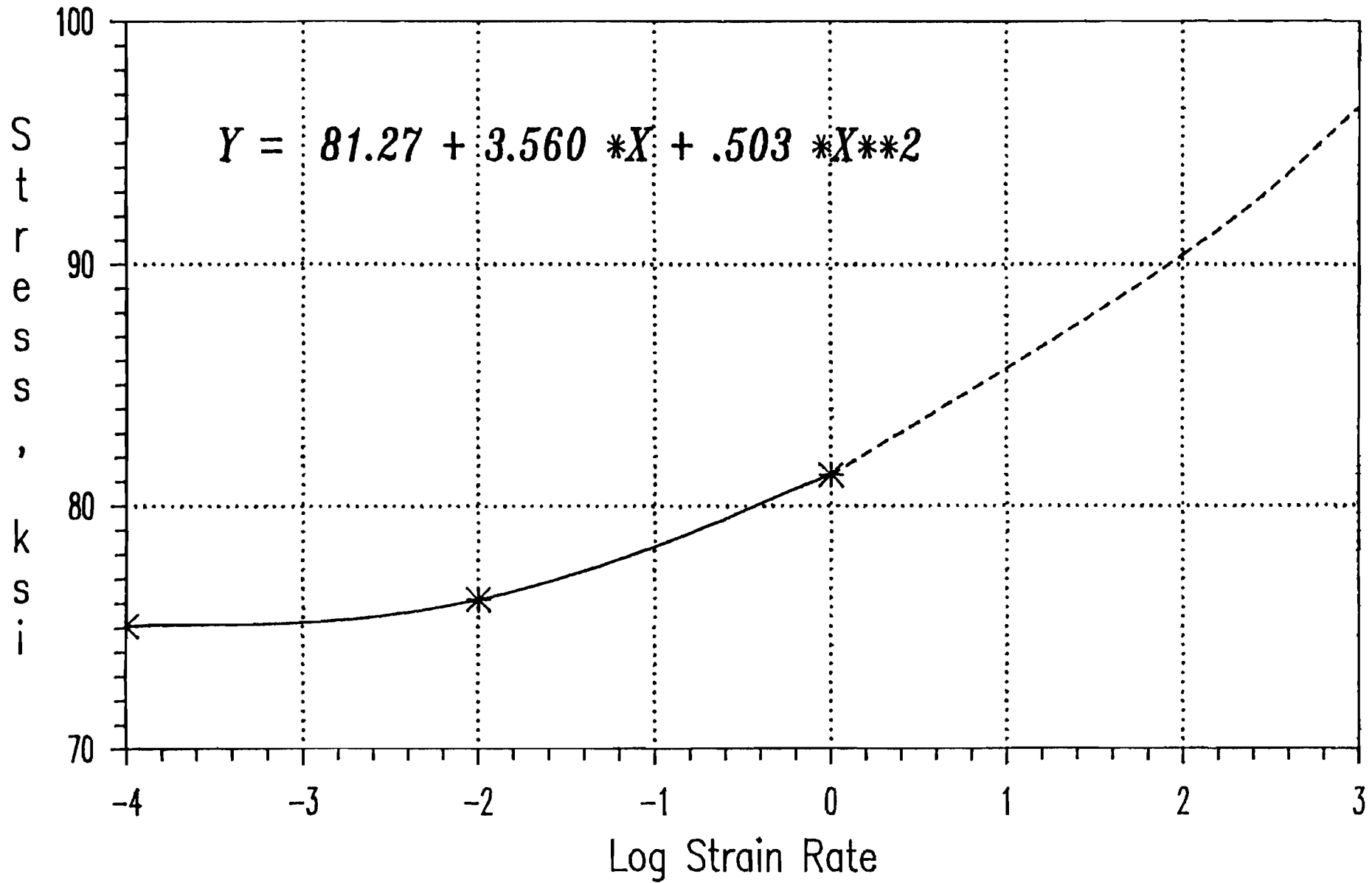
Fig. 4.11 Tensile Ultimate Stress vs Logarithmic Strain Rate Curve
for 50XF-LT, (2% Cold-Stretched, Aged Material)
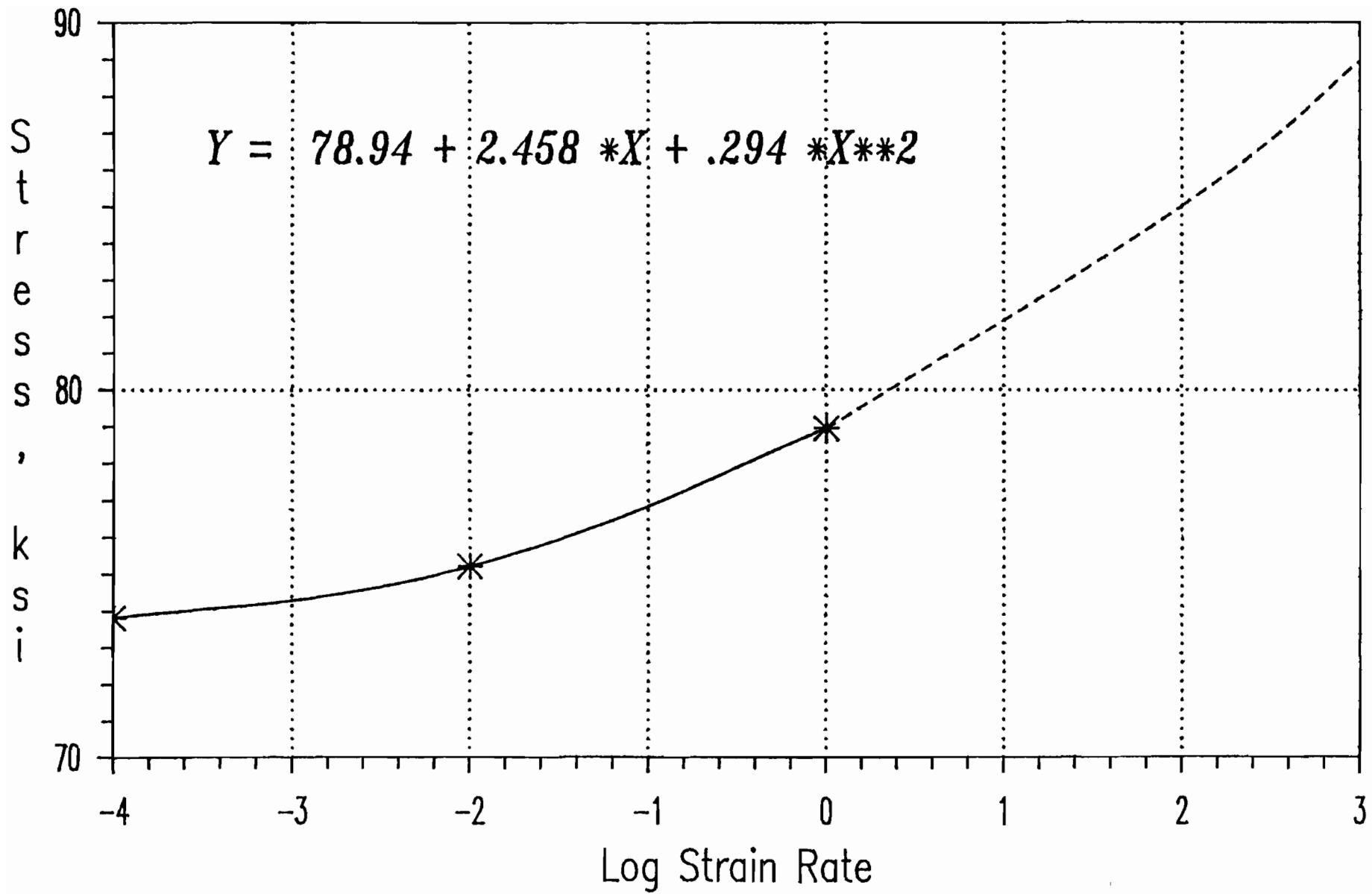
Fig. 4.12 Tensile Ultimate Stress vs Logarithmic Strain Rate Curve
for 50XF-LT, (8% Cold-Stretched, Aged Material)
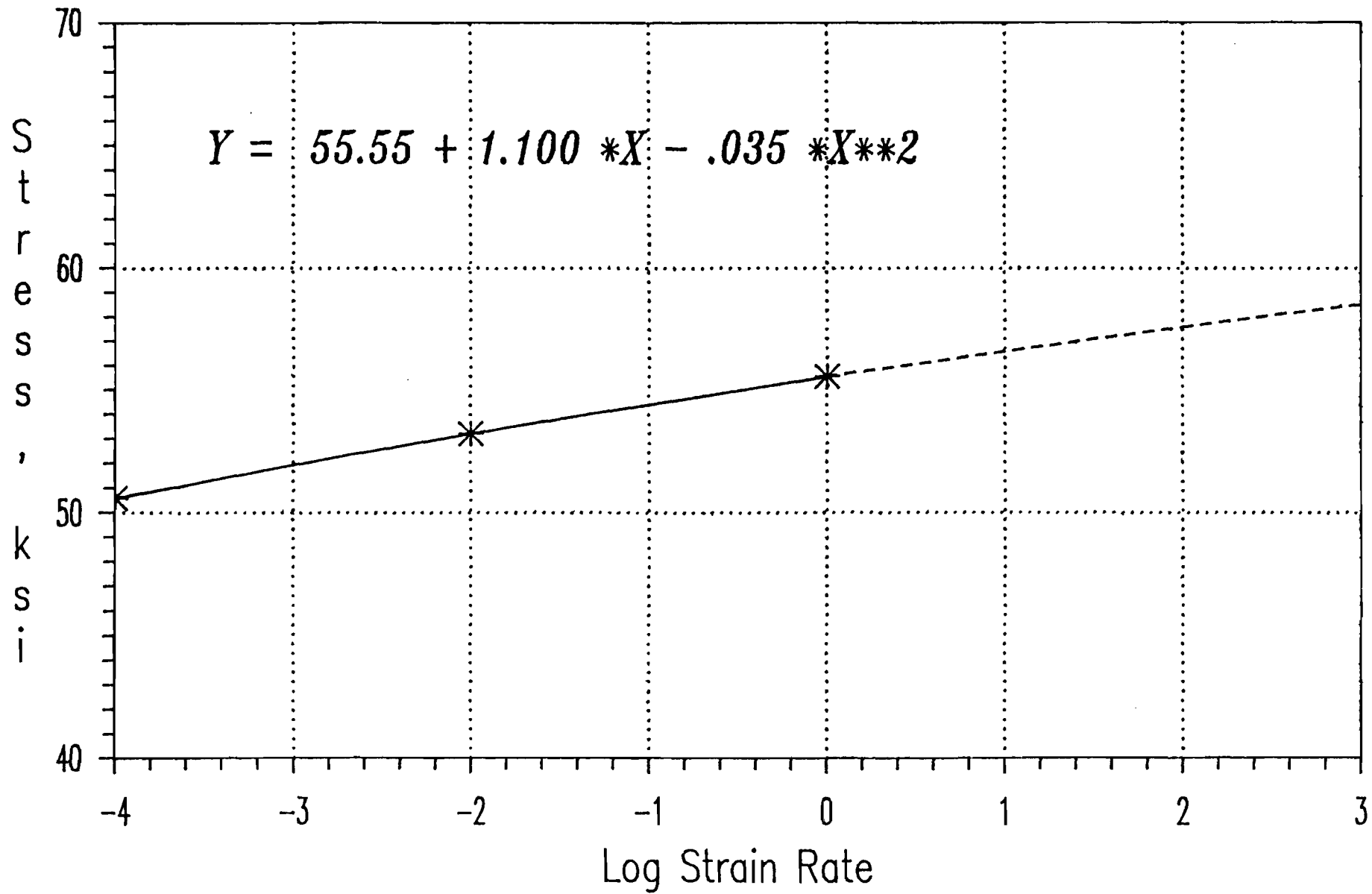
Fig. 4.13 Tensile Yield Stress vs Logarithmic Strain Rate Curve
for 50XF-TT, (Virgin Material)

$$Y = 79.91 + 3.552 *X + .484 *X**2$$
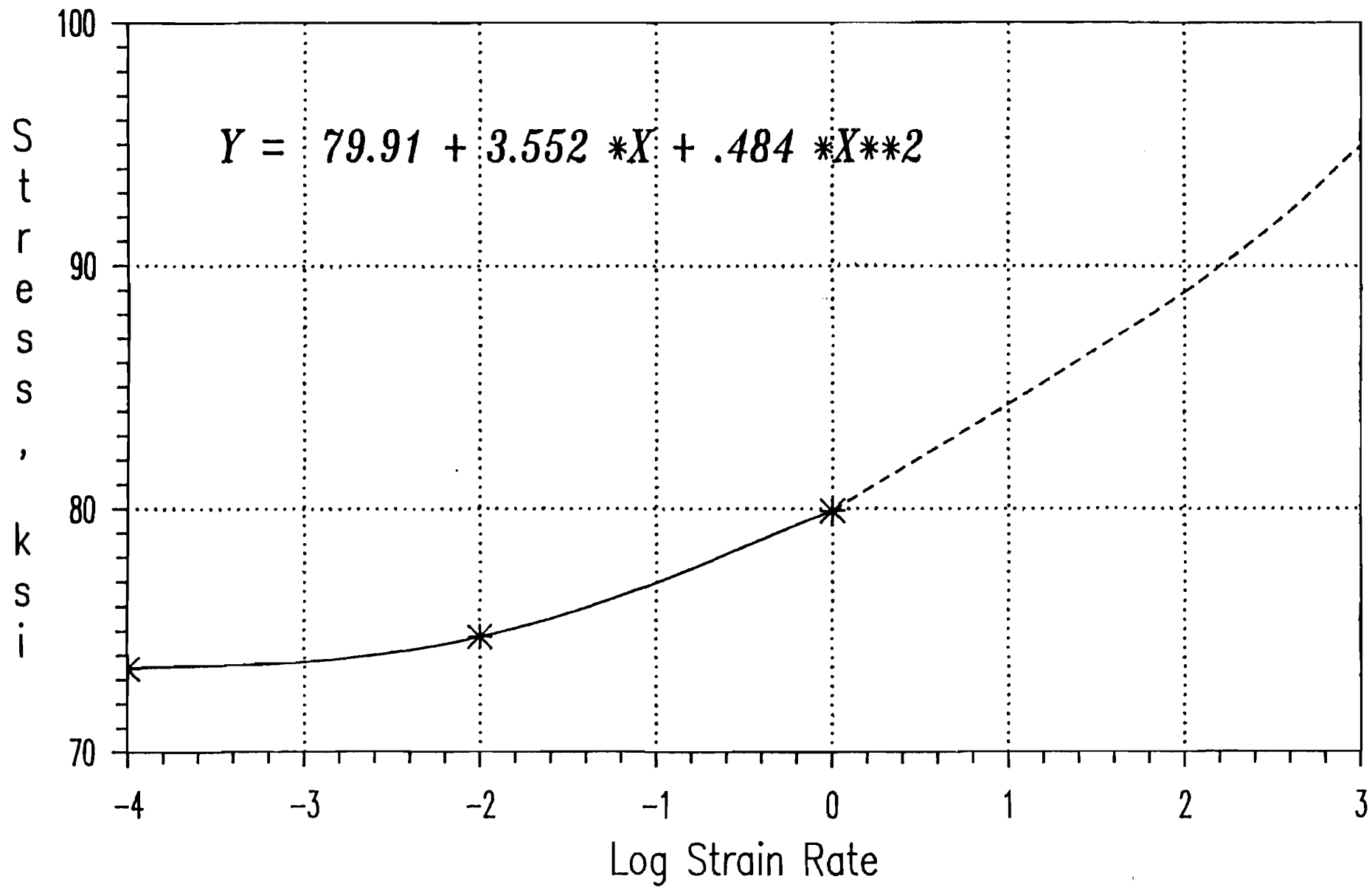
Fig. 4.14 Tensile Ultimate Stress vs Logarithmic Strain Rate Curve
for 50XF-TT, (Virgin Material)

$$Y = 42.37 + 3.595 * X + .305 * X**2$$
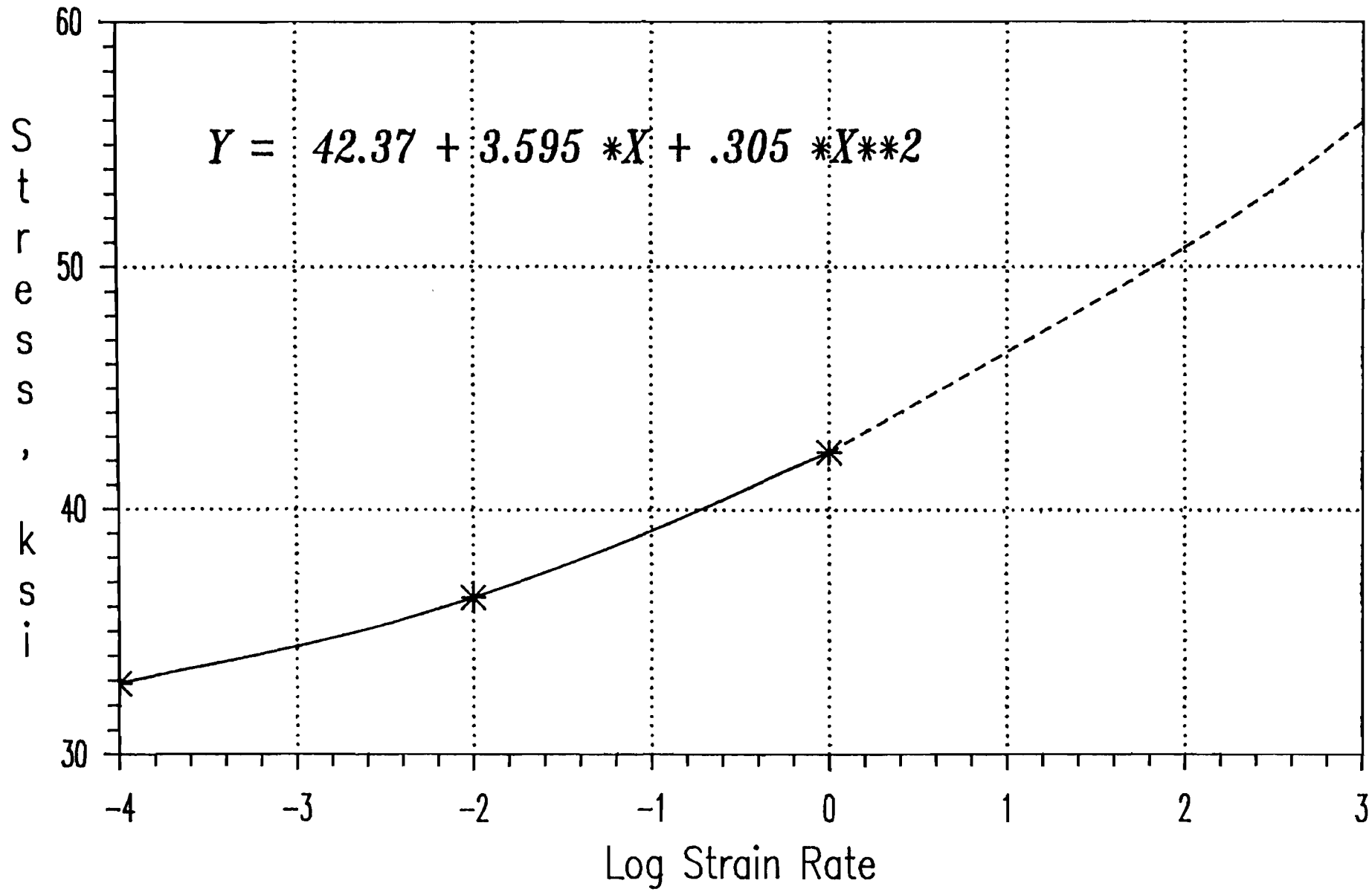
Fig. 4.15 Tensile Yield Stress vs Logarithmic Strain Rate Curve
for 35XF-LT, (Virgin Material)
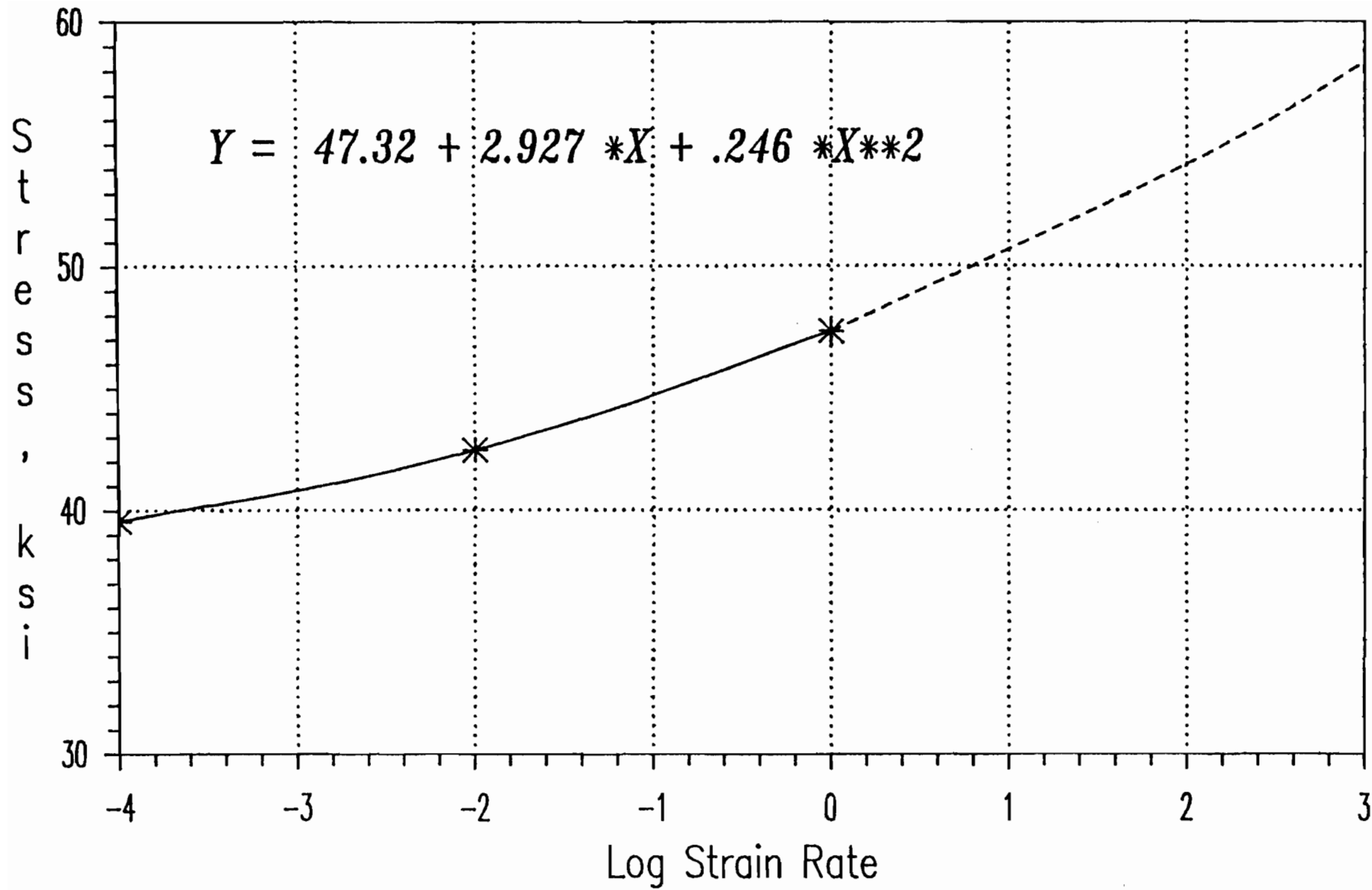
Fig. 4.16 Tensile Yield Stress vs Logarithmic Strain Rate Curve
for 35XF-LT, (2% Cold-Stretched, Non-Aged Material)

$$Y = 52.90 + 2.102 * X + .114 * X**2$$
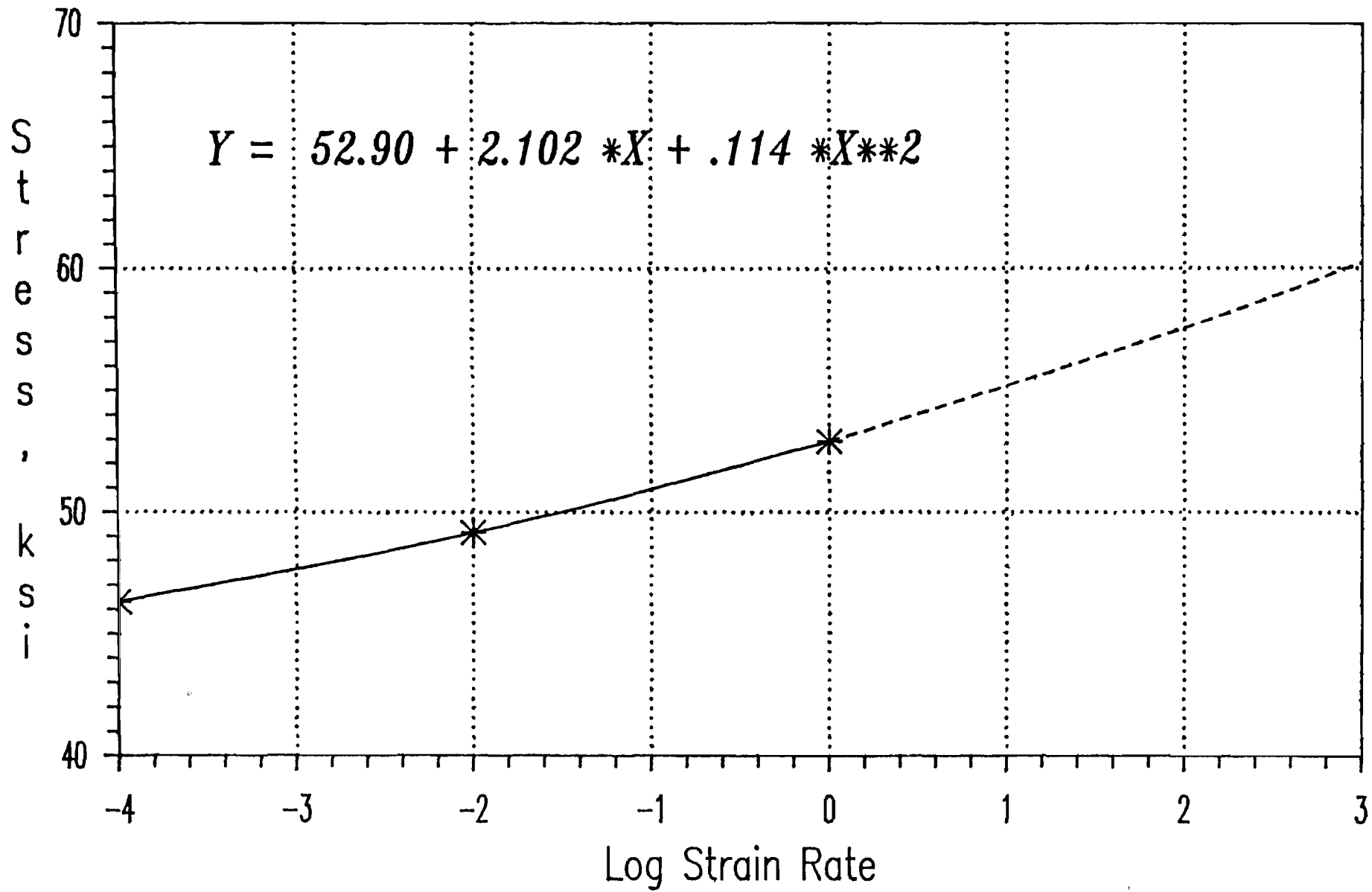
Fig. 4.17 Tensile Yield Stress vs Logarithmic Strain Rate Curve
for 35XF-LT, (8% Cold-Stretched, Non-Aged Material)

$$Y = 47.40 + 4.008 *X + .536 *X**2$$
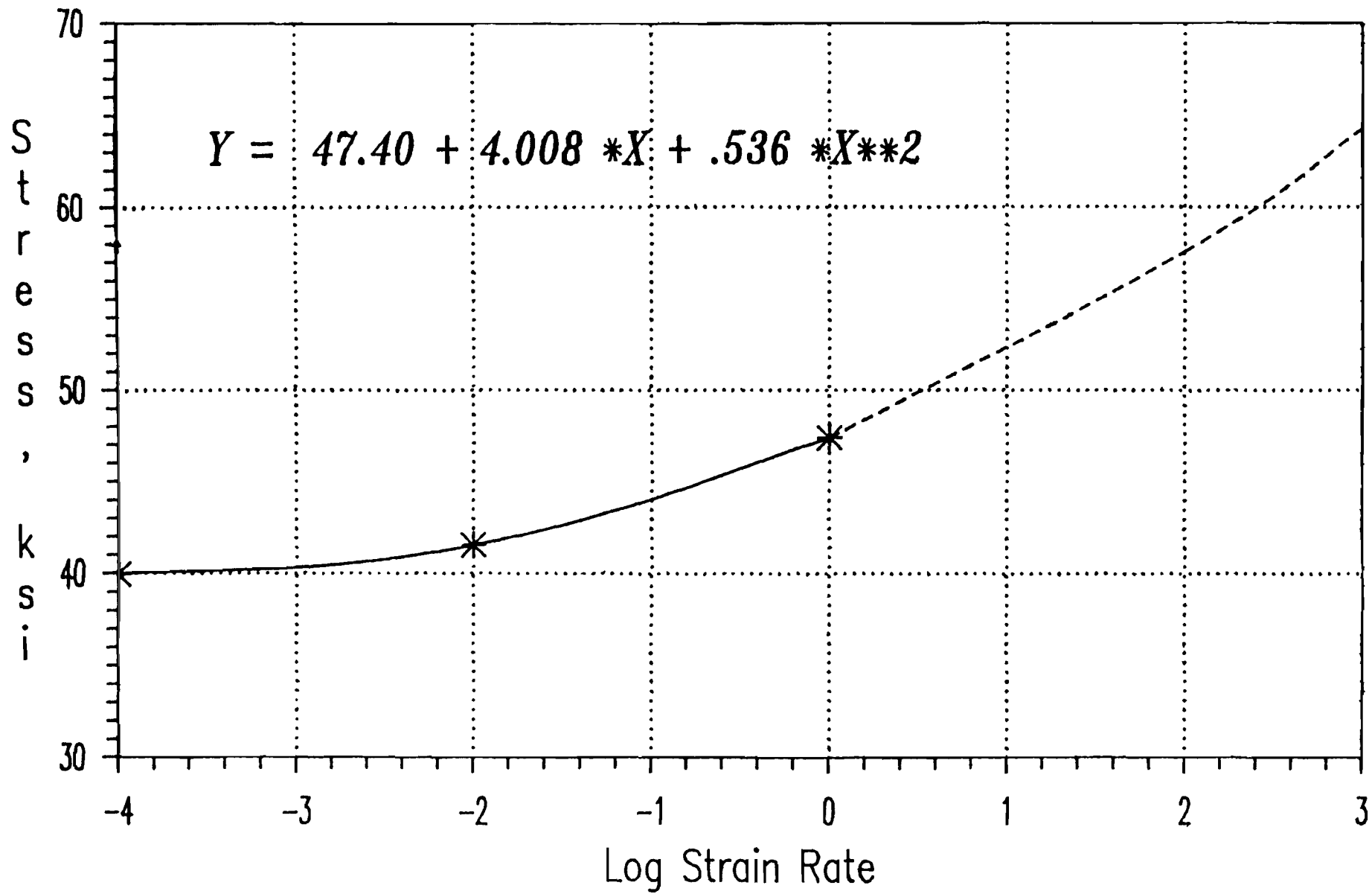
Fig. 4.18 Tensile Yield Stress vs Logarithmic Strain Rate Curve
for 35XF-LT, (2% Cold-Stretched, Aged Material)

$$Y = 53.67 + 2.520 * X + .160 * X ** 2$$
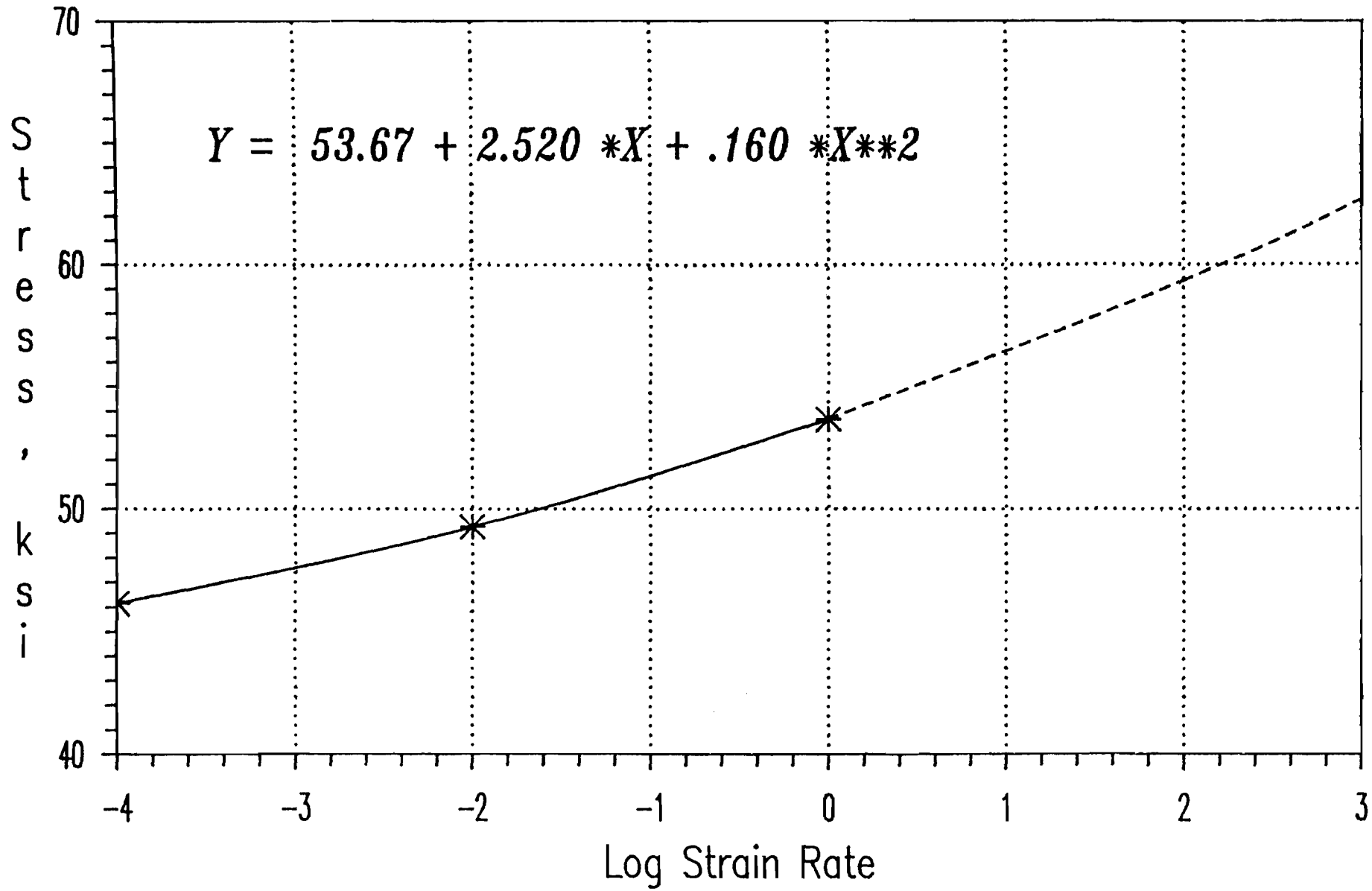
Fig. 4.19 Tensile Yield Stress vs Logarithmic Strain Rate Curve
for 35XF-LT, (8% Cold-Stretched, Aged Material)

$$Y = 56.63 + 3.050 * X + .308 * X**2$$
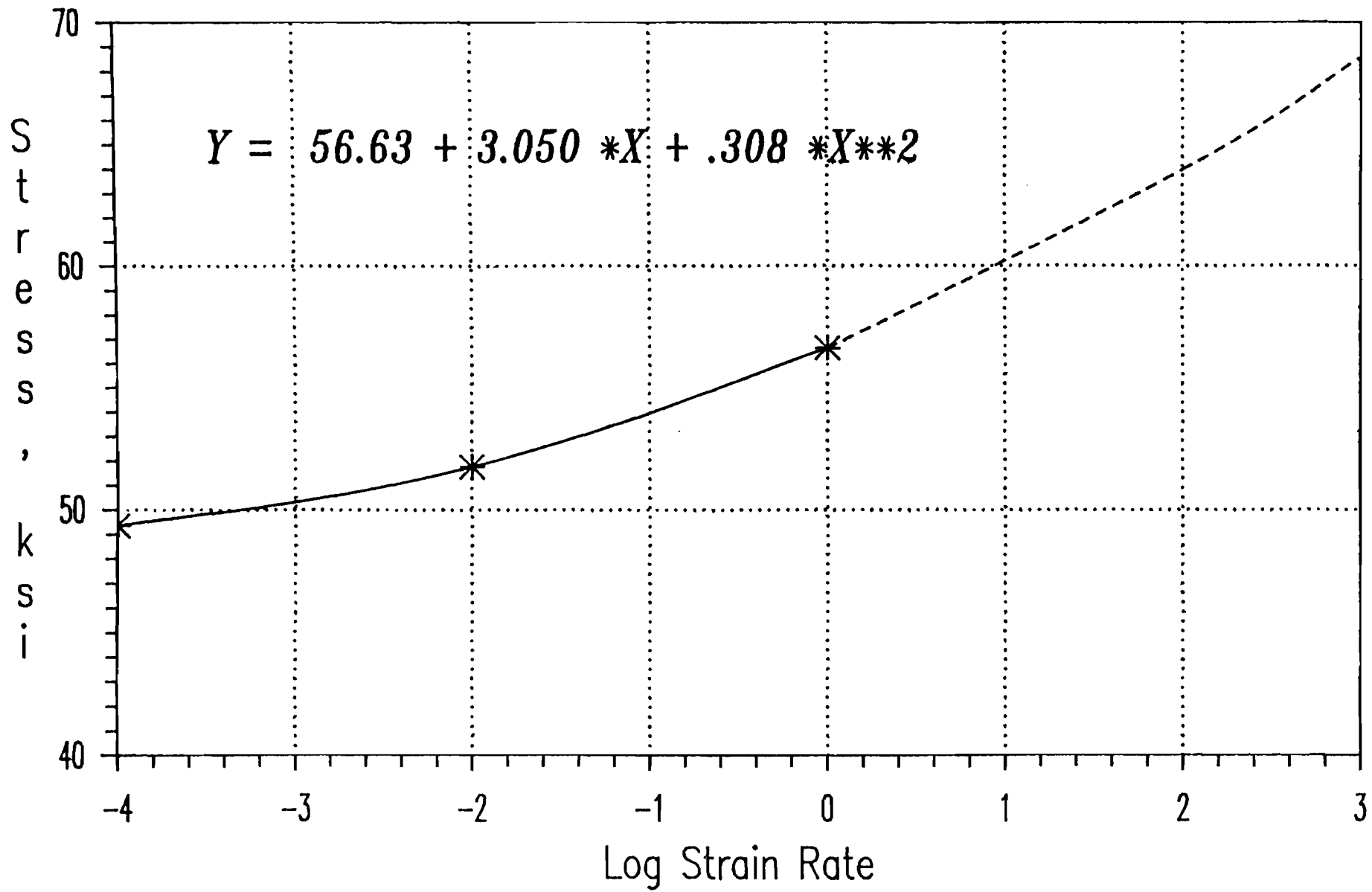
Fig. 4.20 Tensile Ultimate Stress vs Logarithmic Strain Rate Curve
for 35XF-LT, (Virgin Material)

$$Y = 57.05 + 2.885 * X + .248 * X**2$$
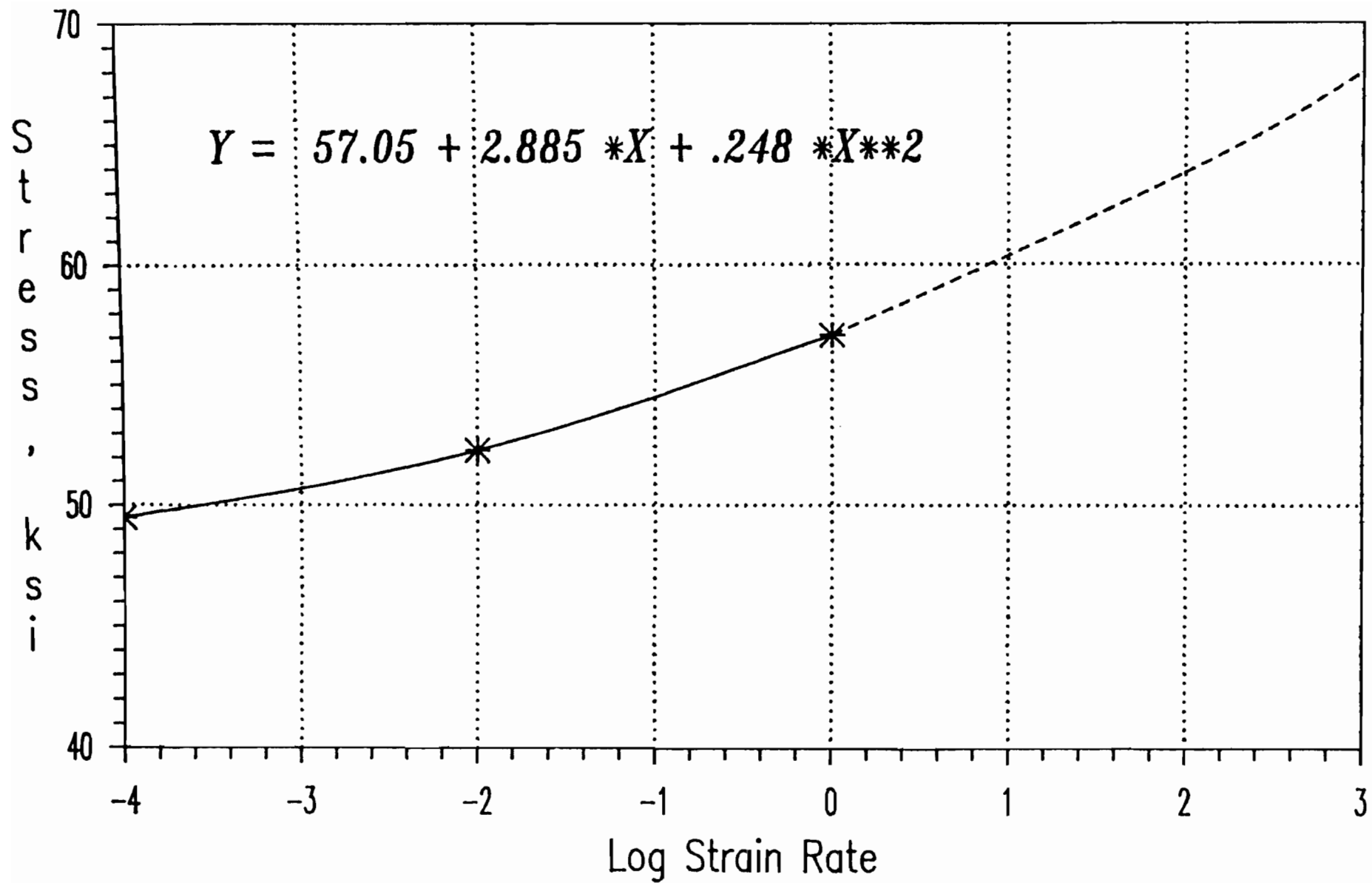
Fig. 4.21 Tensile Ultimate Stress vs Logarithmic Strain Rate Curve
for 35XF-LT, (2% Cold-Stretched, Non-Aged Material)

$$Y = 57.21 + 2.890 *X + .225 *X**2$$
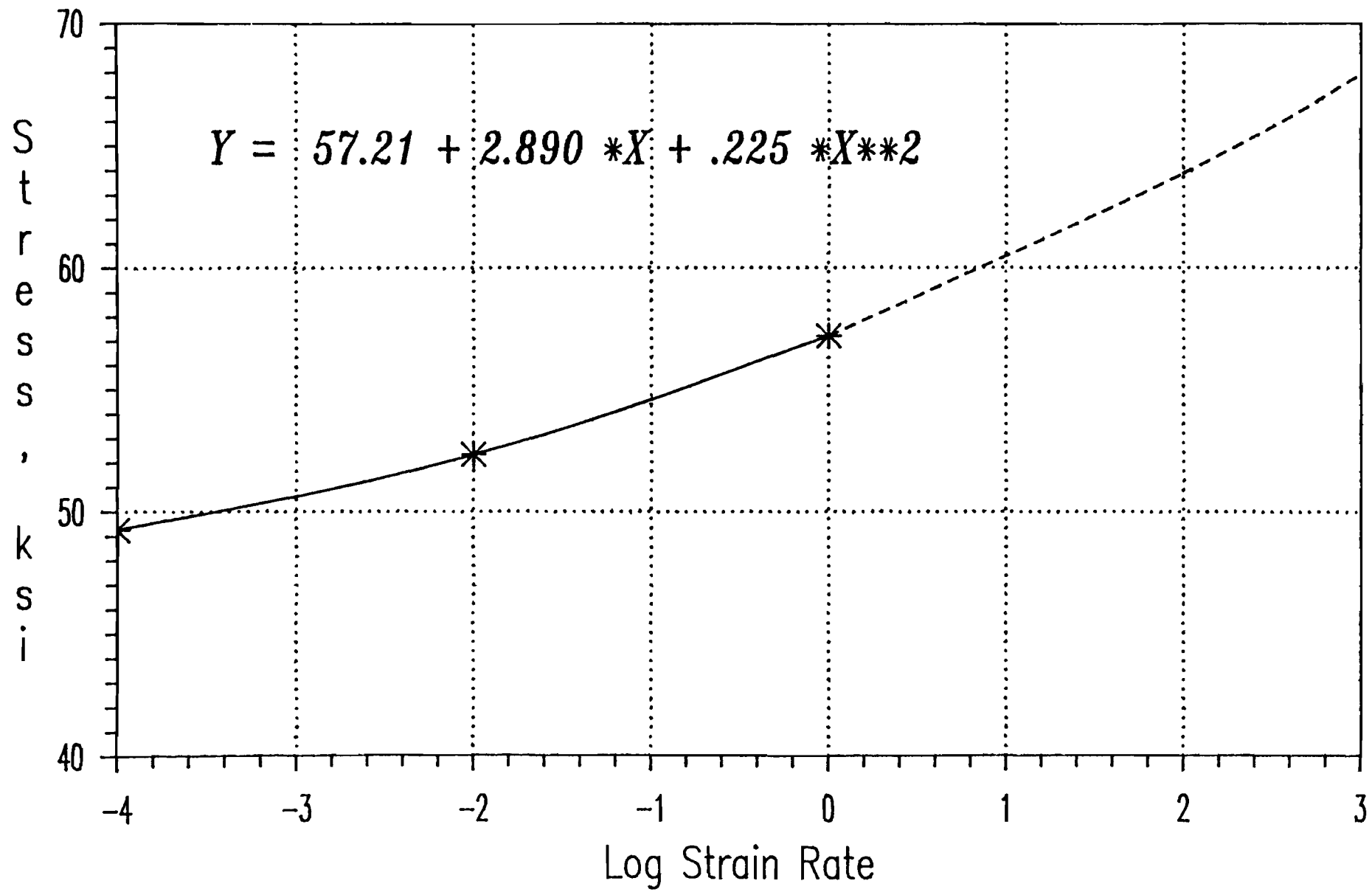
Fig. 4.22 Tensile Ultimate Stress vs Logarithmic Strain Rate Curve
for 35XF-LT, (8% Cold-Stretched, Non-Aged Material)

$$Y = 56.85 + 3.595 * X + .453 * X ** 2$$
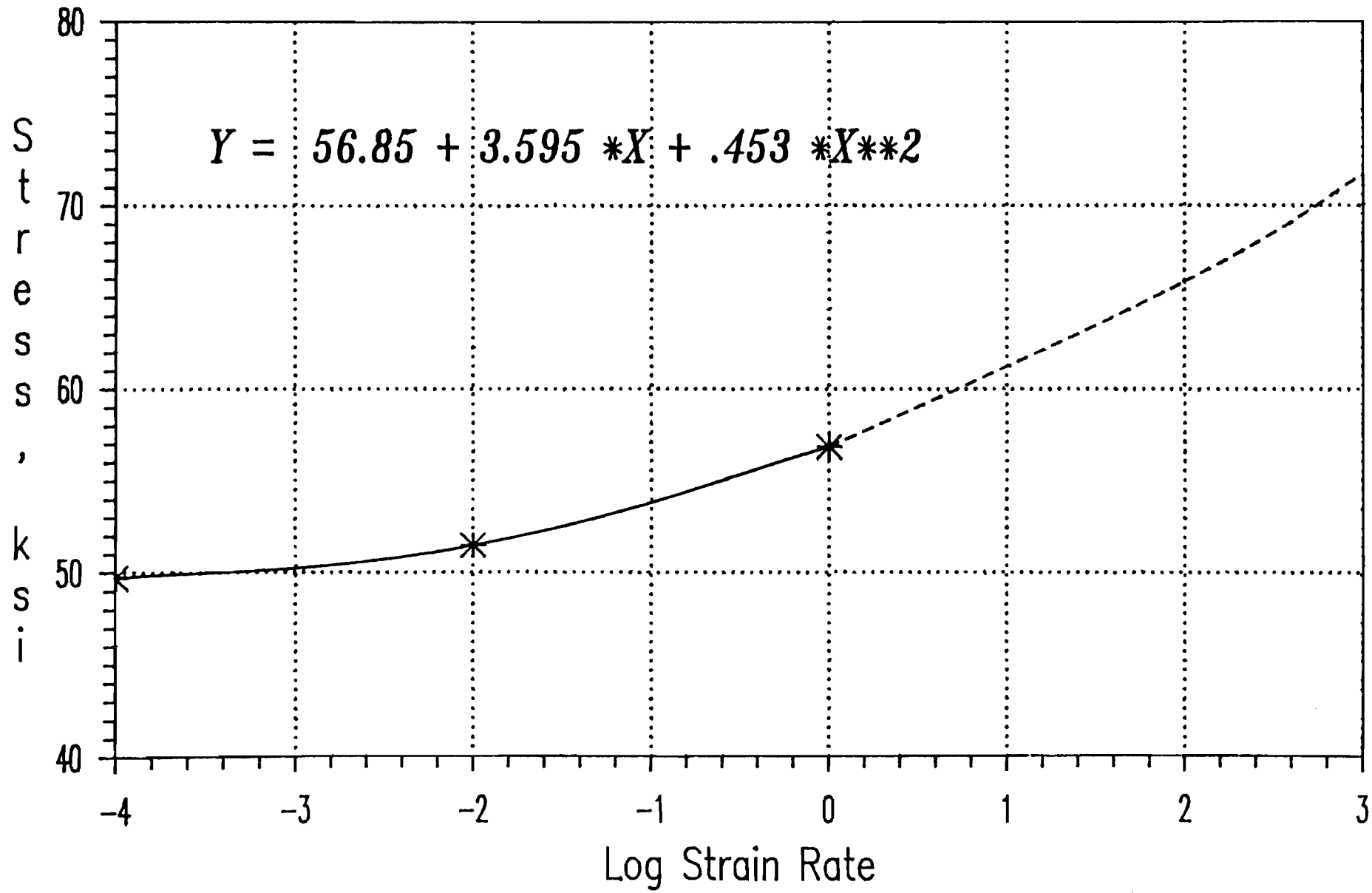
Fig. 4.23 Tensile Ultimate Stress vs Logarithmic Strain Rate Curve
for 35XF-LT, (2% Cold-Stretched, Aged Material)

$$Y = 57.53 + 3.270 *X + .263 *X**2$$
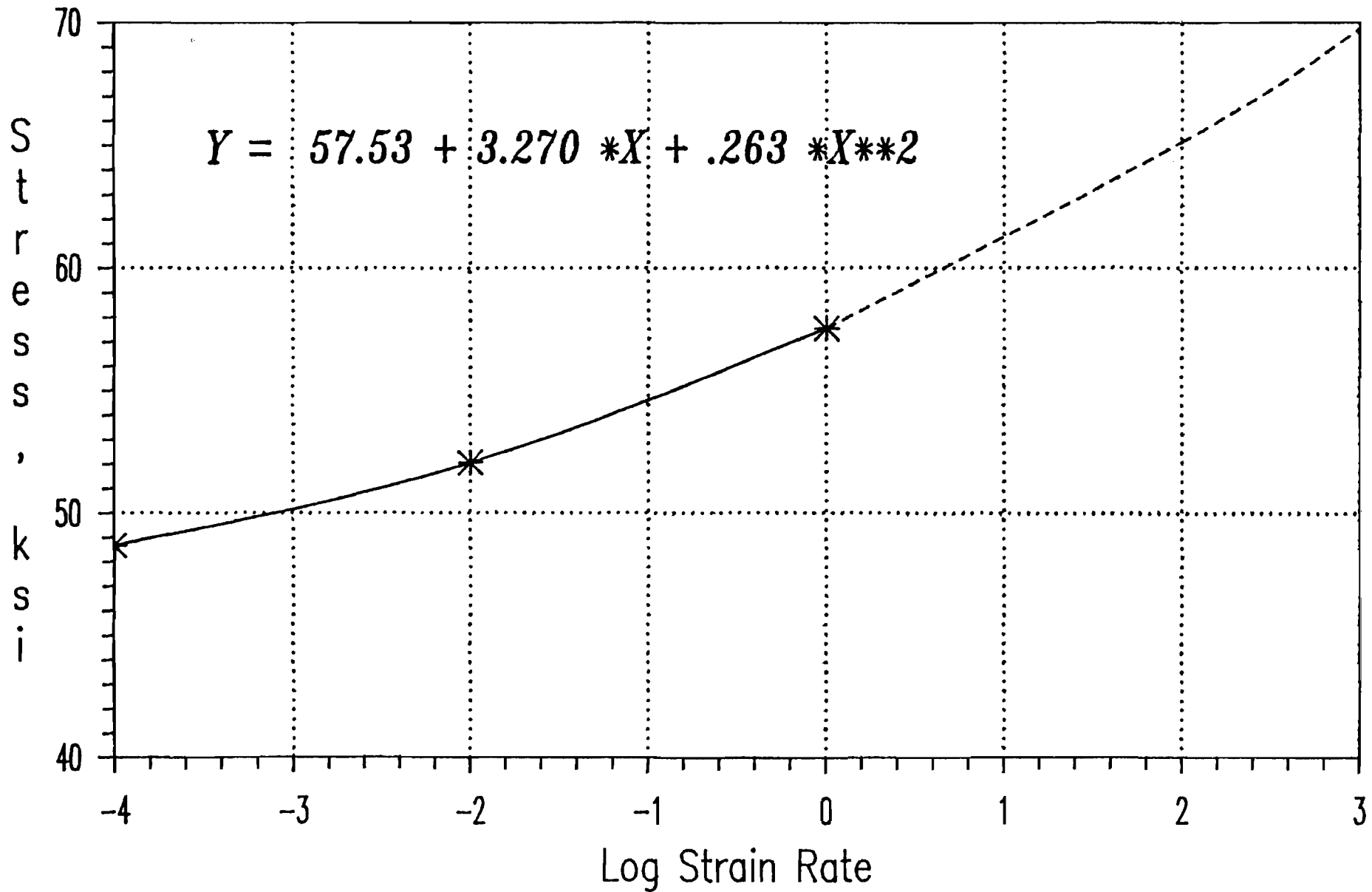
Fig. 4.24 Tensile Ultimate Stress vs Logarithmic Strain Rate Curve
for 35XF-LT, (8% Cold-Stretched, Aged Material)
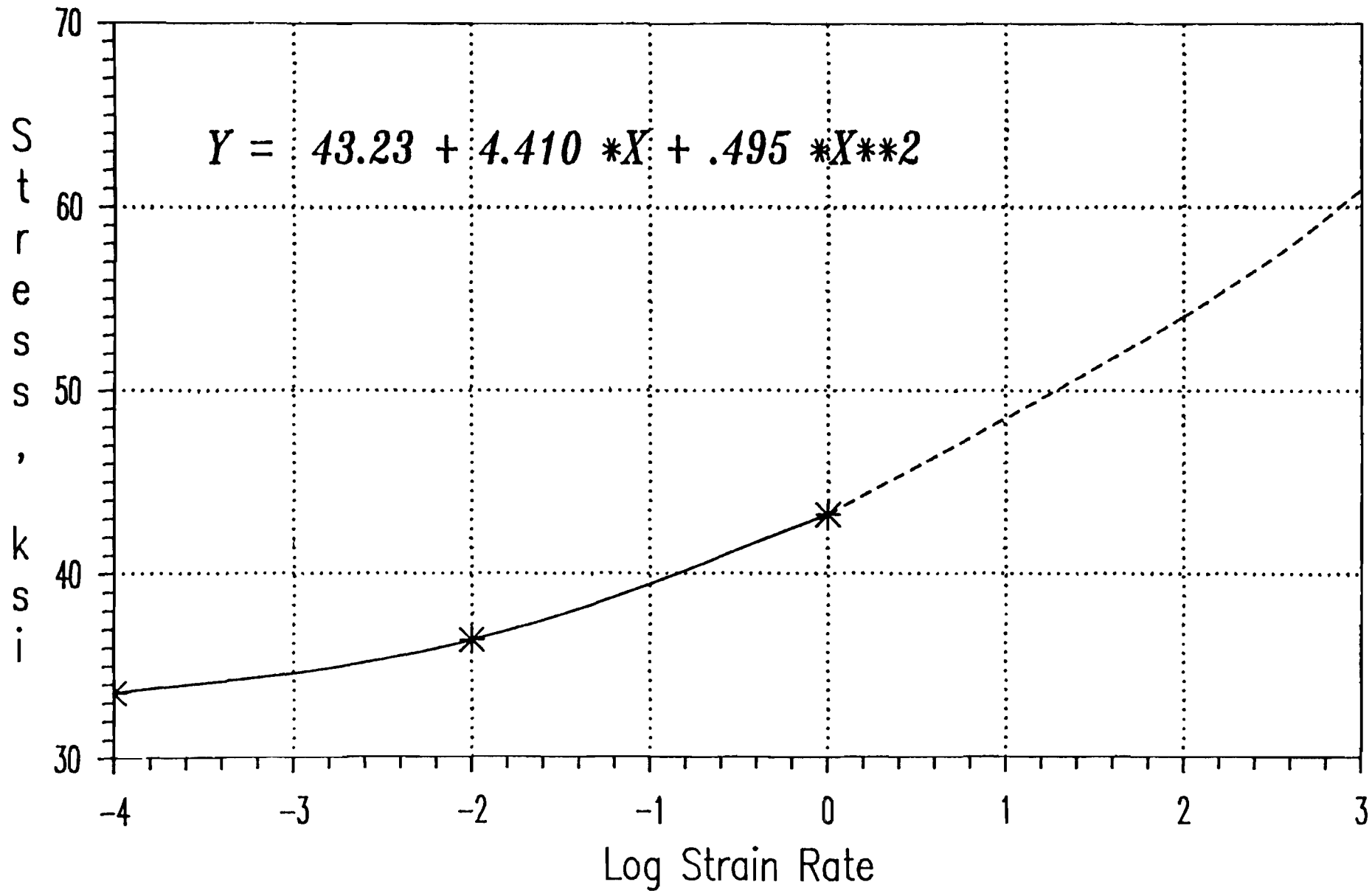
Fig. 4.25 Tensile Yield Stress vs Logarithmic Strain Rate Curve
for 35XF-TT, (Virgin Material)

$$Y = 55.93 + 3.232 *X + .394 *X**2$$
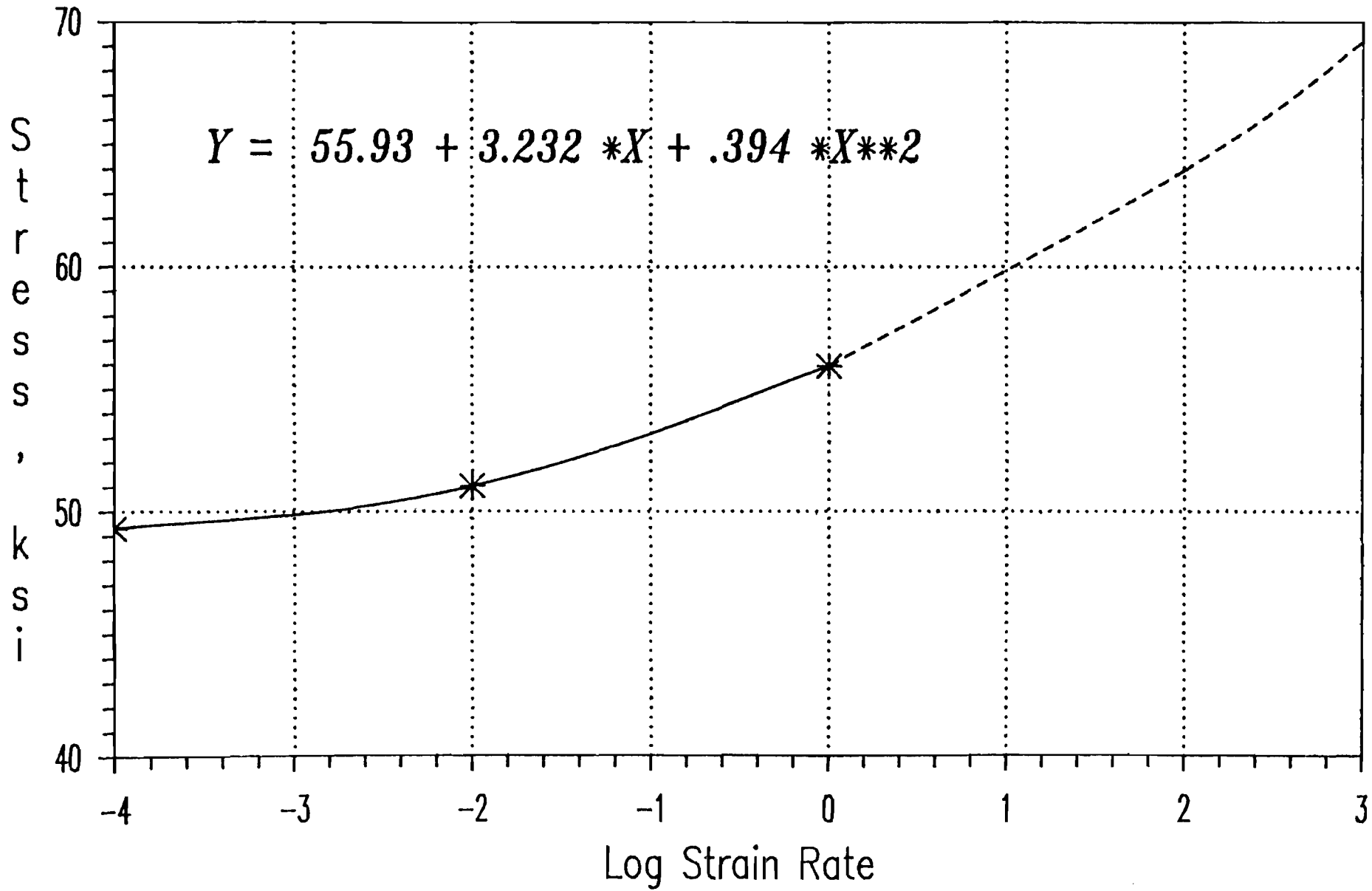
Fig. 4.26 Tensile Ultimate Stress vs Logarithmic Strain Rate Curve
for 35XF-TT, (Virgin Material)